DETERMINATION OF SEISMIC SOURCE PARAMETERS FROM LONG-PERIOD TELESEISMIC WAVES

Lawrence S. Turnbull, et al

Texas Instruments, Incorporated

Prepared for:

Air Force Office of Scientific Research
Advanced Research Project

31 May 1974

UNCLASSIFIED

SECURITY CLASSIFICATION OF THIS PAGE (When Data Entered)

AD-784898

REPORT DOCUMENTATION PAGE

READ INSTRUCTIONS BEFORE COMPLETING FORM

1. REPORT NUMBER: AFOSR - TR - 74 - 1132
2. GOVT ACCESSION NO.
3. RECIPIENT'S CATALOG NUMBER

4. TITLE (and Subtitle): DETERMINATION OF SEISMIC SOURCE PARAMETERS FROM LONG-PERIOD TELESEISMIC WAVES

5. TYPE OF REPORT & PERIOD COVERED: Technical

6. PERFORMING ORG. REPORT NUMBER: ALEX(02)-TR-74-01-PART A

7. AUTHOR(s): Lawrence S. Turnbull, David Sun, and David G. Black

8. CONTRACT OR GRANT NUMBER(s): F44620-73-C-0055

9. PERFORMING ORGANIZATION NAME AND ADDRESS: Texas Instruments Incorporated, Equipment Group, Dallas, Texas 75222

10. PROGRAM ELEMENT, PROJECT, TASK AREA & WORK UNIT NUMBERS: ARPA Program Code No. F10

11. CONTROLLING OFFICE NAME AND ADDRESS: Advanced Research Projects Agency, Nuclear Monitoring Research Office, Arlington, Virginia 22209

12. REPORT DATE: 31 May 1974

13. NUMBER OF PAGES: 109

14. MONITORING AGENCY NAME & ADDRESS (if different from Controlling Office): Air Force Office of Scientific Research, 1400 Wilson Boulevard, Arlington, Virginia 22209

15. SECURITY CLASS. (of this report): UNCLASSIFIED

15a. DECLASSIFICATION/DOWNGRADING SCHEDULE

16. DISTRIBUTION STATEMENT (of this Report)

APPROVED FOR PUBLIC RELEASE, DISTRIBUTION UNLIMITED

17. DISTRIBUTION STATEMENT (of the abstract entered in Block 20, if different from Report)

18. SUPPLEMENTARY NOTES

ARPA Order Number 1827

19. KEY WORDS (Continue on reverse side if necessary and identify by block number)

Surface Waves
Spectral Fitting Procedure
Focal Depth Estimate
Source Region Crustal Structure

20. ABSTRACT (Continue on reverse side if necessary and identify by block number)

Spectral-fitting procedures are applied to teleseismic surface wave data for determining seismic source parameters, especially depth. From an examination of theoretical Rayleigh and Love wave spectra as a function of source structure, significant variation of the spectra can result from differences of gross tectonic structure in most cases. For very shallow events (less than 5 km), though, the effect of source structure is minimal.

DD FORM 1 JAN 73 1473 EDITION OF 1 NOV 65 IS OBSOLETE

UNCLASSIFIED

SECURITY CLASSIFICATION OF THIS PAGE (When Data Entered)

20. continued

Since major variations of spectra with focal depth occur in the 10 to 20 second period range, the data recorded on VLPE instruments is not as desirable as that recorded at NORSAR and ALPA because of the very low instrument response in that period range.

Seven Eurasian events are analyzed for source mechanisms. For those with known depth from bodywave phases, knowledge of the source region crustal structure is crucial to obtain focal depth agreement from spectral fitting. These source structures were then applied to events in the same region with no independent depth estimates.

ABSTRACT

Spectral-fitting procedures are applied to teleseismic surface wave data for determining seismic source parameters, especially depth. From an examination of theoretical Rayleigh and Love wave spectra as a function of source structure, significant variation of the spectra can result from differences of gross tectonic structure in most cases. For very shallow events (less than 5 km), though, the effect of source structure is minimal.

Since major variations of spectra with focal depth occur in the 10 to 20 second period range, the data recorded on VLPE instruments is not as desirable as that recorded at NORSAR and ALPA because of the very low instrument response in that period range.

Seven Eurasian events are analyzed for source mechanisms. For those with known depth from bodywave phases, knowledge of the source region crustal structure is crucial to obtain focal depth agreement from spectral fitting. These source structures were then applied to events in the same region with no independent depth estimate.

TABLE OF CONTENTS

LIST OF FIGURES

LIST OF FIGURES
(continued)

LIST OF FIGURES
(continued)

LIST OF FIGURES
(continued)

LIST OF FIGURES
(continued)

LIST OF TABLES

SECTION I
INTRODUCTION

This report presents the results from a continuing effort at Texas Instruments to obtain source parameter estimates (especially depth) from long period teleseismic surface waves. Previous work (Tsai (1972 a, b), Tsai and Shen (1972), and Turnbull, et. al. (1973)) has been mainly concerned with methodology and verification of the methods with synthetic and continental events (i. e., Southeastern Missouri Earthquake of 1965). In this report, we are attempting to determine the limitations of our approach in obtaining source parameter estimates of Central Asian events using teleseismic surface waves. The data base used in the analysis of these events consists of VLPE stations and the NORSAR and ALPA arrays.

In Section II, a brief summary of the theoretical source description is given, with the variation of Rayleigh and Love wave spectra discussed as a function of source depth and source structure. The requirements on the data for effective depth determination (the inverse problem) are then presented in light of this spectral behavior.

The analysis of the Central Asian events is given in Section III. These events are divided into two groups; those with depth of focus known from bodywave data and those where no source depth is known. Each event is discussed in terms of the data quality, source-station travel path, and the geology in the source region.

Finally, in Section IV, a summary of the results given in the previous sections are presented, and the directions this investigation expects to take in the future are discussed.

SECTION II

THEORETICAL CONSIDERATIONS

In fitting long period surface wave data, one must assume a theoretical source description. Most investigators use the far-field description of a double-couple source in a plane-layered half-space. We can write the transform of the source excitation function as:

$$S(\omega) = ML(\omega)k(\omega)N(\omega, h)X(\omega, \theta, \lambda, \Delta, h)\, e^{i\phi}$$

where

M - Seismic moment

$k(\omega)$ - Rayleigh or Love wave number

$L(\omega)$ - Transform of the source-time function

$N(\omega)$ - Medium amplitude response

$X(\omega)$ - Complex radiation pattern

After correcting the observed spectra for the instrument response and source-station travel path effects, we can describe the source as above, which varies as a step function in time whose strength is M. In fitting the observed source spectra, the seismic moment (M), strike (θ), dip (Δ), slip (λ), and depth (h) are varied.

We are primarily interested in the latter parameter, depth, because of its importance as a discriminant between underground nuclear explosions and earthquakes. Most explosions occur at quite shallow depths, generally less than 3 km. The maximum depth possible, from oil exploration experience, is about 8 km. Therefore, an event occurring from a region of interest with a depth of focus less than 10 km would invite extensive analysis

($M_s : m_b$, spectral ratios, etc.). In obtaining our depth estimate, a systematic spectral fitting procedure is applied; the source parameters are varied until the closest match of the theoretical spectral shape with the observed spectra is achieved.

A. THE VARIATION OF SOURCE SPECTRA WITH STRUCTURE

In a previous study (Turnbull, et. al. 1973), spectra and radiation patterns were theoretically generated for many source parameter combinations. One of the most important conclusions from this analysis was that the variation of source depth produces larger spectral change than the variation of any other source parameter. It is precisely this fact that enables our spectral fitting techniques to be sensitive to source depth.

Also, in this same study, the effect of the earth structure in the source region was examined by an indirect method in the analysis of the Southeastern Missouri Earthquake of October 21, 1965. Four earth structures were used in the spectral fitting procedure, their main differences lying in the upper 30 km of the crust. These structures had very little effect on our source depth determination, the minimum depth being 3 km and the maximum being 5 km. Therefore, for very shallow events, we concluded that geology made very little difference. In the present study, we arrive at this same conclusion (see discussion of CENAP+75 in Section III), but for events with focal depths approximately 10 km or greater, large structural changes have a significant effect on the focal depth (see discussion in Section III).

A direct confirmation of this effect was found by generating spectra for a structure representing some of the major fold systems in Central Asia (structure S-2) , and comparing this to spectra previously generated for a standard Gutenberg structure. Table A-1 lists the elastic parameters for these structures, with group velocity curves and spectra for Rayleigh and Love waves

given in Figures A-1 through A-9. Structure S-2 has the dominant characteristic of a very thick, high velocity crust. This results in spectral levels in the 10 to 20 second period range which are much higher than those for a Gutenberg structure. These spectral levels are not entirely unexpected, because a thicker, higher velocity crust should emphasize short period energy.

From this comparison, we see how important it is to have, at least, the correct gross structure in the source region. For example, if a Gutenberg structure was used incorrectly in place of the S-2 structure, a shallower focal depth would result from the fitting process. Conversely, if a Gutenberg structure was used incorrectly in place of a structure with low velocity upper layers (i. e., to model sediments), a deeper focal depth would be obtained.

B. DATA REQUIREMENTS FOR DEPTH DETERMINATIONS

Because of the need for 10 to 20 second period surface wave data with a fair degree of accuracy, it is important to examine the instrument response of the VLPE sites, ALPA, and NORSAR. Examples of the VLPE instrument response are given in Figures B-1 through B-4 for ALQ, TLO, EIL, and CHG. In most cases, the vertical component peaks between 35-40 second period, with the horizontal component peaking at a 5 to 10 second higher period. For ALPA and NORSAR, both the vertical and horizontal components peak at approximately 25 second period (see Figures B-5 and B-6). The period of peak response and the number of dB down from the peak at a 10 second period at each site is given in Table B-1. For the VLPE sites, we see that the 10 second period response of the vertical components is on the average 27 dB down from the peak, while ALPA is 20 dB down and NORSAR is 12 dB down. Obviously, for the purpose of determining depth using a spectral fit technique, NORSAR data should furnish the more accurate spectra. The question of spectral accuracy

becomes quite important when the response of the instrument is very low at the periods of interest, and the information becomes difficult to recover.

We see that modification of the VLPE instrument response to a NORSAR type response would be advantageous in the determination of depth from far-field surface waves. The only drawback to this modification would be if the long period information yielded by the VLPE instruments in their present configuration would be lost by making such a change. Studies show, though, that no information is lost. Massé (1970), in an analysis of seismic signals recorded on both a NORSAR type instrument and a VLPE type instrument placed at TFO, revealed that these systems yield equivalent information concerning long period energy in the signals. The response of these instruments is shown in Figure B-7; with comparative spectra of a typical event shown in Figure B-8.

Modification of the VLPE instrument response to a NORSAR type response can easily be accomplished by adjustment of the free period of the instrument (Sykes, 1971), which has a range of 0.033 Hz. In this way, the peak response can be adjusted to 0.04 Hz and have little change on the magnification of the system. Also, the long period detection levels can be retained by using the appropriate bandpass filter to eliminate microseismic noise in the analog recording.

SECTION III
ANALYSIS OF SEVERAL EURASIAN EVENTS

Keeping in mind the importance of accurate source structure and good data quality, seven Eurasian events were analyzed using teleseismic, long period surface wave data. The geographic locations of these events are shown in Figure III-1, with examples of the travel paths encountered to the VLPE stations, NORSAR, and ALPA also shown. These locations are shown again in Figure III-2a, but this time in relation to the major geologic features. Cross sections along the broken line DD' - D'D'' - D''D''' are shown in Figures III-2b, -2c, -2d, respectively, giving the major structural parameters.

The seven Eurasian events are discussed in two groups; those with and without an independent source depth estimate. For each event, the solution is presented in terms of the local structure, data quality, and travel path corrections. The procedure used in the analysis of the events was as follows:

- Data Handling - Applying a series of narrowband filters (see Appendix C), each component was analyzed for evidence of multipathing. At each period, group velocities were determined for each multipath, and then compared to the standard group velocity curves for the type of travel path encountered (see example in Appendix E). Estimating the correct multipath from this comparison, the spectra is then corrected for attenuation (as in Turnbull, et. al., 1973) and instrument response.
- Source Parameter Determination - Spectral fitting procedures (Turnbull, et. al., 1973) are then applied to the corrected

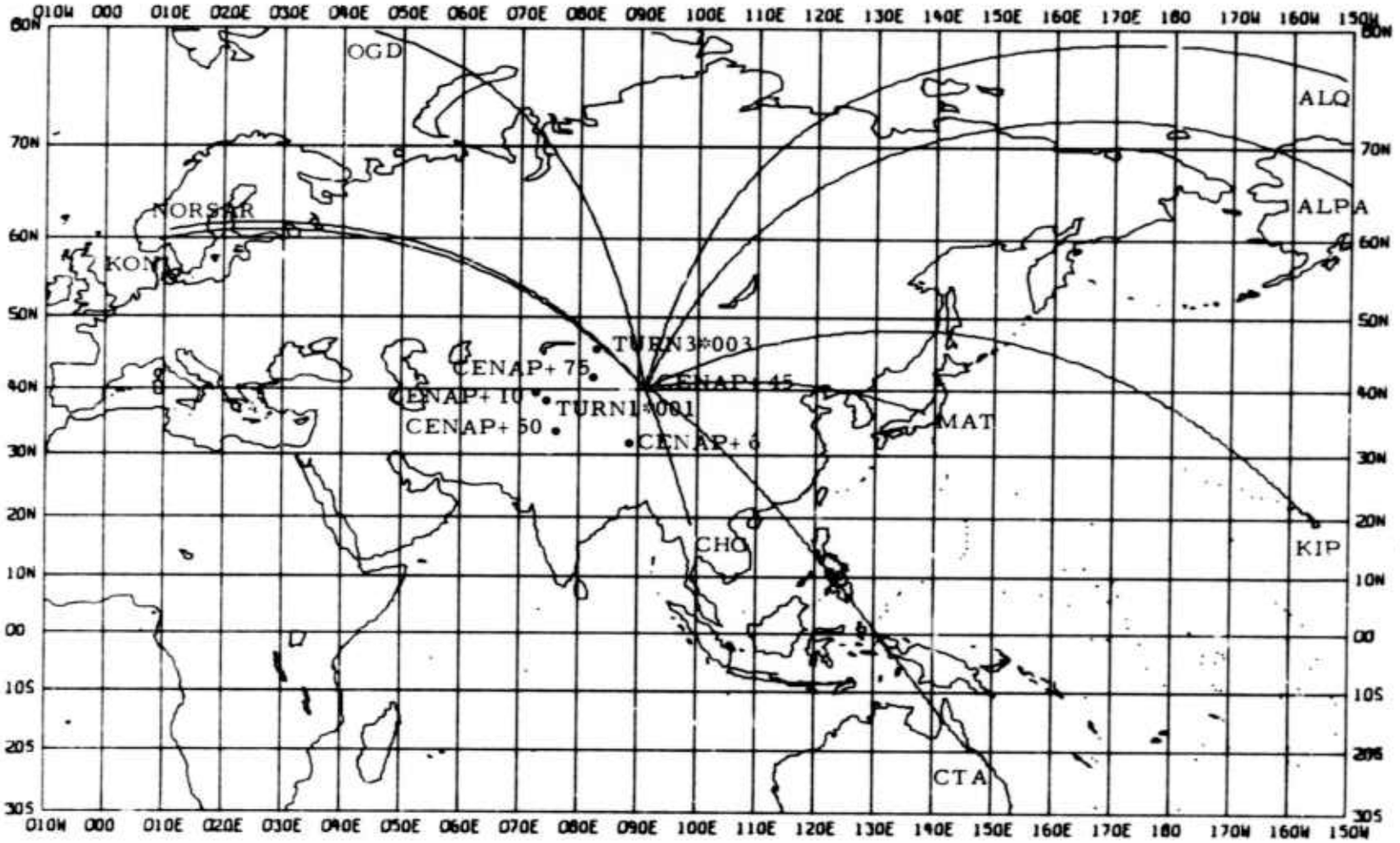

MILLER MODIFIED MERCATOR PROJECTION
MAP SCALE: 0.400 IN./ 10 DEG. LONGITUDE

FIGURE III-1

MAP OF EURASIAN EVENTS WITH TRAVEL PATHS TO RECORDING STATIONS

FIGURE III-2a

EURASIAN EVENTS AND LOCAL GEOLOGY

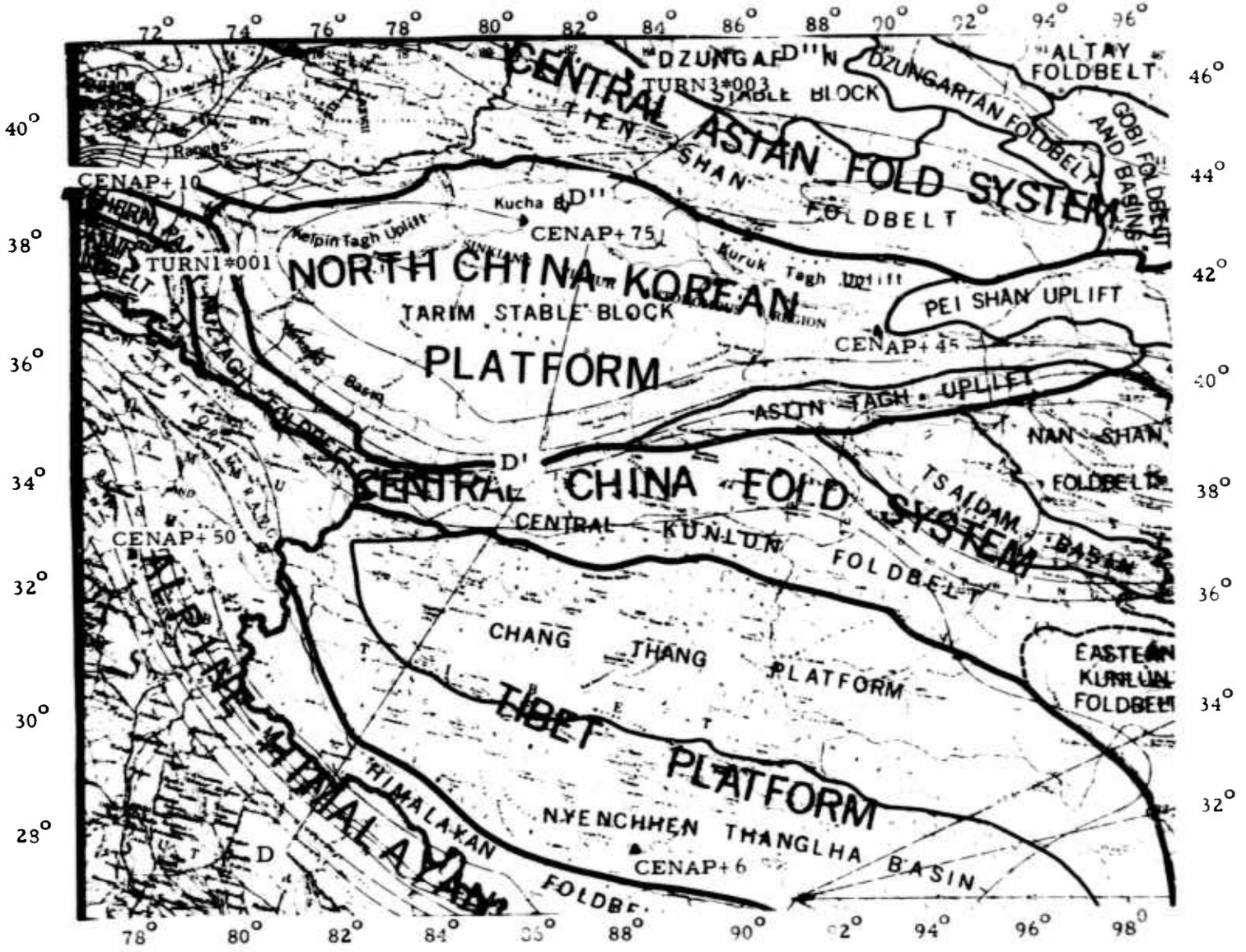

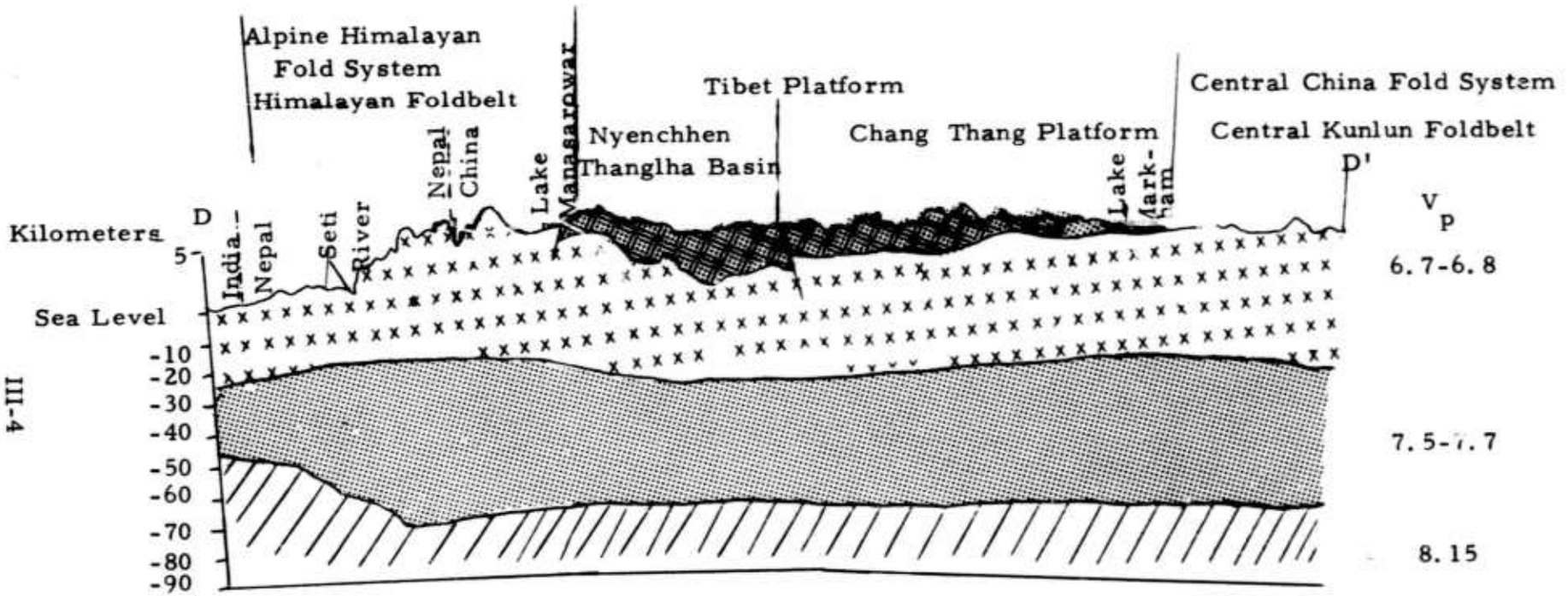

FIGURE III-2b

PROFILE D D' - THE TIBET PLATFORM

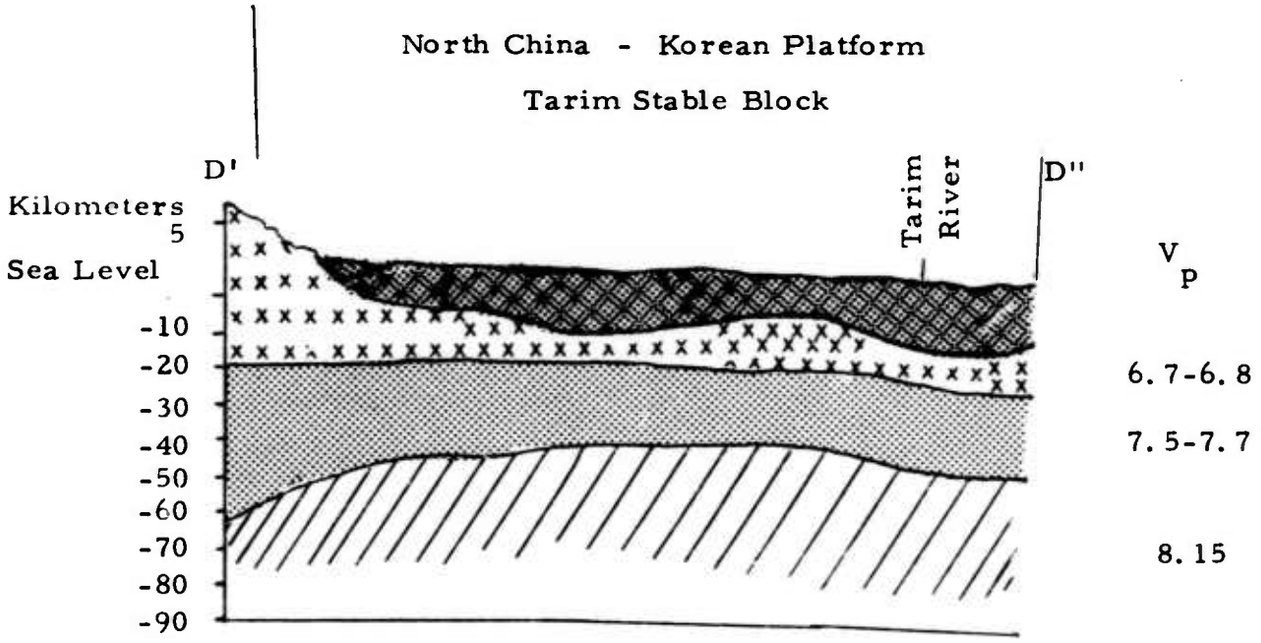

FIGURE III-2c

PROFILE D' D'' - THE NORTH CHINA-KOREAN PLATFORM

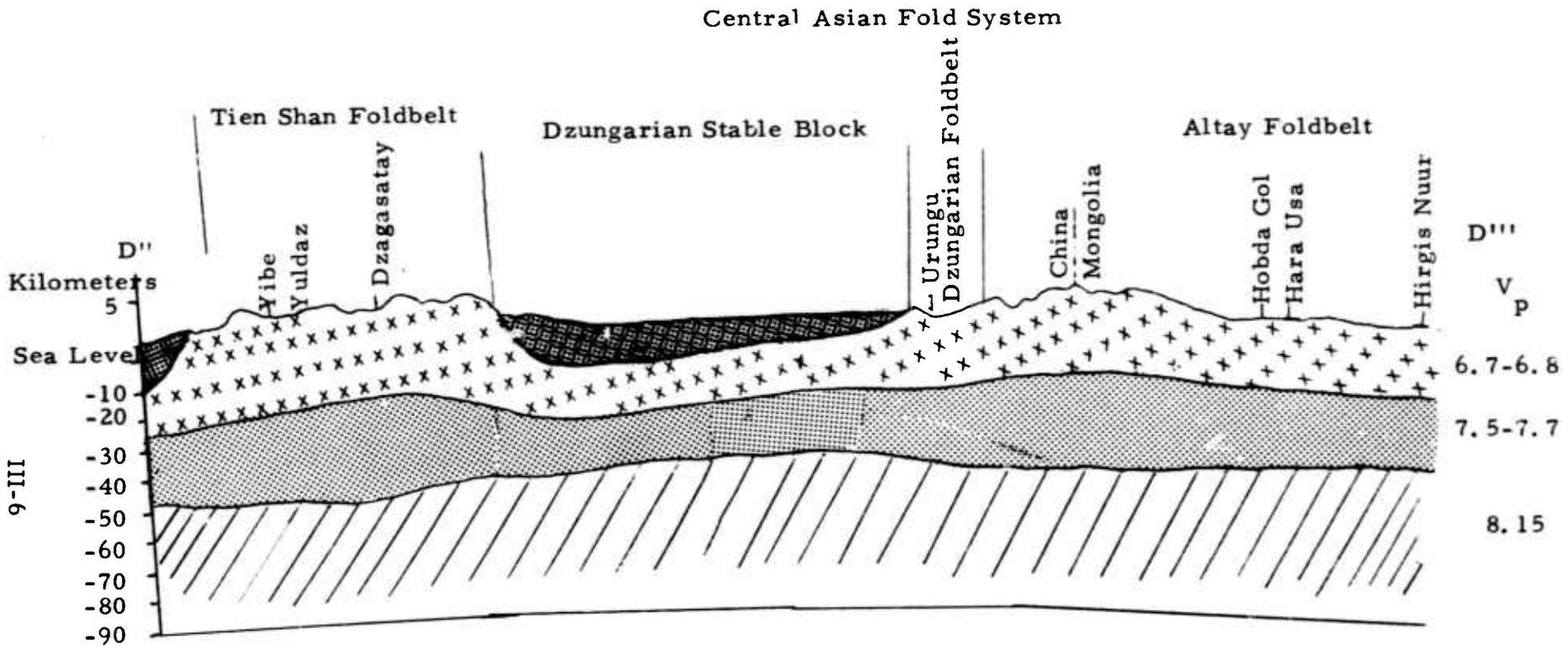

FIGURE III-2d

PROFILE D'' D''' - THE CENTRAL ASIAN FOLD SYSTEM

spectra, using a theoretical model placed in a source structure closely approximating the known geology. If a depth estimate is known from independent evidence, the structural parameters are perturbed within reasonable limits until the depth obtained from the fitting procedure is in close agreement with the known depth. The final structure used in this procedure is then applied to events in the same region where no source depth is known.

After discussing each event individually, their source parameter estimations are summarized; in particular, our seismic moment estimate in relation to bodywave magnitude.

A. ANALYSIS OF EURASIAN EVENTS WITH KNOWN SOURCE DEPTH

Four events were analyzed which had independent estimates of the source depth. The first three had their depth determined from the multiple station observations by NOAA of depth phases (CENAP+45, TURN3*003, TURN1*1), while the fourth (CENAP+50) was determined from analysis of the relative arrivals of several bodywave phases. The depths of the first three events are considered quite reliable, and with their relatively large magnitudes they can be considered the best data from which to develop spectral fitting procedures.

1. LX+CENAP+45: The event identification and recording station data are listed in Table III-1. Depth phases yielded a 13 km depth. The event occurred in Southern Sinkiang Province; more precisely, at Lop Nor. The travel paths to the recording stations are discussed in detail in Appendix E. The source structure used was a basic Gutenburg-Bullen, because the event lies on the North China - Korean Platform. The spectral fits are

TABLE III-1

EVENT IDENTIFICATION: LX+CENAP+45

Event I. D. : LX+CENAP+45

Location: 40.4N Lat., 91.1E Long.

Magnitude: m_b = 5.1

Date: 1/15/73

Origin Time: 12:55:44

Recording Station (No. -Station)	Location		Azimuth from Source (degrees)	Δ (km)
	Lat.	Long.		
2-CHG	18.8N	99.0E	160.2	2511.5
6-KON	59.7N	9.6E	-39.4	5794.1
8-KIP	21.4N	158.0W	60.4	10127.0
9-ALQ	34.9N	106.5W	14.7	11471.5
ALPA	36.6N	138.3E	23.3	7242.3
NORSAR	60.8N	10.9E	-38.2	5688.2

shown in Figures III-3a, -3b. For NORSAR and ALPA, both Rayleigh and Love wave data was used, while for the VLPE stations we used only the Rayleigh wave data. As will be seen in the discussion of these events, VLPE Love wave data was considered unreliable because of the large instrument response correction and the usually severe multipathing.

The spectral fit yields a depth of approximately 8 km, with a dip-slip mechanism (see Figure III-4). It is felt that knowledge of the sediment thickness at Lop Nor, and its inclusion in our source structure, would yield a source depth quite close to that determined from bodywave phases.

2. LX*TURN3*003: Table III-2 lists the event identification and recording station data. Depth phases yield a source depth of 26 km. The event occurred in the Central Asian Fold System, and structure S-0A (see Appendix A) was found to be a good approximation. This structure's main feature is a thinner sedimentary layer and higher velocity layers in the upper 50 km than the Gutenburg-Bullén structure. Only NORSAR data was used in the spectral fit because of the overall poor quality of the VLPE data that was available. ALPA data were not available at the time of processing. For the VLPE stations CTA, KIP, and OGD, multipathing was a severe problem; KON essentially duplicated the NORSAR data.

The spectral fit can, at best, be said to 'average' the observed spectra (Figure III-5). The optimal solution yielded a nearly vertical strike slip fault mechanism with an approximate source depth of 22 km (see Figure III-6). A one station determination such as this can only be thought of as a rough solution.

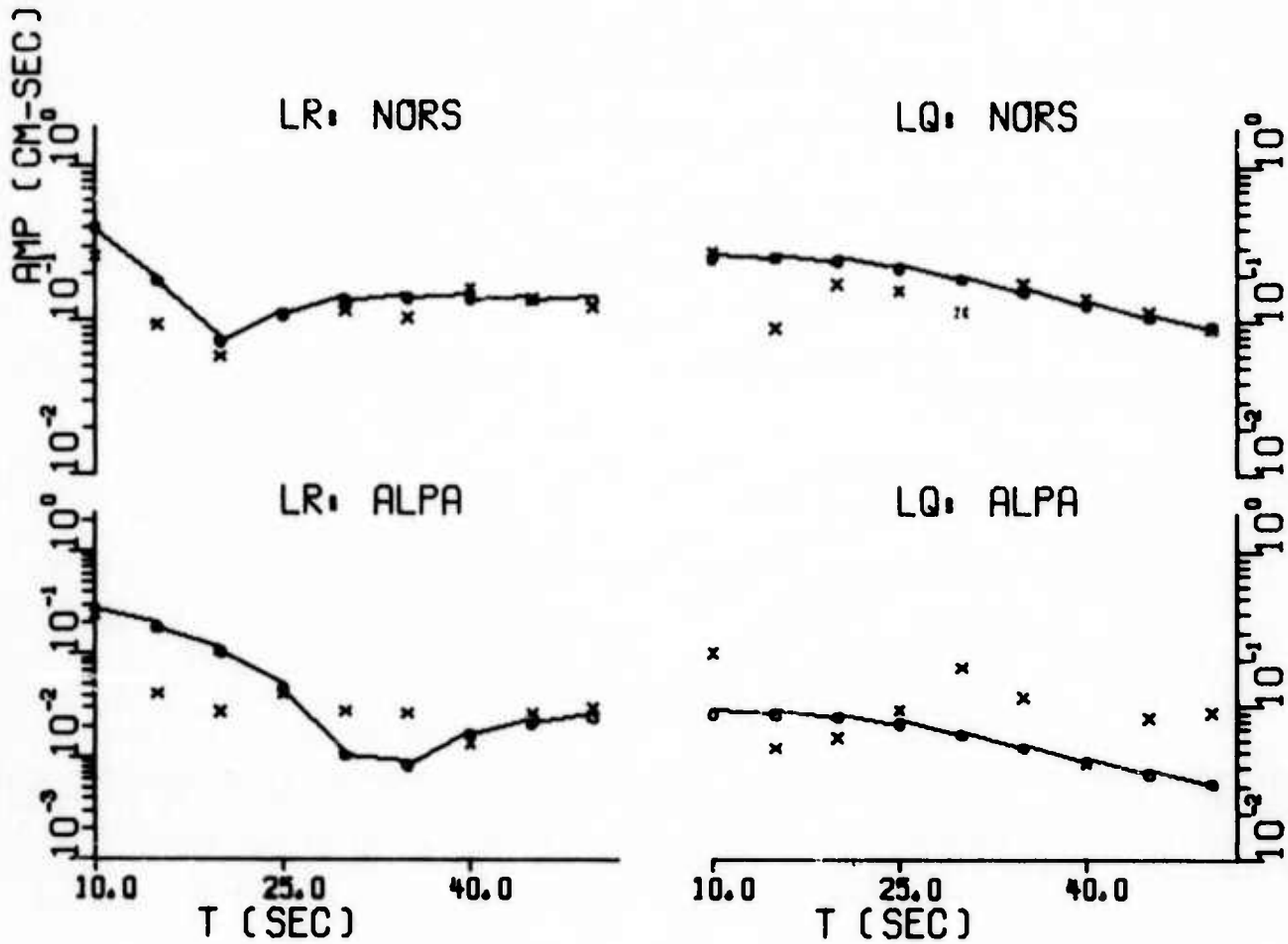

FIGURE III-3a

AMPLITUDE SPECTRA
LX+CENAP+45

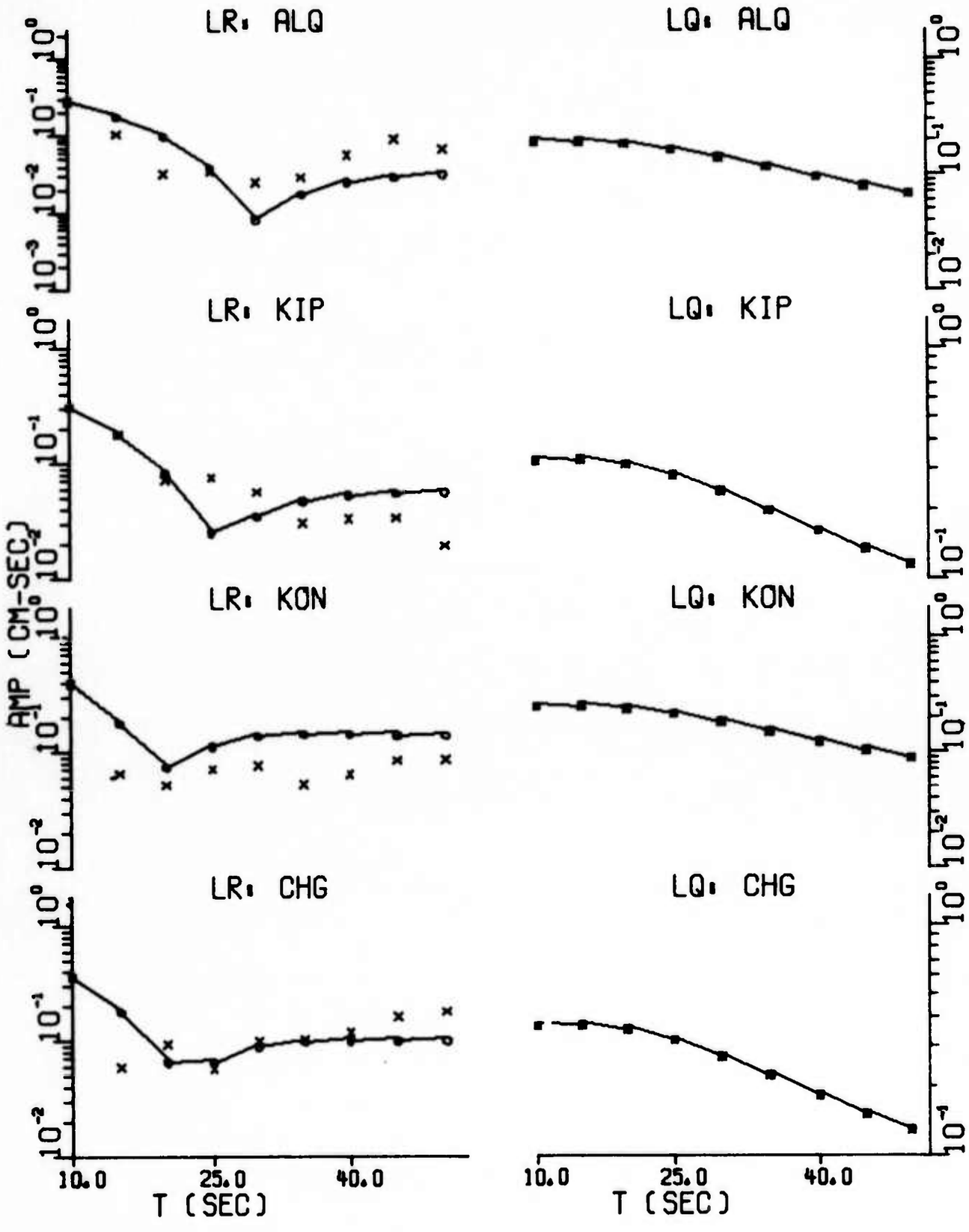

FIGURE III-3b

AMPLITUDE SPECTRA
LX+CENAP+45

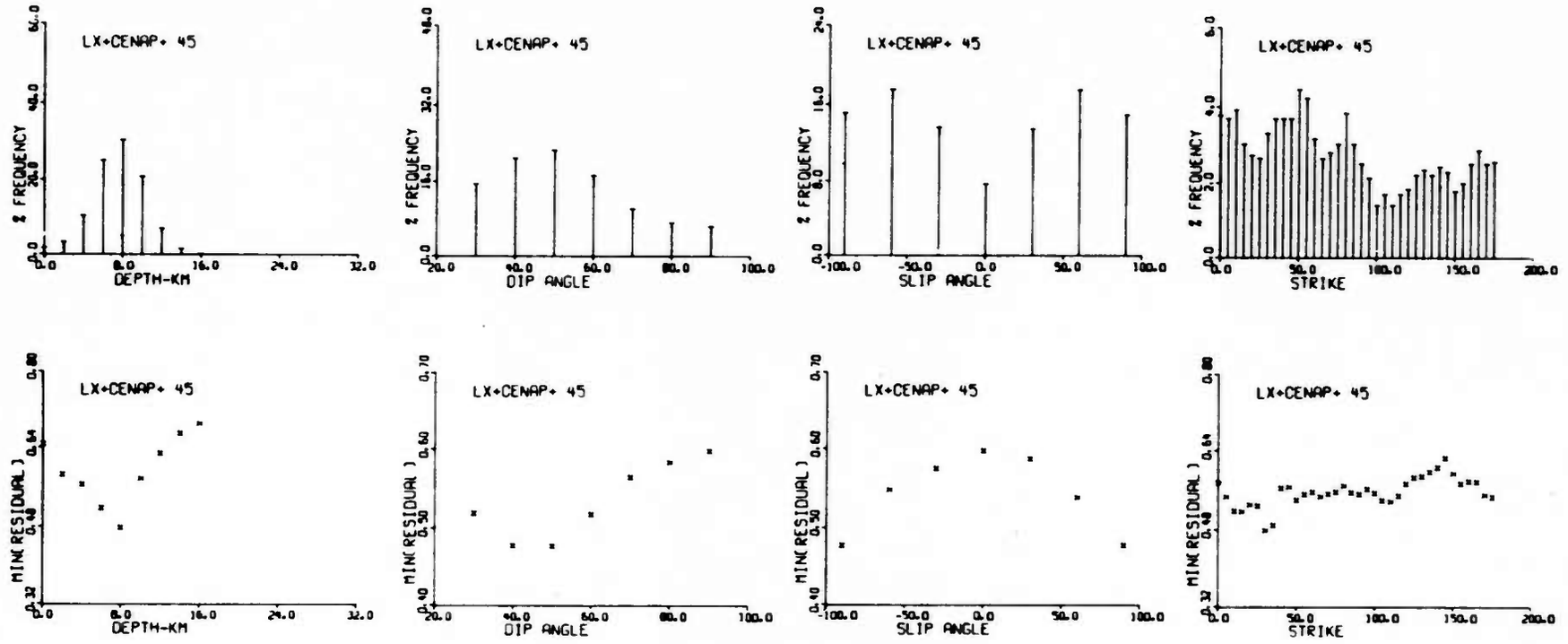

FIGURE III-4

SOURCE PARAMETER DISTRIBUTIONS FOR LX+ CENAP+ 45

TABLE III-2

EVENT IDENTIFICATION: LX*TURN3*003

Event I. D. : LX*TURN3*003

Location: 44.1N Lat., 83.6E Long.

Magnitude: m_b = 5.8

Date: 6/2/73

Origin Time: 23:57:04

Recording Station (No. -Station)	Location		Azimuth from Source (degrees)	Δ (km)
	Lat.	Long.		
1-CTA	20.1S	146.3E	123.0	9540.7
6-KON	59.7N	9.6E	-42.9	5077.8
7-OGD	41.1N	74.6E	-16.3	10323.9
8-KIP	21.4N	158.0W	55.1	10431.4
NORSAR	60.8N	10.9E	-41.5	4976.5

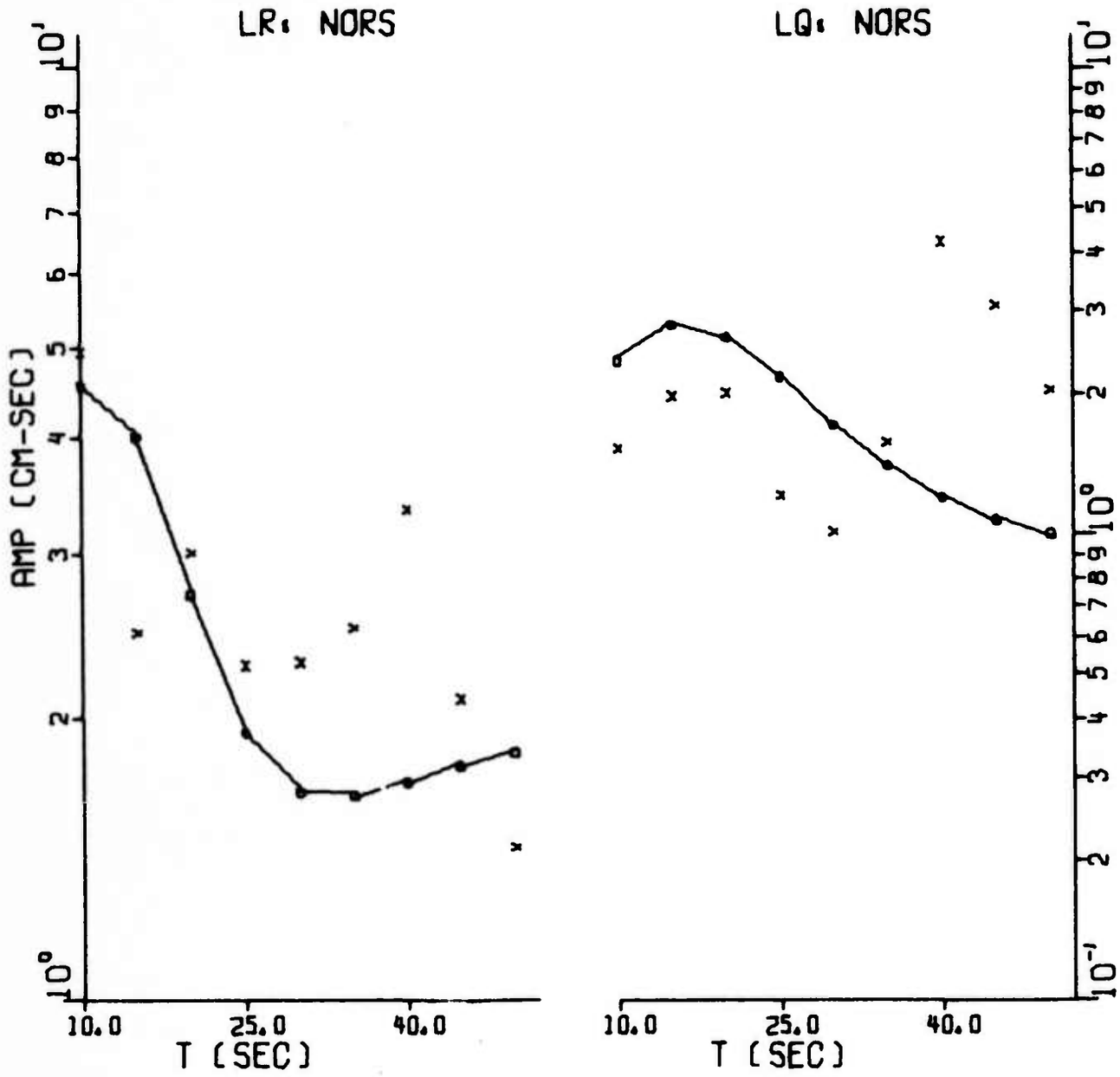

FIGURE III-5

AMPLITUDE SPECTRA
LX*TURN3*003

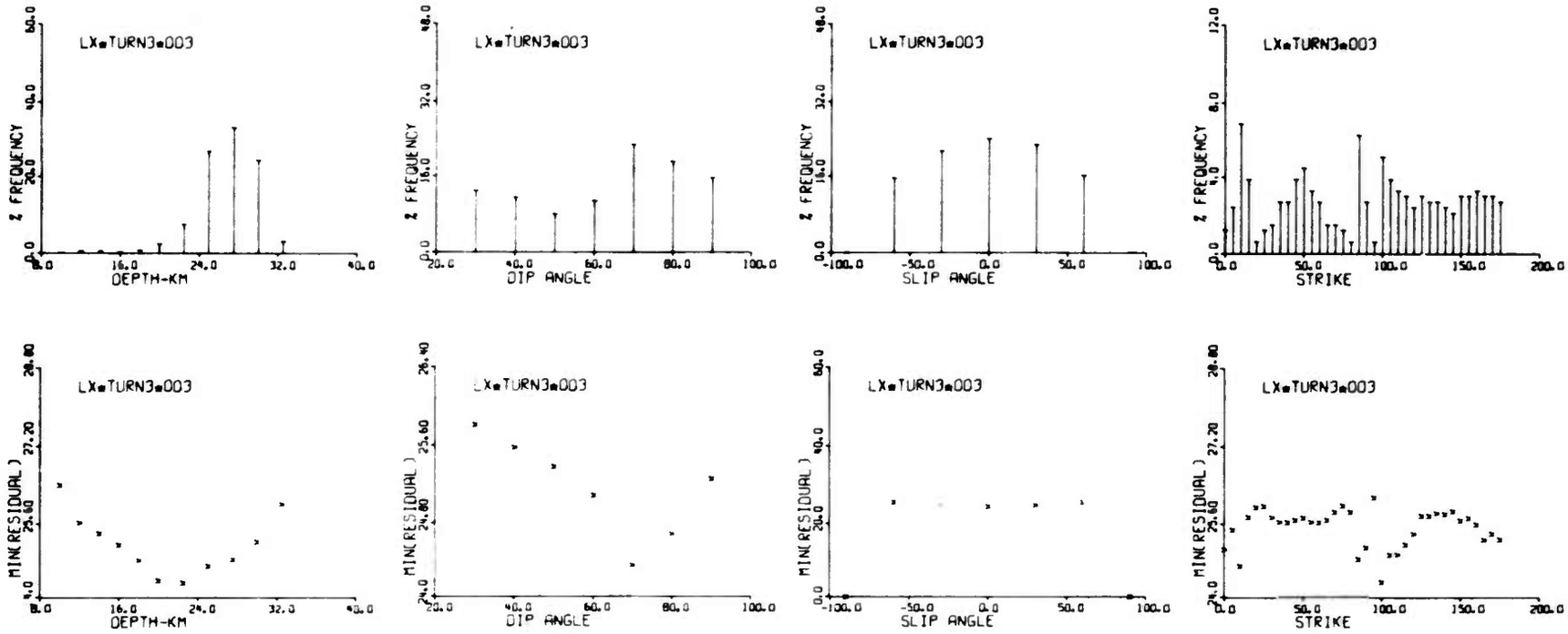

FIGURE III-6

SOURCE PARAMETER DISTRIBUTIONS FOR LX*TURN3*003

3. LX*TURN1*001: As a contrast to the two fairly shallow events discussed previously, an event was chosen with a known deep focus (123 km - from depth phases). The event identification and available recording station information are listed in Table III-3. The first structure used in the fitting process was the standard Gutenburg-Bullen. The data available was again quite sparse, with CHG and MAT of very poor quality, and KON essentially duplicating NORSAR.

The spectral fit (Figure III-7), while quite good above 20 seconds period, becomes succeedingly worse below this period. The optimal solution yielded a moderatly dipping strike-slip fault, with a depth of 125 km (Figure III-8). While this result is in close agreement with the bodywave data, we consider this agreement fortuitous. High quality spectra and several azimuths are needed. Also, the structure used is only a first approximation. The location places the event in a foldbelt system where structural parameters were not available. Using foldbelt structures from the D''D''' cross-section, a depth greater than 150 km was obtained.

4. LX+CENAP+50: This event differs from the first three in that a bodywave depth estimate was obtained from body phase arrival times rather than from depth phase. From this method, a source depth of 42 km was obtained. The event identification and available recording station information are listed in Table III-4. The event occurred in the Alpine-Himalayan fold system, and a structure was derived from the DD' profile. This structure's main feature (S-2: see Appendix A) is an abnormally thick (70 km), high velocity crust. Again, only NORSAR data was used in the spectral fit because of the poor quality of the VLPE data below 20 seconds period.

TABLE III-3

EVENT IDENTIFICATION: LX*TURN1*001

Event I. D. : LX*TURN1*001 Location: 38.3N Lat., 73.9E Long. Magnitude: m_b = 5.3 Date: 3/26/73 Origin Time: 07:58:42				
Recording Station (No. -Station)	Location		Azimuth from Source (degrees)	Δ (km)
	Lat.	Long.		
2-CHG	18.8N	99.0E	124.7	3250.5
6-KON	59.7N	9.6E	-40.1	5018.1
11-MAT	36.5N	138.2E	70.9	5573.2
NORSAR	60.8N	10.9E	-38.5	4945.0

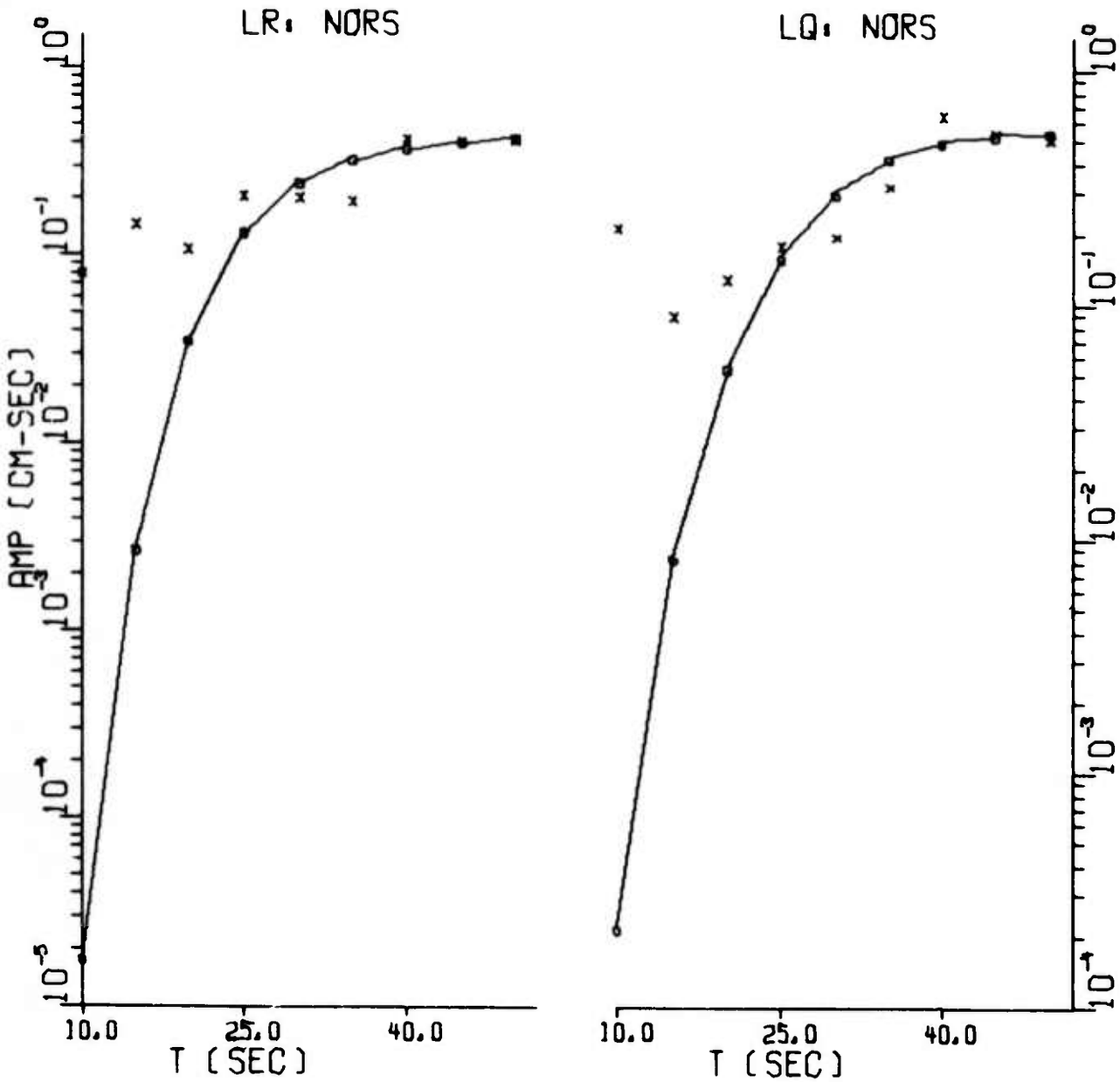

FIGURE III-7

AMPLITUDE SPECTRA
LX*TURN1*001

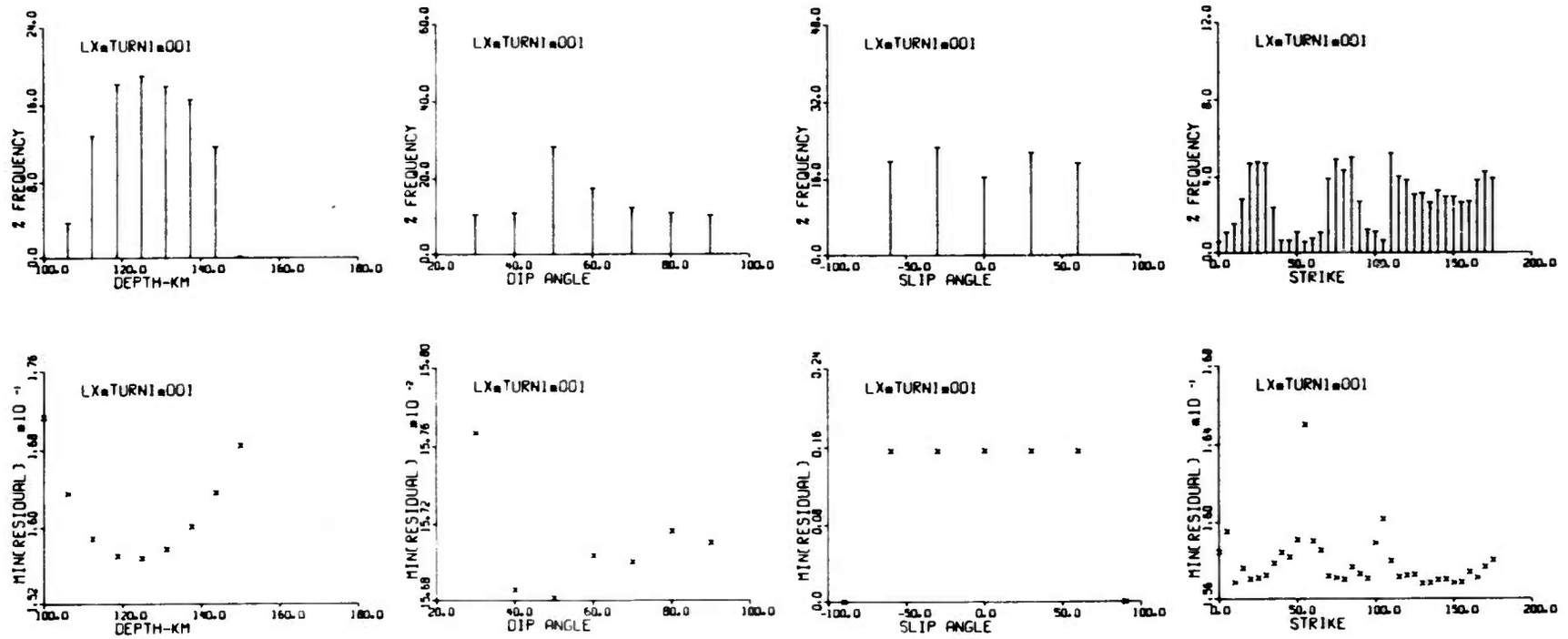

FIGURE III-8

SOURCE PARAMETER DISTRIBUTIONS FOR LX*TURN1*001

TABLE III-4

EVENT IDENTIFICATION: LX+CENAP+50

Event I. D. : LX+CENAP+50
Location: 33.2N Lat., 75.6E Long.
Magnitude: m_b = 5.1
Date: 1/16/73
Origin Time: 21:31:26

Recording Station (No. -Station)	Location		Azimuth from Source (degrees)	Δ (km)
	Lat.	Long.		
2-CHG	18.8N	99.0E	118.8	2813.9
6-KON	59.7N	9.6E	-37.2	5562.7
8-KIP	21.4N	158.0W	51.0	11708.9
9-ALQ	34.9N	106.5W	1.9	12458.2
NORSAR	60.8N	10.9E	-35.1	5586.4

The spectral fit is shown in Figure III-9, and is quite good, especially for the Love waves. The optimal solution yielded a depth of 57 km, with 90% of the solutions lying from 45 km to 58 km (Figure III-10). This estimate of the depth is considered reasonable in the absence of depth phase information.

B. ANALYSIS OF EURASIAN EVENTS WITH UNKNOWN SOURCE DEPTH

Three events were analyzed which did not have an independent source depth estimate. We did, though, have some control on our solution, through the use of structures which proved successful in the analysis of events with known source depths.

1. LX+CENAP+6: The event identification and available recording station information are listed in Table III-5. Four VLPE stations yielded relatively good Rayleigh wave spectra. The event occurred on the southern edge of the Tibet Planform (Figure III-2a) whose structural cross section is shown in profile DD' (Figure III-2b). Hence, structure S-2 was used for the theoretical source.

   The spectral fit is shown in Figure III-11, which is quite good except for that at KIP. Theoretical Love wave curves, which were generated using the best fit source parameters, are also shown. In Figure III-12 is shown the optimal solution, which is a strike slip fault mechanism with a depth of 16 km. Of the models generated, 91 per cent had a focal depth between 6 km and 18 km.

   A measure of the structural effect on the source depth was obtained by fitting the spectra using a Gutenburg structure.

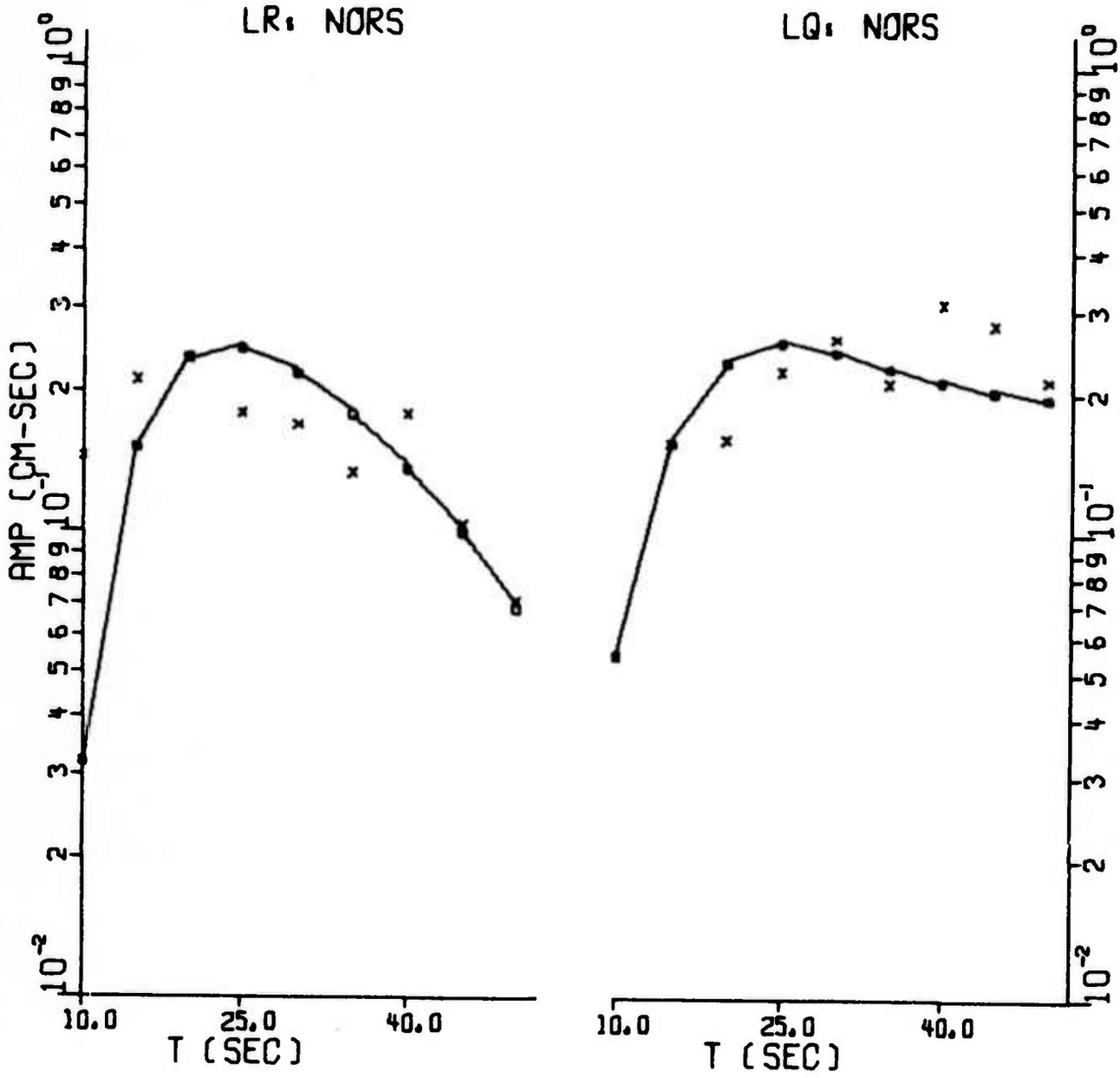

FIGURE III-9

AMPLITUDE SPECTRA
LX+CENAP+50

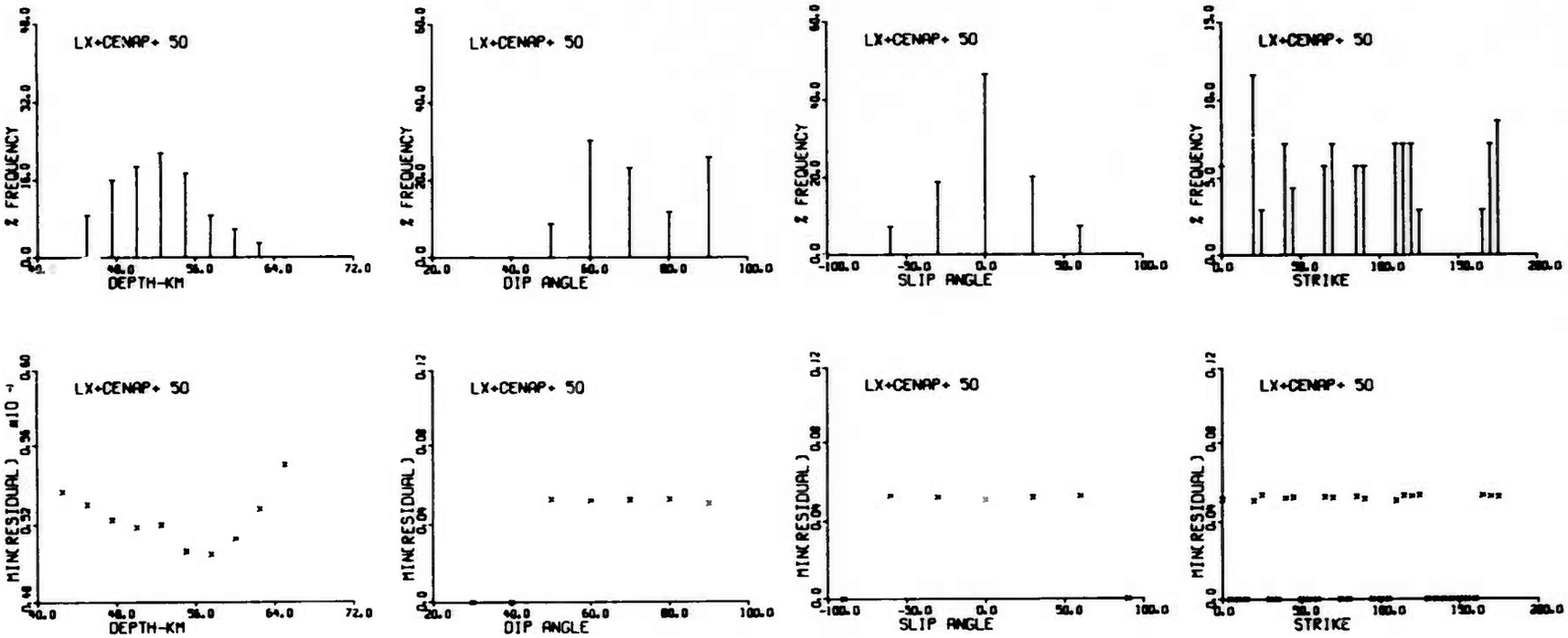

FIGURE III-10

SOURCE PARAMETER DISTRIBUTIONS FOR LX+ CENAP+ 50

TABLE III-5

EVENT IDENTIFICATION: LX+CENAP+6

Event I. D. : LX+CENAP+6 Location: 31.2 N Lat., 88.1E Long. Magnitude: m_b = 5.2 Date: 1/2/73 Origin Time: 22:27:19				
Recording Station (No. -Station)	Location		Azimuth from Source (degrees)	Δ(km)
	Lat.	Long.		
2-CHG	18.8N	99.0E	138.9	1757.3
5-EIL	29.6N	35.0E	-77.7	5062.1
6-KON	59.7N	9.6E	-35.9	6438.0
8-KIP	21.4N	158.0W	59.1	10876.7

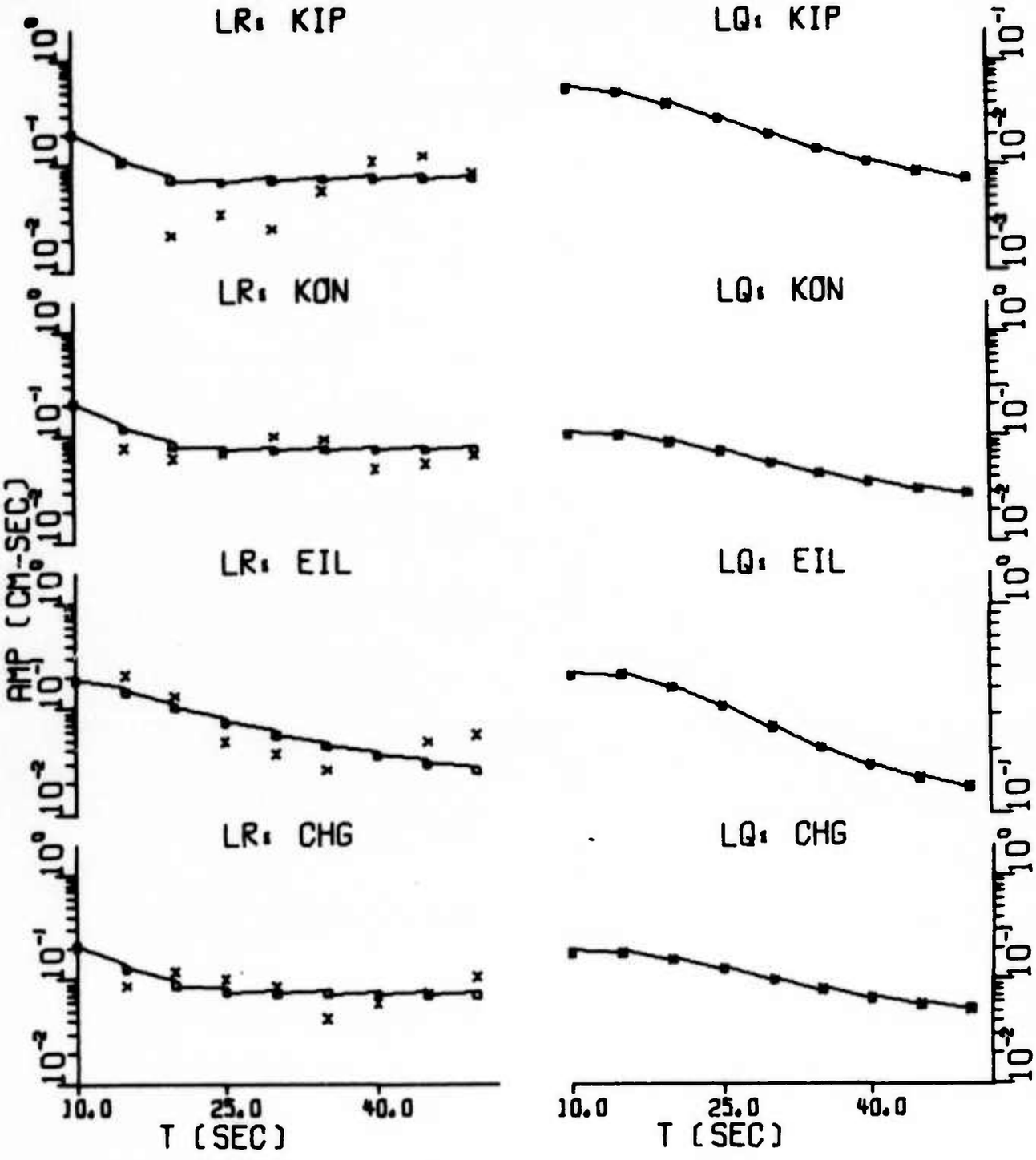

FIGURE III-11

AMPLITUDE SPECTRA
LX+CENAP+6

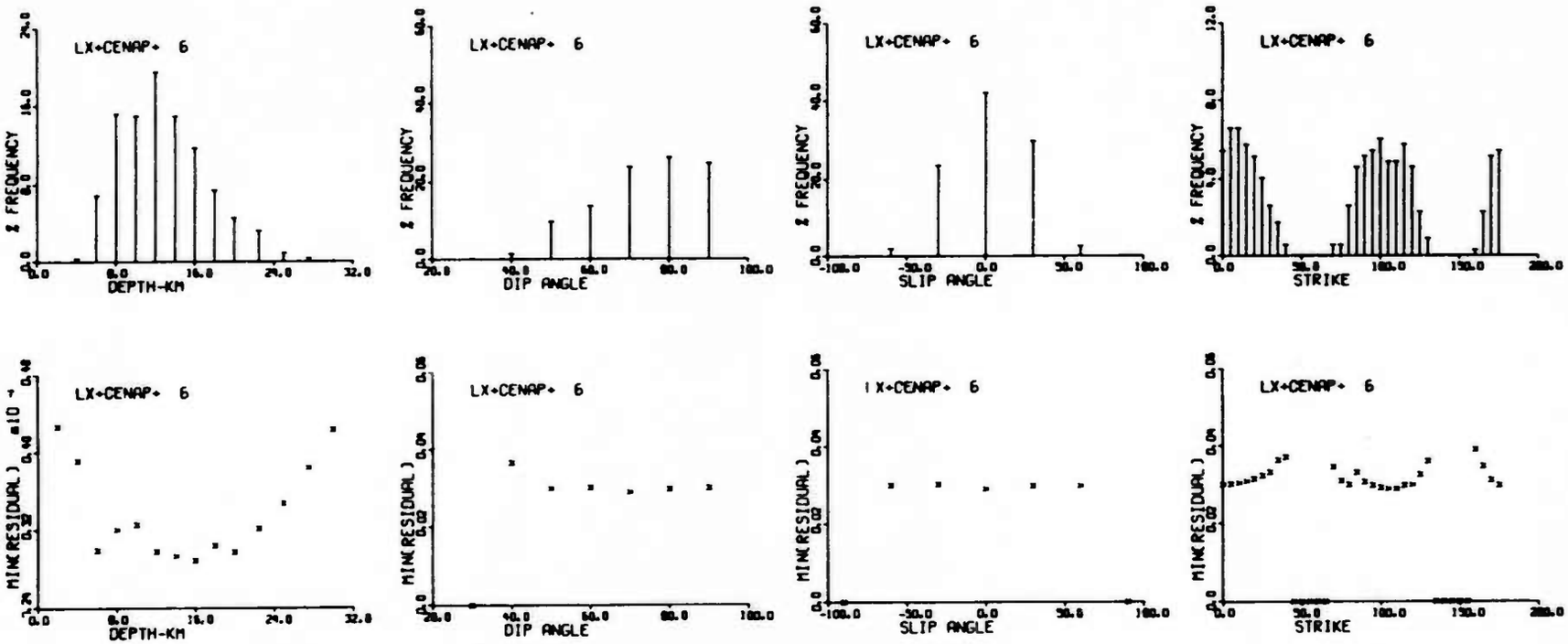

FIGURE III-12

SOURCE PARAMETER DISTRIBUTIONS FOR LX+ CENAP+ 6

This resulted in a 10 km focal depth, because of the lower velocity crustal layers (see Section II).

2. LX+CENAP+10: This event was located within a few degrees of LX*TURN1*001 (see Table III-6). Therefore, a standard Gutenburg-Bullen structure was used because of its successful use in the latter event. Both Rayleigh and Love wave data were used from five VLPE stations (EIL, KON, KIP, ALQ, MAT), with a sixth (CHG) having only Rayleigh waves of reasonable quality. The use of both surface wave components was felt to be justified because of the appearance of the data, a direct result of the large m_b (5.5).

In Figures III-13a, -13b, are shown the spectral fits, which are of mixed quality. While those at ALQ and MAT could be considered good, the fits at KON and EIL can be considered, at best, average. The optimal solution is shown in Figure III-14, yielding a strike-slip fault with a 63 km focal depth. It can be inferred from this result and that of LX*TURN1*001 that the source region is one of deep tectonic activity.

3. LX+CENAP+75: The identification and available recording station information for this last event is given in Table III-7. The Rayleigh wave spectra from four VLPE stations were used in the fitting process. The event occurred near the center of the North China-Korean Platform (Figure III-2a) whose structural cross section is shown in profile D'D'' (Figure III-2c). A slightly modified Gutenburg-Bullen structure was used for the theoretical source.

The spectral fit for the Rayleigh waves, along with the theoretical Love wave curves, is shown in Figure III-15. This

TABLE III-6

EVENT IDENTIFICATION: LX+CENAP+10

Event I. D. : LX+CENAP+10

Location: 39.1N Lat., 71.9E Long.

Magnitude: m_b = 5.5

Date: 1/3/73

Origin Time: 14:31:04

Recording Station (No. -Station)	Location		Azimuth from Source (degrees)	Δ (km)
	Lat.	Long.		
2-CHG	18.8N	99.0E	123.0	3444.7
5-EIL	29.6N	35.0E	-96.0	3534.4
6-KON	59.7N	9.6E	-40.7	4838.6
8-KIP	21.4N	158.0W	47.1	11537.3
9-ALQ	34.9N	106.5W	-1.4	11805.1
11-MAT	36.5N	138.2E	70.6	5711.7

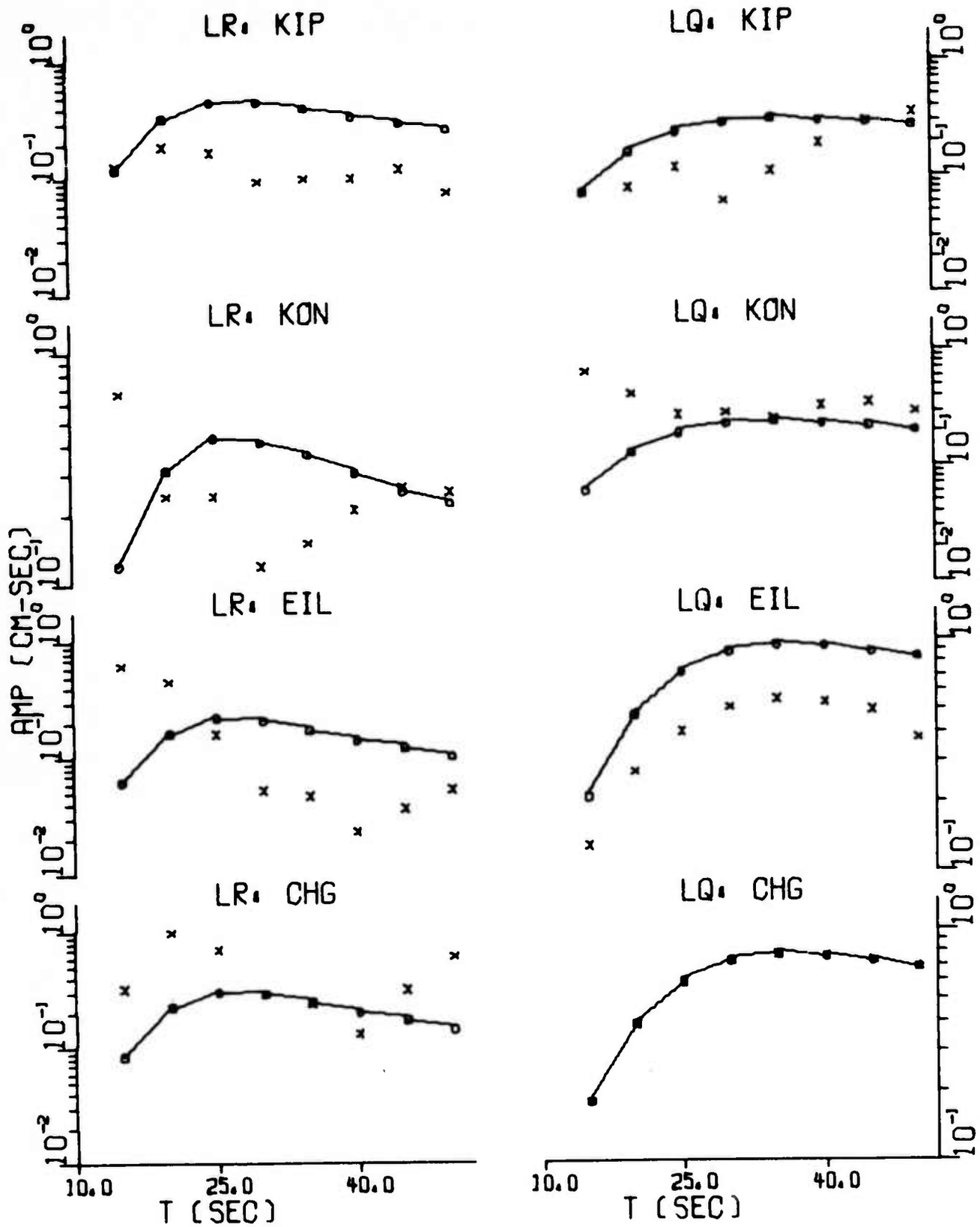

FIGURE III-13a

AMPLITUDE SPECTRA
LX+CENAP+10

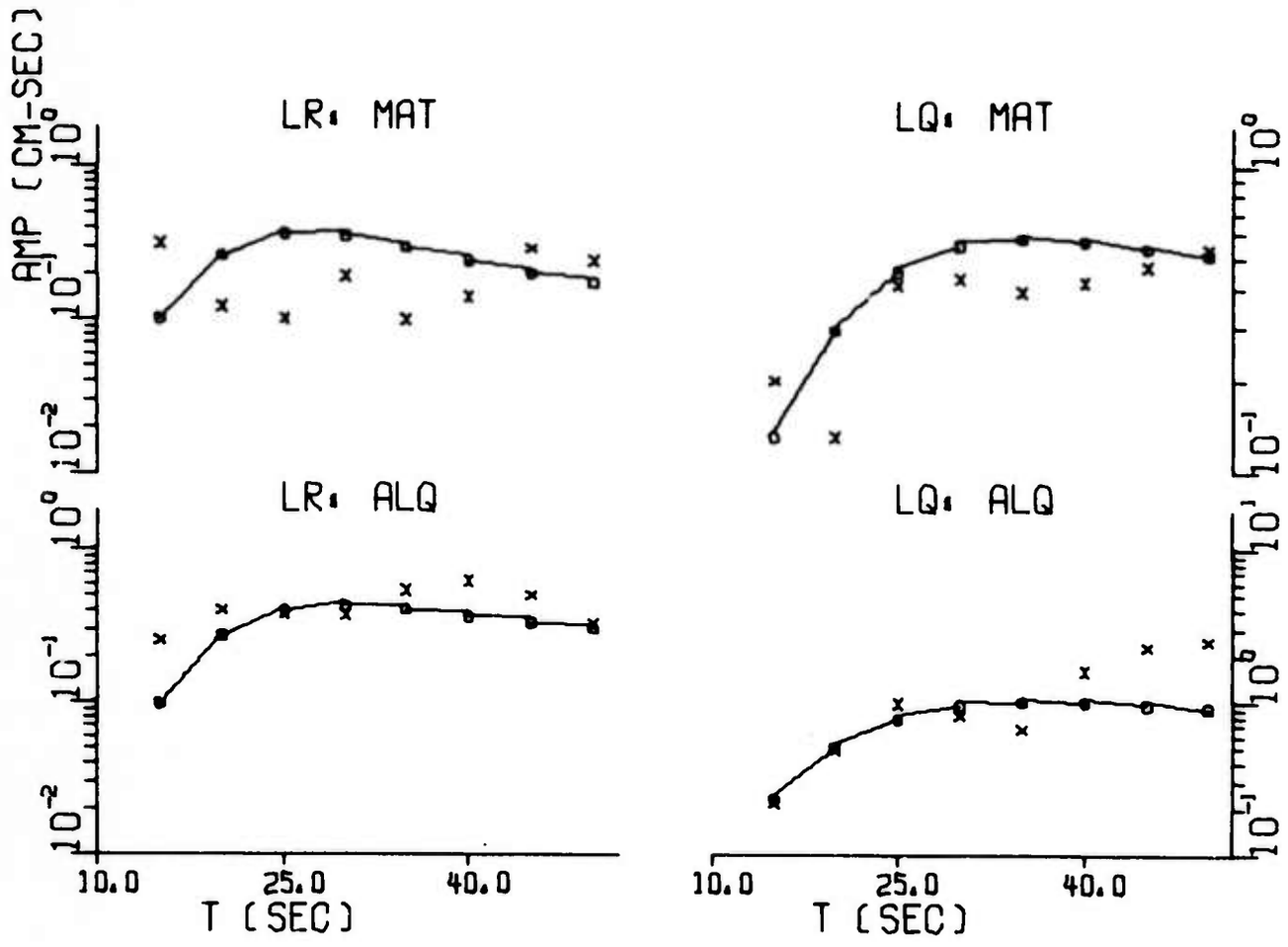

FIGURE III-13b

AMPLITUDE SPECTRA
LX+CENAP+10

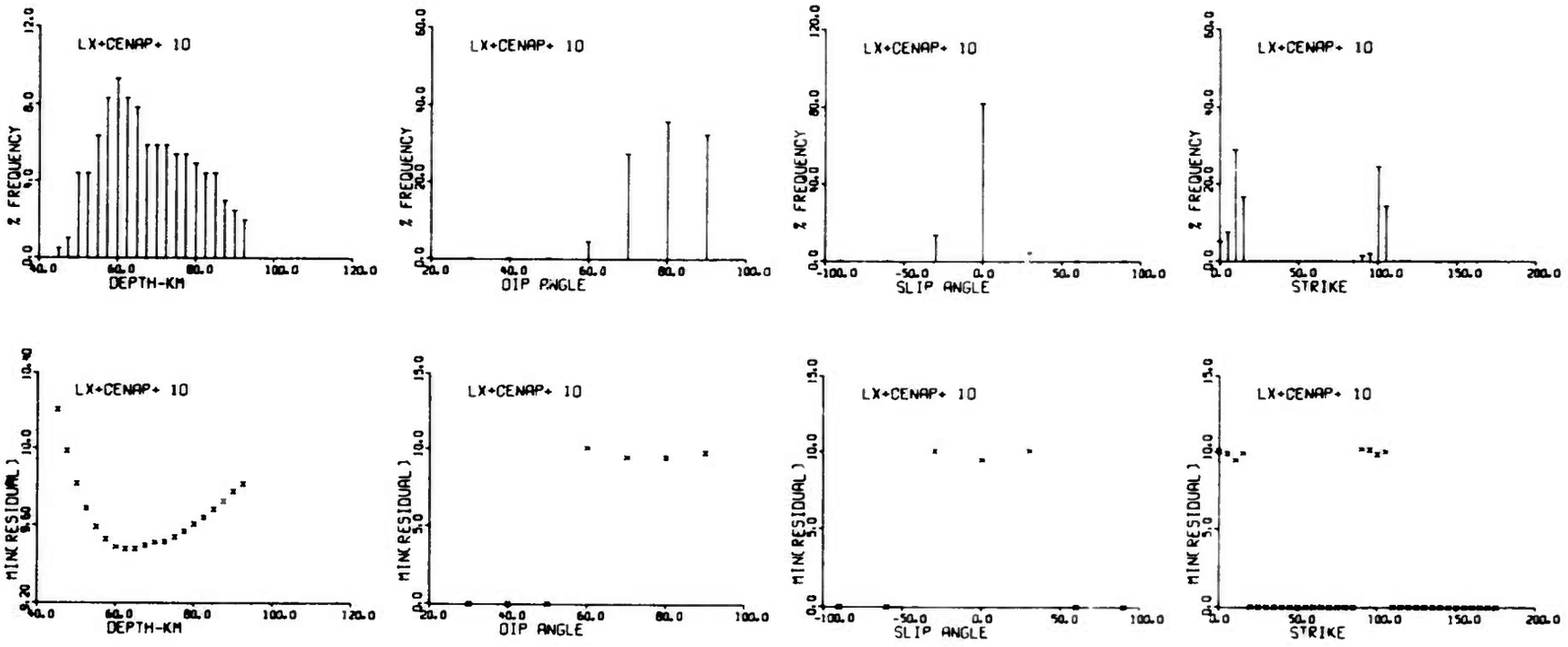

FIGURE III-14

SOURCE PARAMETER DISTRIBUTIONS FOR LX+ CENAP+10

TABLE III-7

EVENT IDENTIFICATION: LX+CENAP+75

Event I. D. : LX+CENAP+75
Location: 41.0N Lat., 82.2E Long.
Magnitude: m_b = 5.1
Date: 1/24/73
Origin Time: 03:20:20

Recording Station (No. -Station)	Location		Azimuth from Source (degrees)	Δ(km)
	Lat.	Long.		
2-CHG	18.8N	99.0E	142.0	2935.7
6-KON	59.7N	9.6E	-41.2	5256.5
8-KIP	21.4N	158.0W	54.3	10724.3
10-ZLP	16.5S	68.1W	-54.6	16082.6

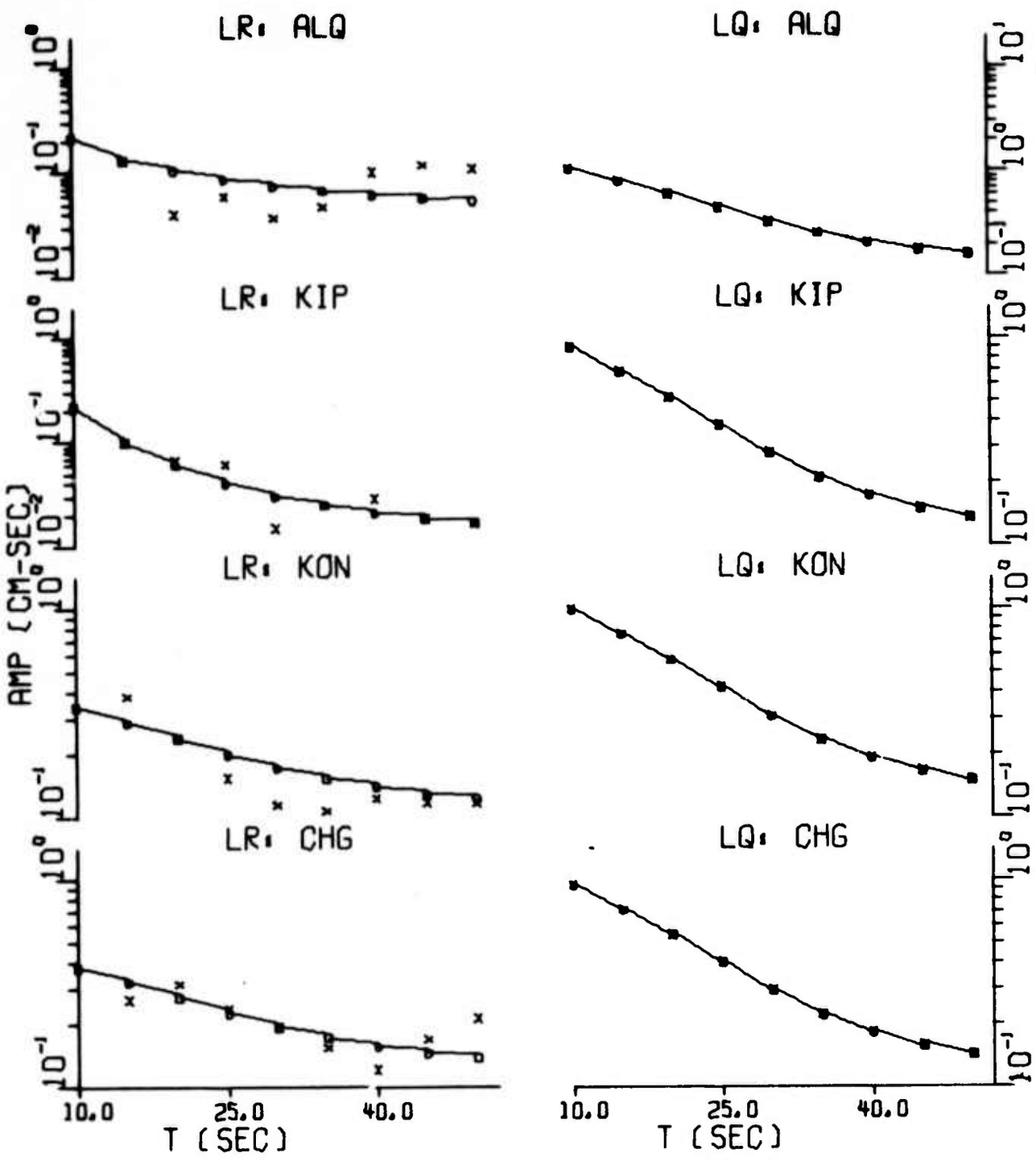

FIGURE III-15

AMPLITUDE SPECTRA
LX+CENAP+75

fit is quite good for all stations. The optimal solution (Figure III-16) describes a very shallow focus event (2 km) with a moderate dip angle (60^{o}) and low slip angle (30^{o}). The structural effect on this solution is quite similar to that encountered previously for the Southeastern Missouri Earthquake written about previously (Turnbull, et. al., 1973). Both high and low velocity crustal models were applied to the data, resulting in very little change in the depth ($\pm$ 1 km). This implies that little change in spectral shape occurs for shallow depths between different source structures in the frequency range of interest.

C. SUMMARY OF PARAMETER ESTIMATES

A summary of optimal solutions for the seven Eurasian events that have been discussed is given in Table III-8, with the statistics of these solutions listed in Table III-9. From this latter table, we see the following properties of the solutions:

- In general, we can usually determine a reasonably probable range of focal depth values with a high degree of confidence. For very shallow events, this range is fairly narrow (less than 5 km), while for deep events this range is quite broad (greater than 15 km).
- The probable range of the dip and slip values is more ambiguous than that for focal depth, and the probable range for the strike direction is in many cases unknown. This latter result is due to poor azimuthal coverage.

Finally in Figure III-17, we have plotted the seismic moment (M_o) versus bodywave (m_b) magnitude for each event in relation to the ω^2-model determined by Tsai (1972b). We see that there is close agreement,

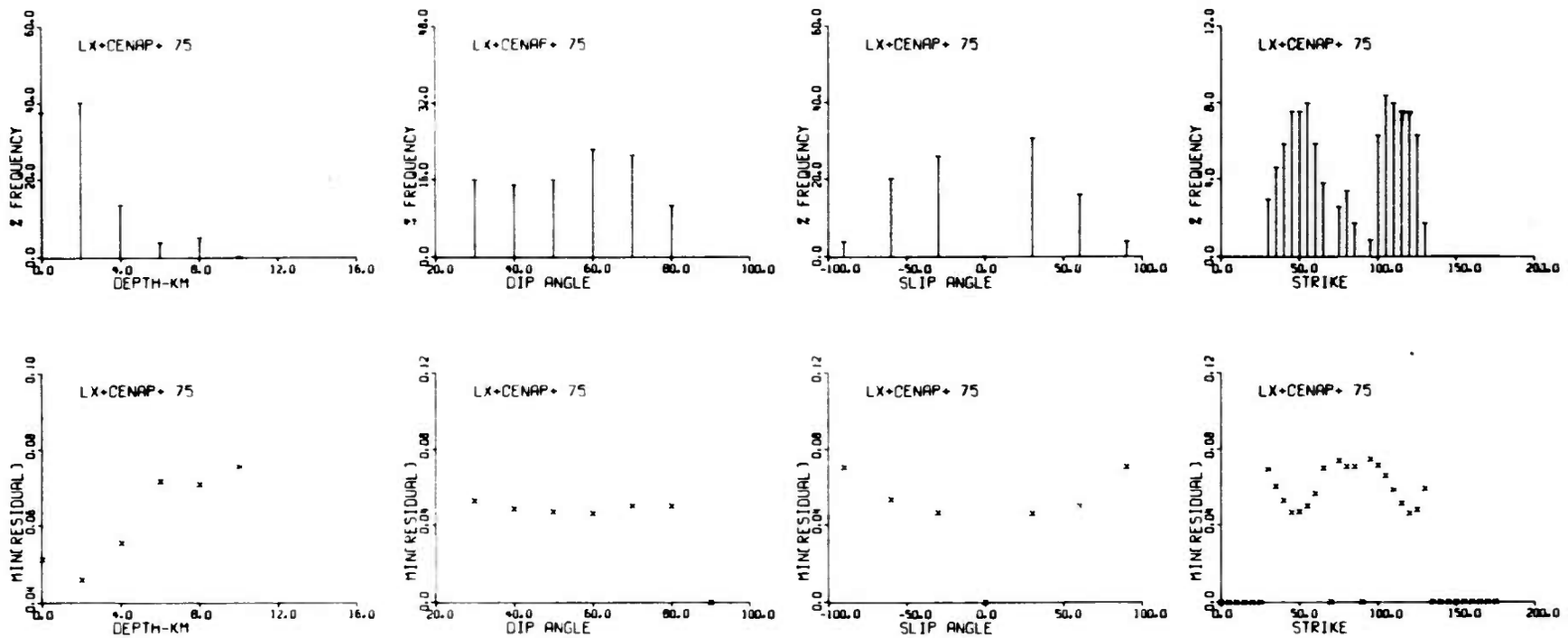

FIGURE III-16

SOURCE PARAMETER DISTRIBUTIONS FOR LX+ CENAP+ 75

TABLE III-8

SUMMARY OF OPTIMAL SOLUTIONS FOR EURASIAN EVENTS

Event I. D.	Optimal Solution				
	Depth h km	Dip Angle δ degree	Slip Angle λ degree	Strike Nϕ^{o}E	Moment 10^{25} dyne-cm
LX+CENAP+10	62.5	70.0	0.0	10	0.236
LX+CENAP+50	57.5	90.0	0.0	110	0.193E 00
LX+CENAP+75	2.0	60.0	30.0	120	0.485E-01
LX+CENAP+6	16.0	70.0	0.0	105	0.347E-01
LX+CENAP+45	8.0	40.0	90.0	30	0.391E-01
LX*TURN1*001	125.0	50.0	30.0	130	0.263E 00
LX*TURN3*003	22.5	70.0	0.0	100	0.126E 01

TABLE III-9

SUMMARY OF SOURCE PARAMETER STATISTICS OF EURASIAN EVENTS

Event I. D.	Source Parameters							
	Depth h km		Dip Angle δ°		Slip Angle λ°		Strike $N\phi^{\circ}E$	
	Probable Range	% Confidence	Probable Range	% Confidence	Probable Range	% Confidence	Probable Range	% Confidence
LX+CENAP+10	55 - 80	74	70 - 90	95	0	82	10 - 15 100 - 105	46 39
LX+CENAP+50	45 - 57.5	91	60 - 70 90	54 26	-30 - +30	85	———	———
LX+CENAP+75	0 - 4	91	40 - 70	74	±30	57	40 - 60 100 - 125	35 44
LX+CENAP+6	6 - 18	91	60 - 90	89	-30 - +30	95	-10 - +20 85 - 120	40 41
LX+CENAP+45	4 - 10	87	30 - 60	84	±60 , ±90	65	———	———
LX*TURN1*001	118 - 138	72	40 - 70	69	±60 , ±30	84	———	———
LX*TURN3*003	22.5 - 30	92	70 - 90	58	-30 - +30	69	———	———

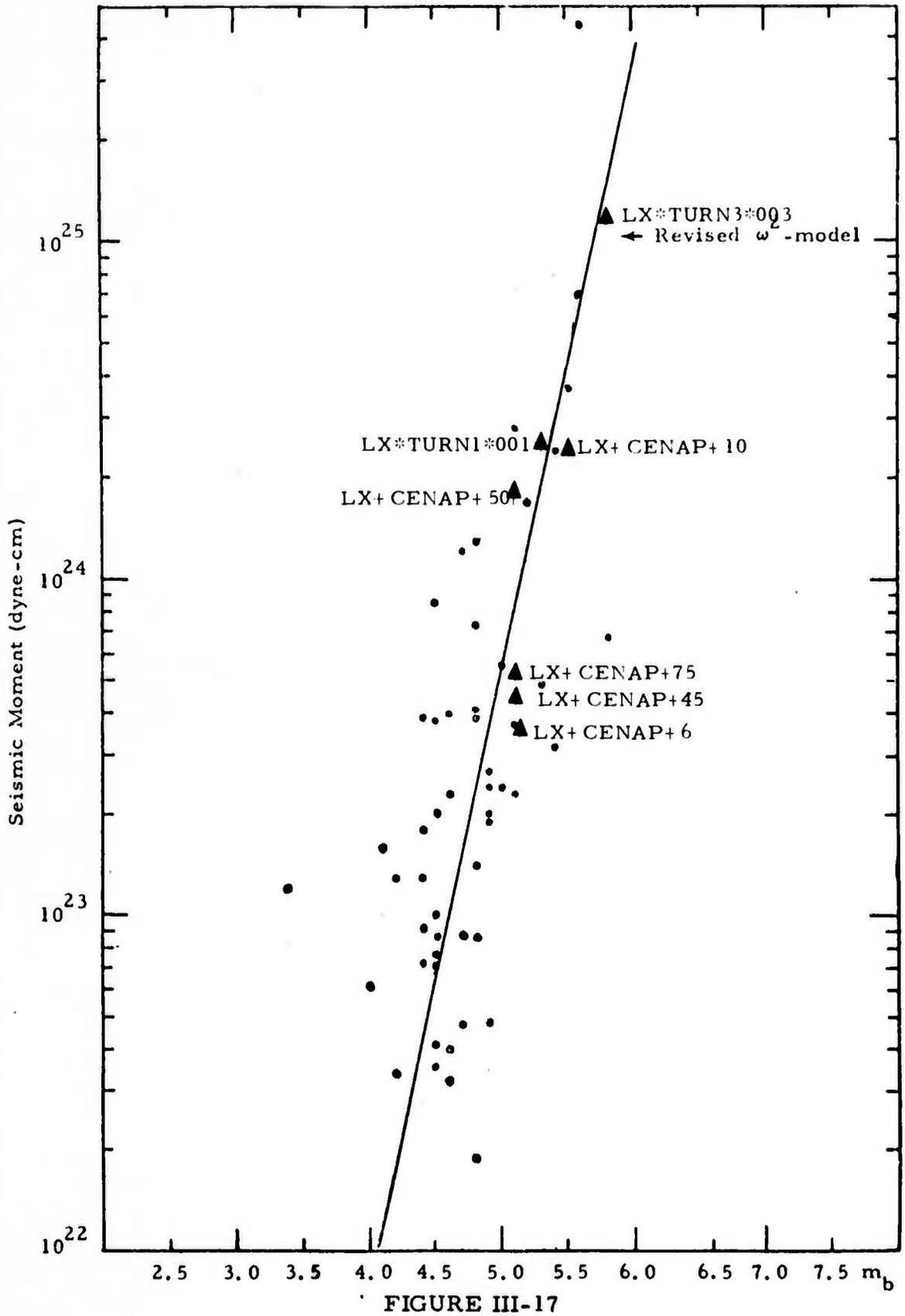

FIGURE III-17

SEISMIC MOMENT ESTIMATES OF THE EURASIAN EVENTS IN RELATION TO THE ω^2-MODEL

but this is possibly deceptive because of the steep slope of the model. Also, all of the events have a bodywave magnitude (m_b) greater than 5.0, so any possible agreement must be limited to that magnitude range.

SECTION 1V
CONCLUSIONS AND RECOMMENDATIONS

We can summarize the remarks in the preceeding sections concerning source parameter estimates obtained from teleseismic surface wave data using spectral fitting procedures with the following points:

- From the analysis of theoretical spectra and of several Eurasian events, it has been shown that a gross knowledge of the source region crustal structure is necessary in most cases. In general terms, if the structural properties are underestimated (low velocities), a shallower focal depth will be obtained. The converse is also true; overestimation yields a deeper focal depth.

- The exception to the above statement occurs for very shallow events (less than 5 km). Using several crustal models in the analysis of a very shallow Eurasian event (CENAP+75) resulted in very little change of the focal depth estimate ($\pm$ 1 km). This implies that little change in spectral shape occurs for shallow depths between different source structures in the frequency range of interest.

- Because the major variations of spectra with focal depth occur in the 10 to 20 second period range (Turnbull, et. al., 1973), it is important to have accurate data at these frequencies. From analysis of the instrument response curves of the VLPE stations, ALPA, and NORSAR, it was found that, in most cases, the VLPE data is unsuitable for accurate depth estimation. The response of these instruments is such that it is

down 27 dB or more at 10 seconds period. For NORSAR and ALPA, though, the response is only 12 to 20 dB down at 10 seconds period. Hence, depth estimates obtained from data recorded on these instruments are felt to be quite adequate.

- The analysis of seven Eurasian events using teleseismic surface wave data yielded the following results: (1) From knowledge of the crustal structure in the source region, depth estimates can be obtained which closely agree with those from bodywave depth phases; (2) After the successful application of a source structure to an event with known depth, this structure should be applied to events in the same tectonic region; (3) We can usually determine a reasonably probable range of focal depth, with the dip and slip values more ambiguous, and the strike direction unknown in many cases; (4) Although there is close agreement of the seismic moment (M_o) versus bodywave magnitude (m_b) for these events with Tsai's ω^2-model, this is possibly deceptive because of the steep slope of the model.

Future studies will be concerned with the following problems:

- The events analyzed in this study have mainly occurred in one tectonic region. We will attempt to analyze other regions, with our interest in a region governed by its seismicity.
- A systematic collection of surface wave group velocity dispersion curves and effective attenuation for particular source-station paths will be undertaken. This information will be used as part of path correction software package, which has been partially developed.

- Events which have been studied using very near field data (less than 10 km), will be analyzed from both intermediate (less than 200 km) and far field distances. Theoretical point source models will be used to obtained source descriptions at these distances, and the results will be compared to those obtained from the very near field.

SECTION V
REFERENCES

Bracewell, R., 1965, The Fourier Transform and Its Applications, McGraw-Hill Book Company, New York, pp. 267-272.

Massé, R. P., 1970, Analysis of Seismic Events as Recorded on Both Wide Band Long Period and Standard VELA Long Period Seismograph Systems, SDL Report No. 260, Teledyne Geotech.

Rodriguez, R. G., 1969, Atlas of Asia and Eastern Europe to Support Detection of Underground Nuclear Testing, U. S. Geological Survey, Volume V.

Tsai, Y. B., 1972a, Utility of Tsai's Method for Seismic Discrimination: Semiannual Technical Report No. 2, Texas Instruments, Incorporated, Dallas, Texas.

Tsai, Y. B., 1972 b, Utility of Tsai's Method for Seismic Discrimination: Semiannual Technical Report No. 2, Texas Instruments, Incorporated, Dallas, Texas.

Turnbull, L. S., D. F. D. Sun, and J. S. Shaub, 1973, Determination of Seismic Source Parameters from Frequency Dependent Rayleigh and Love Wave Radiation Patterns, Semi-Annual Technical Report No. 1-Part C, Texas Instruments, Incorporated, Dallas, Texas.

APPENDIX A

SURFACE WAVE SPECTRAL VARIATION WITH RESPECT TO SOURCE REGION STRUCTURE

In attempting to match the source depths for several Eurasian events obtained from spectral fitting techniques to those obtained from body wave phases, a Gutenberg-Bullen structure was modified using the existing knowledge of the geology (Rodriguez, 1969). Two of the more important modifications (structures S-OA and S-2) are given in Table A-1 and Figures A-1 to A-3. The Rayleigh and Love wave group velocity dispersion of these modifications compared to the Gutenberg-Bullen (G) dispersion is shown in Figures A-4 and A-5. Both of the modified structures exhibit higher group velocities than that for the G structure, especially at the higher frequencies. This is due to the thicker, high velocity crust of both modifications.

Rayleigh and Love wave spectral comparisons between the G-B structure and the S-2 modification are shown in Figures A-6 to A-9 for several fault configurations. The most important feature of this comparison is the increase of the spectral level between 10 and 20 second periods for both the Rayleigh and Love waves of structure S-2. The use of this structure will give a deeper source depth from the spectral fitting procedure.

TABLE A-1

LAYER PARAMETERS FOR EARTH STRUCTURES APPLIED TO SOURCE REGIONS

Gutenberg-Bullen

Layer No.	Layer Thickness (km)	V_p km/sec	V_s km/sec	δ gm/cc
1	22.0	6.03	3.53	2.78
2	15.0	6.70	3.80	3.00
3	13.0	7.96	4.60	3.37
4	25.0	7.85	4.50	3.39
5	50.0	7.85	4.41	3.42
6	75.0	8.00	4.41	3.45
7	50.0	8.20	4.50	3.47
Half space				

Model S-OA

1	8.0	6.14	3.55	2.74
2	6.0	6.50	3.78	3.05
3	6.0	6.90	3.98	3.05
4	30.0	7.70	4.45	3.25

* Normal Gutenberg-Bullen for depths > 50 km

Model S-2

1	20.0	6.70	3.80	3.05
2	20.0	7.50	4.34	3.20
3	30.0	7.70	4.45	3.25

* This thicker crust (70 km) placed on Gutenberg-Bullen structure which begins at 50 km depth.

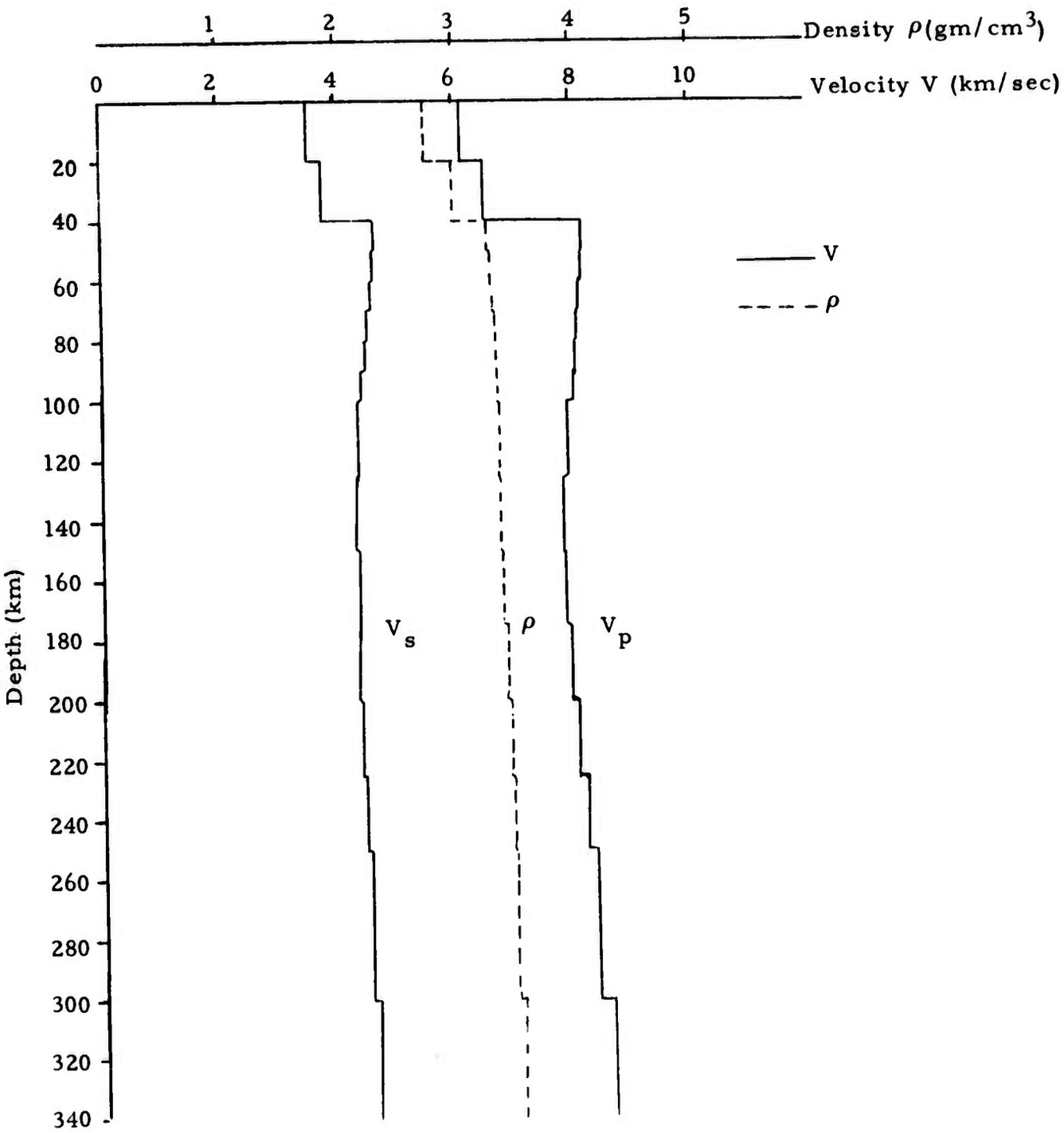

FIGURE A-1

GUTENBERG-BULLEN EARTH MODEL: G

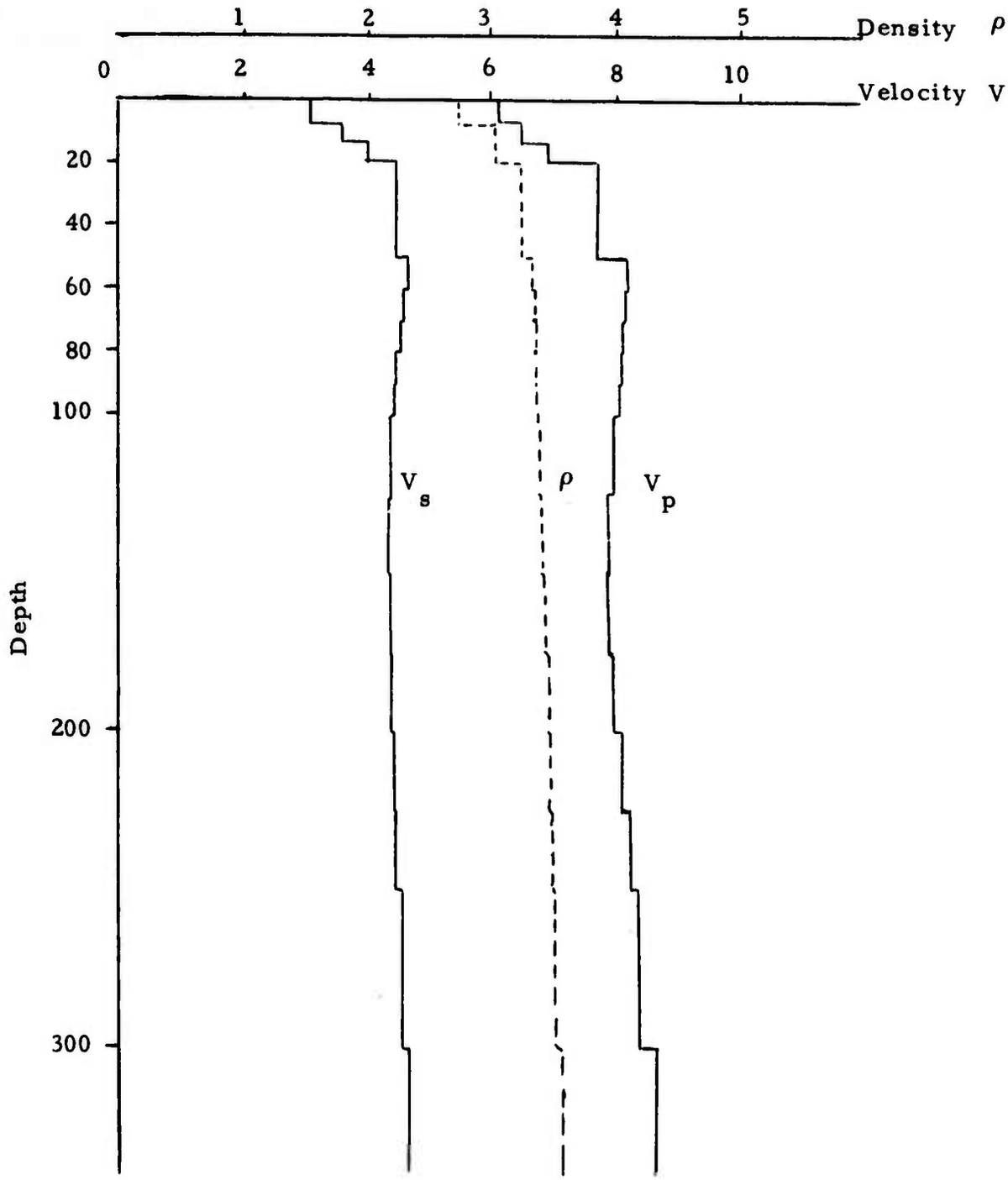

FIGURE A-2

FIRST MODIFICATION OF GUTENBERG-BULLEN MODEL : SO-A

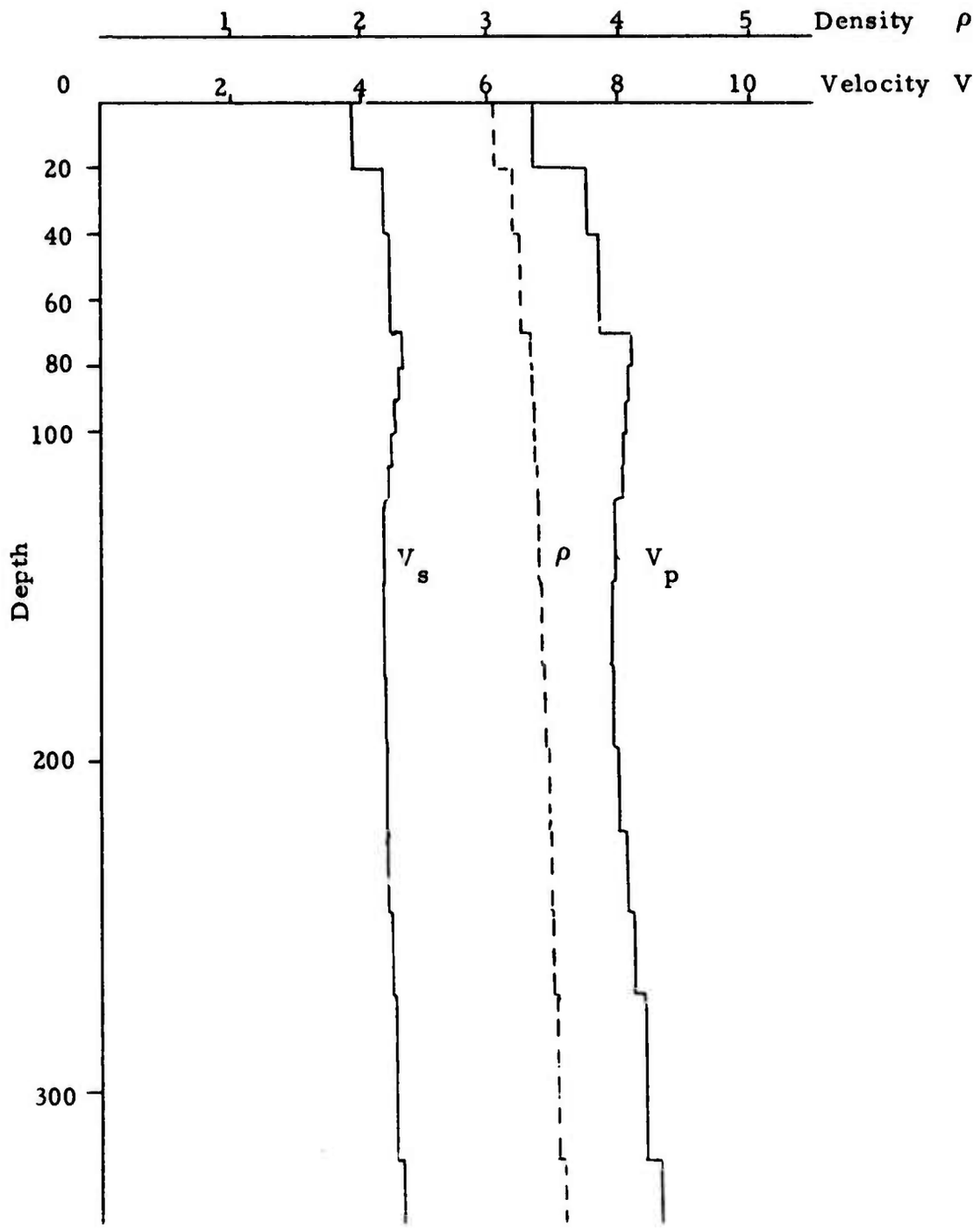

FIGURE A-3

SECOND MODIFICATION OF GUTENBERG-BULLEN MODEL : S-2

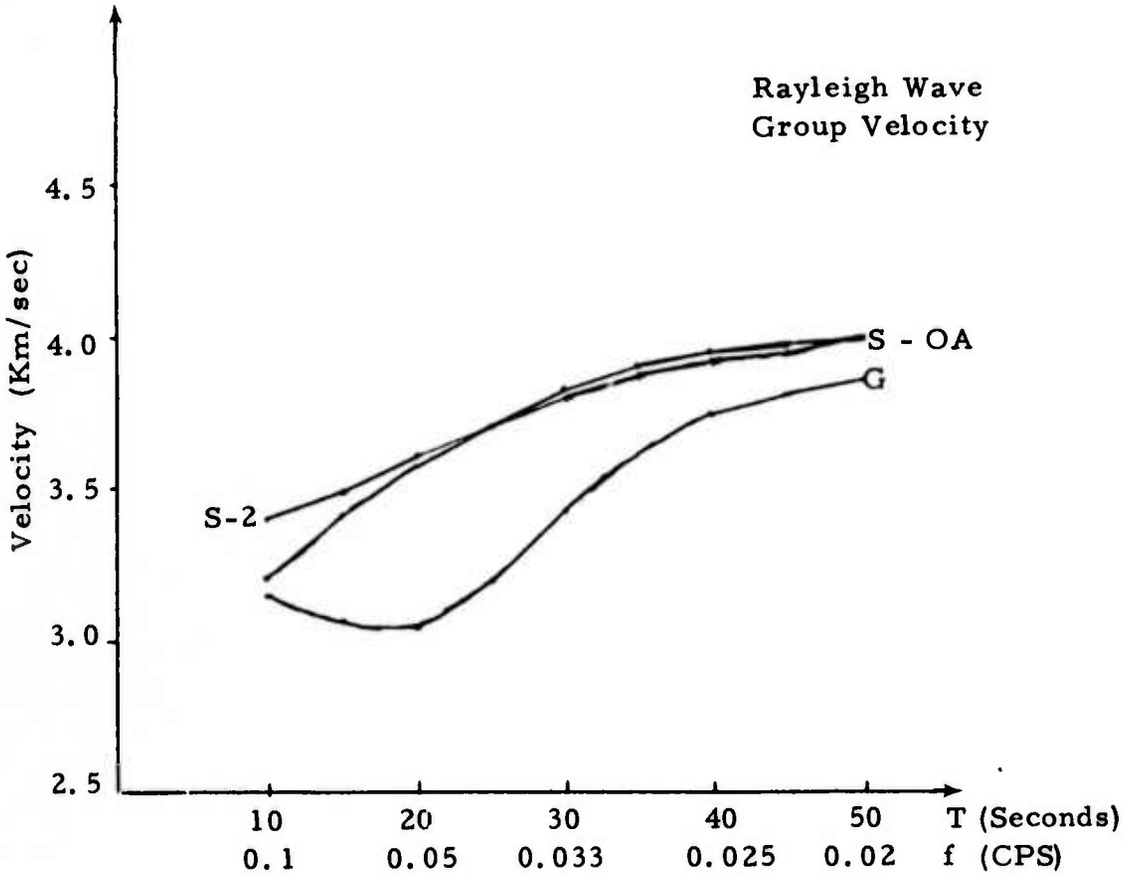

FIGURE A-4

THEORETICAL RAYLEIGH WAVE GROUP VELOCITY CURVES
FOR EARTH STRUCTURES

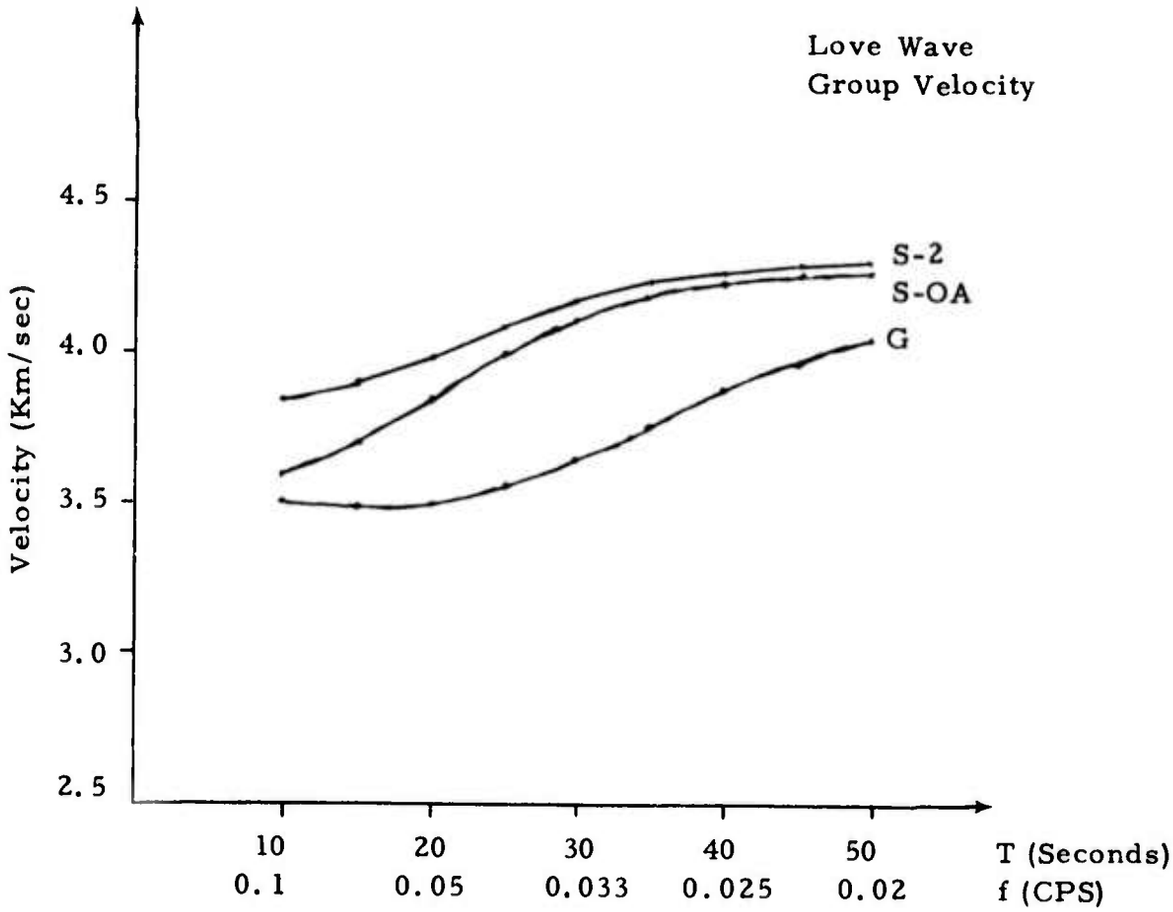

FIGURE A-5

THEORETICAL LOVE WAVE GROUP VELOCITY CURVES
FOR EARTH STRUCTURES

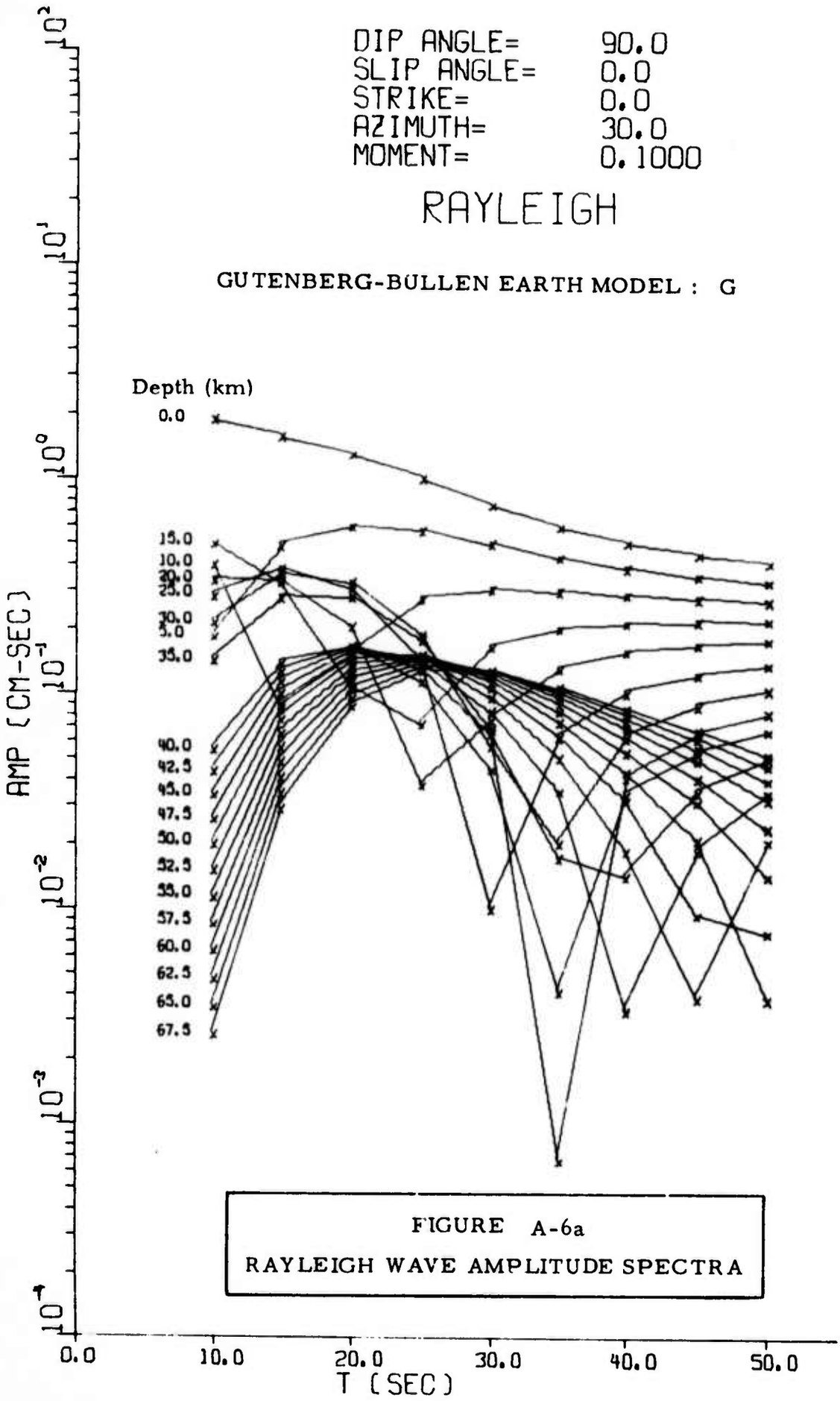

FIGURE A-6a

RAYLEIGH WAVE AMPLITUDE SPECTRA

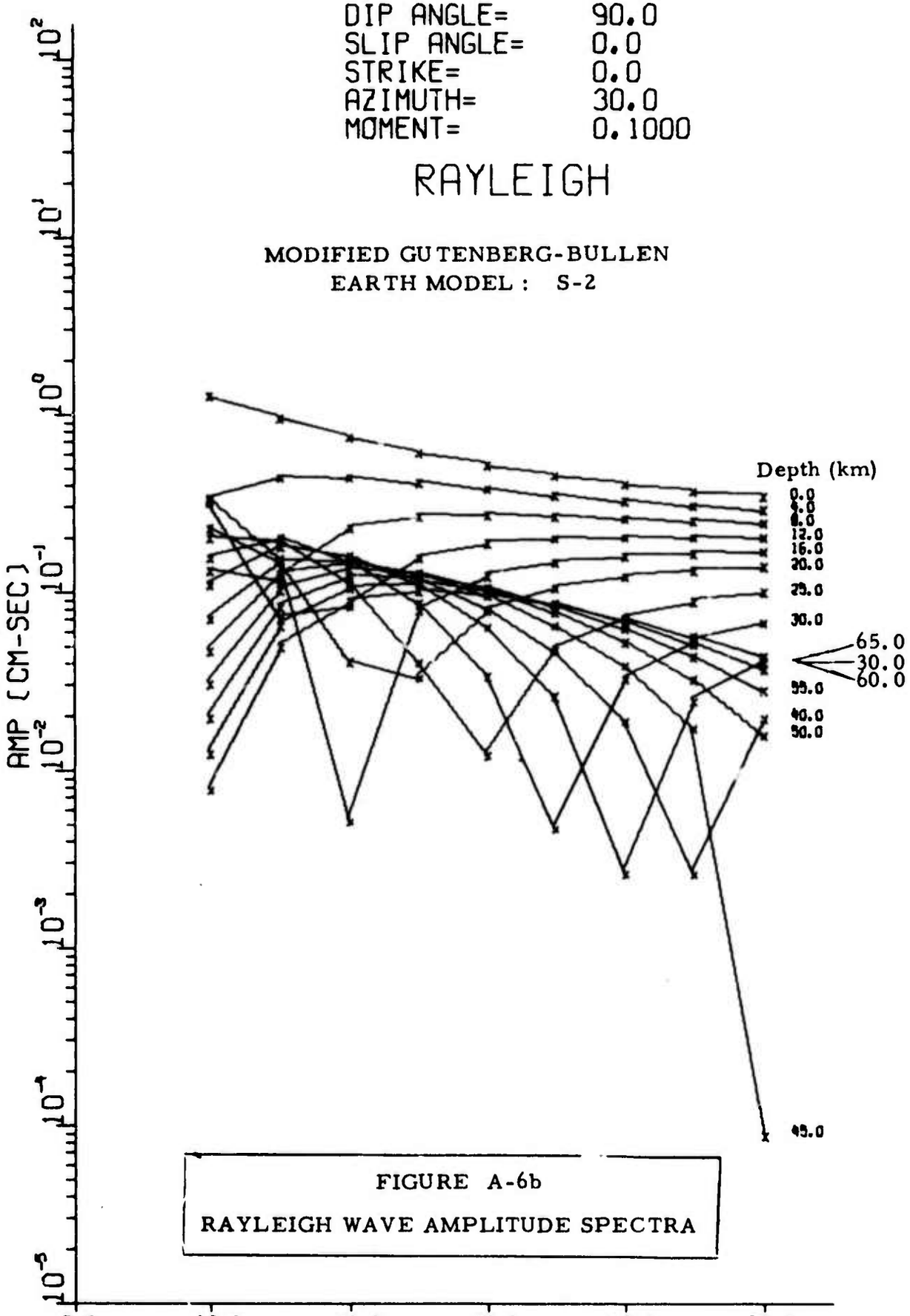

FIGURE A-6b

RAYLEIGH WAVE AMPLITUDE SPECTRA

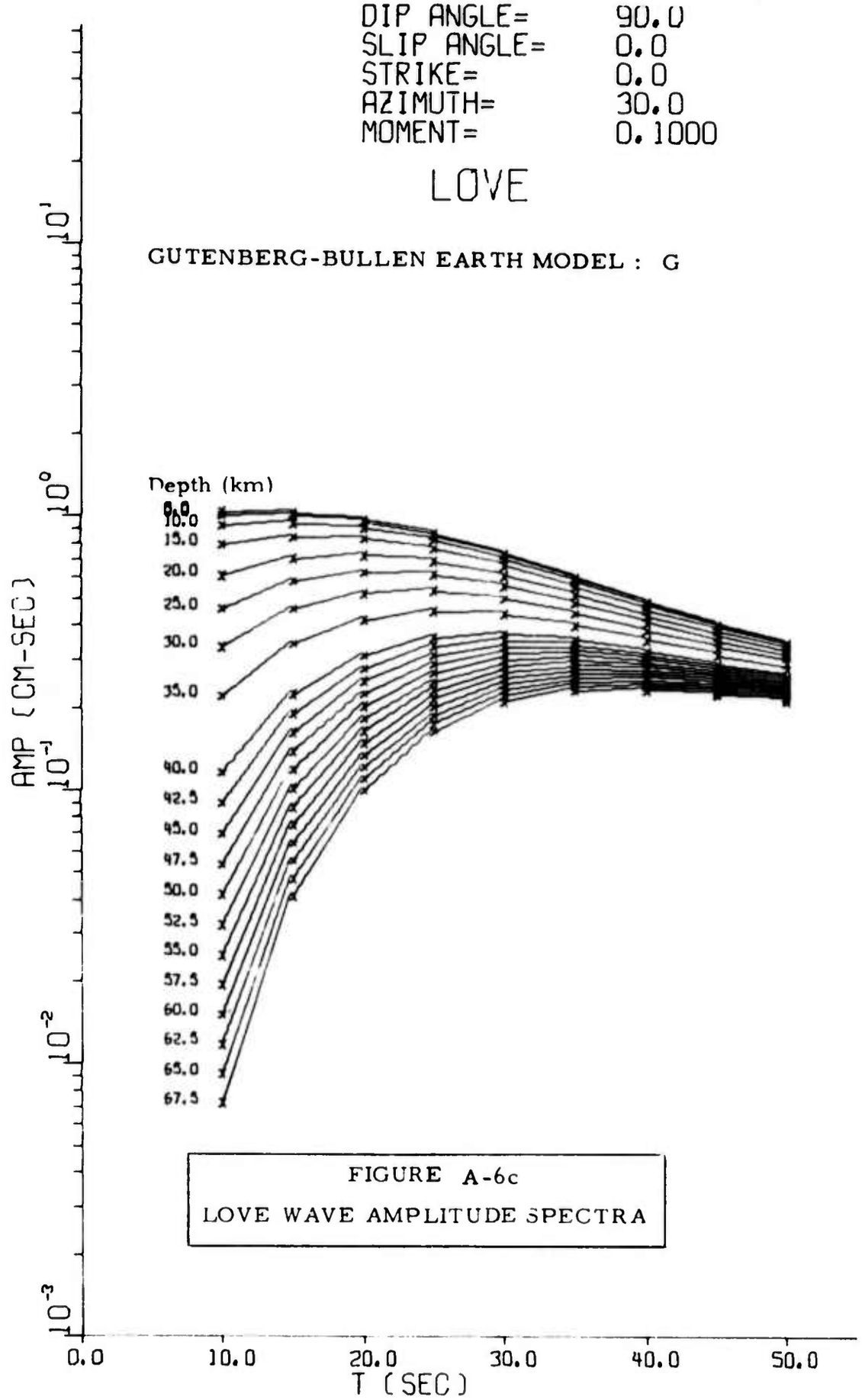

FIGURE A-6c

LOVE WAVE AMPLITUDE SPECTRA

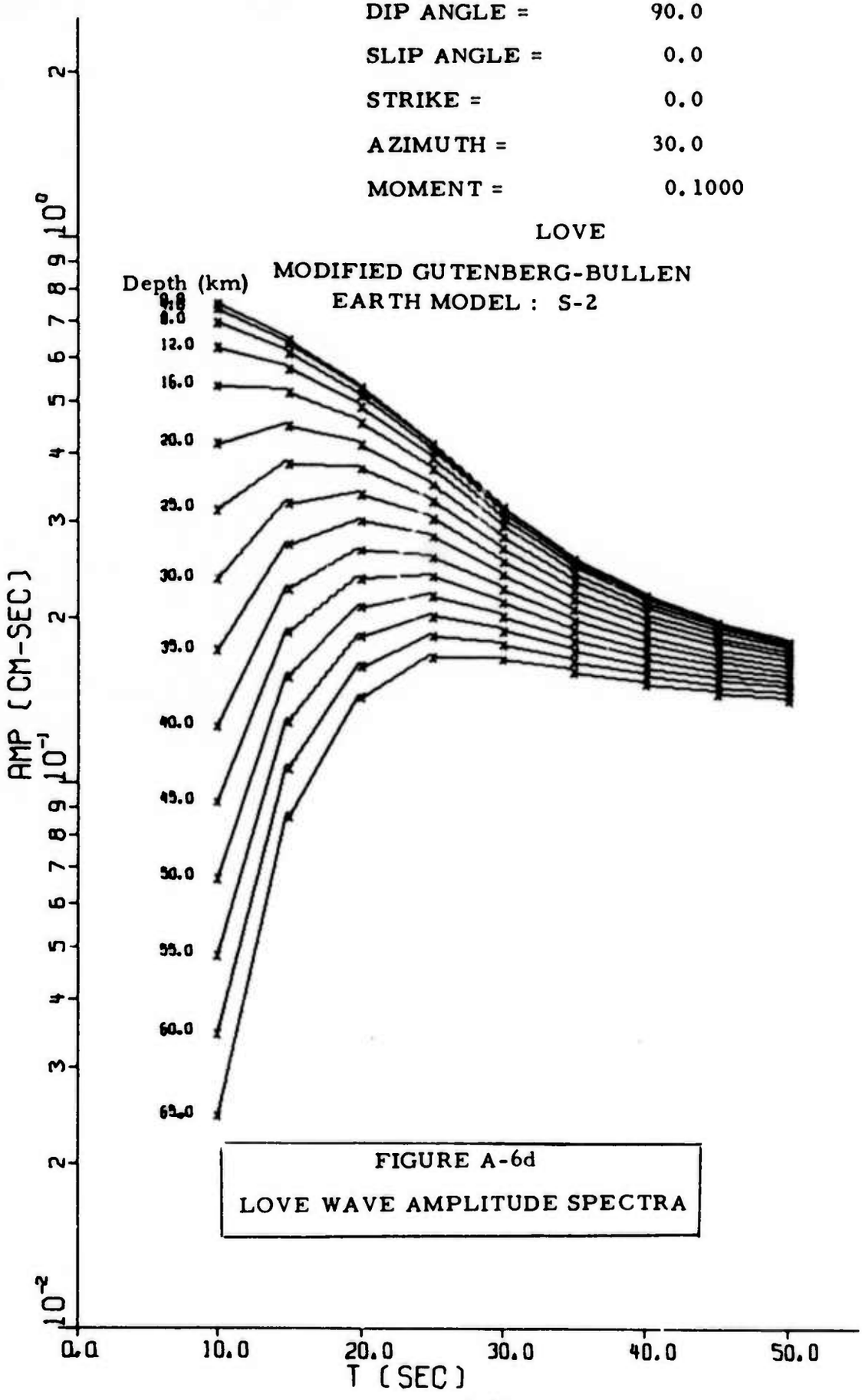

FIGURE A-6d

LOVE WAVE AMPLITUDE SPECTRA

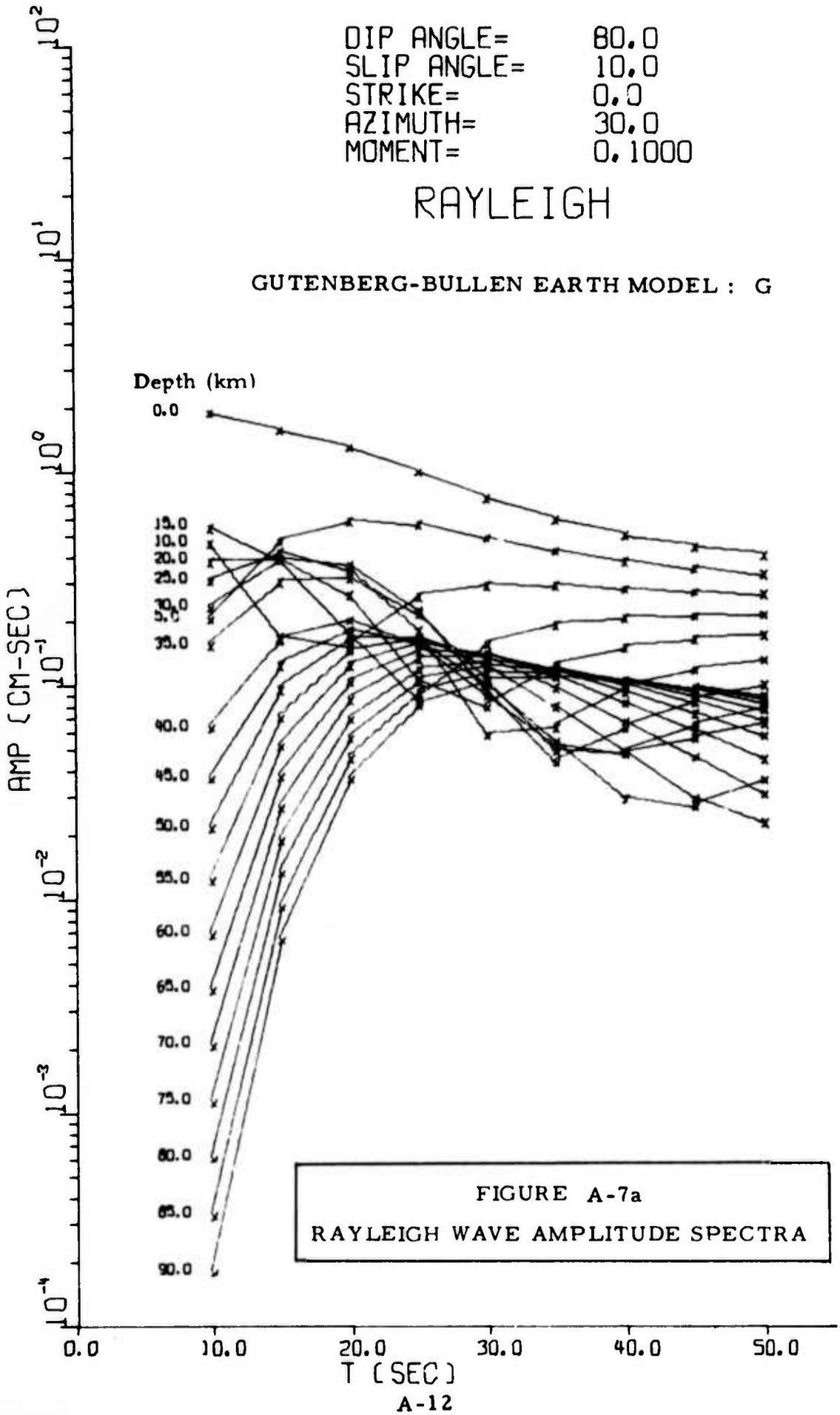

FIGURE A-7a

RAYLEIGH WAVE AMPLITUDE SPECTRA

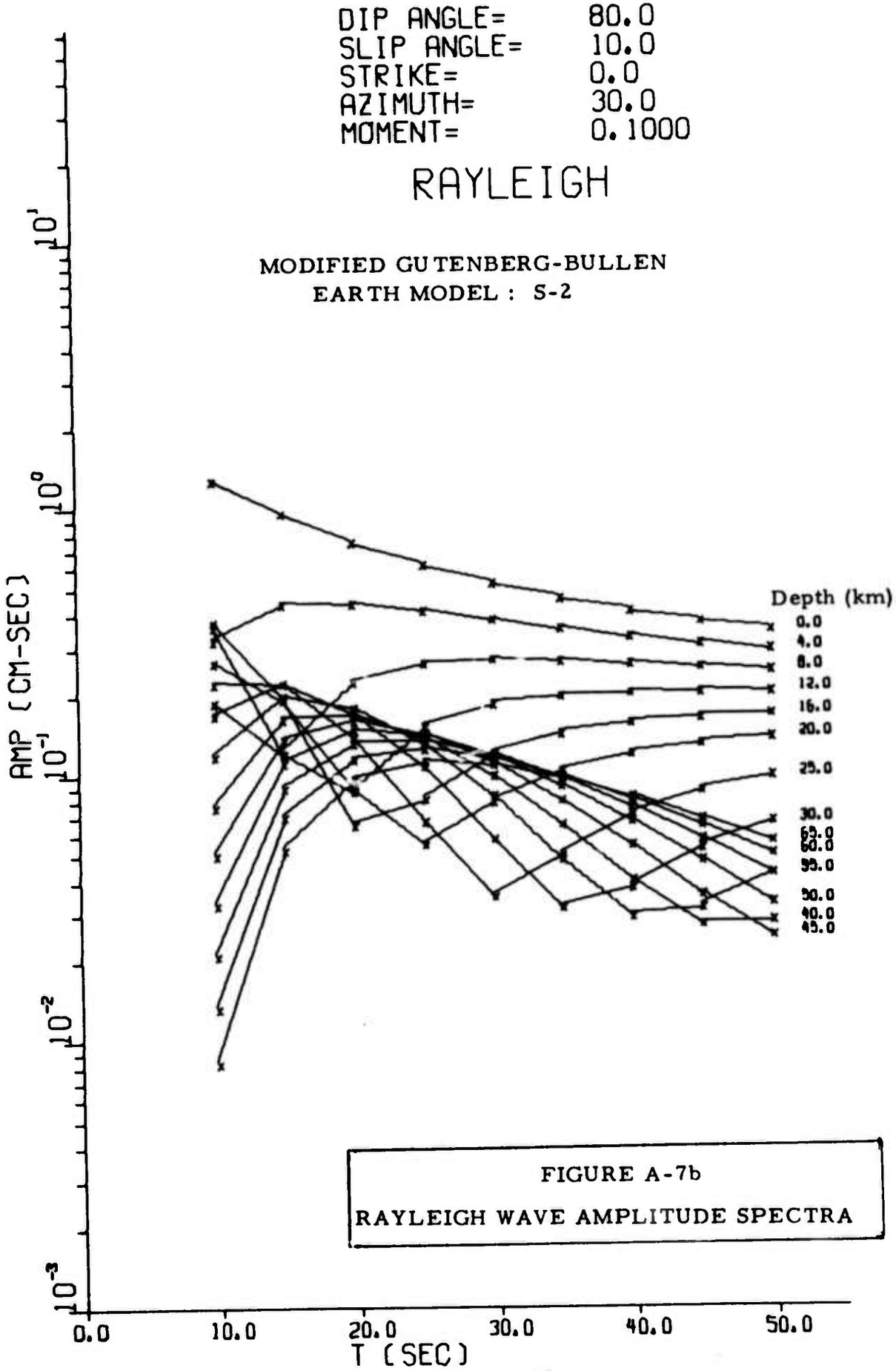

FIGURE A-7b

RAYLEIGH WAVE AMPLITUDE SPECTRA

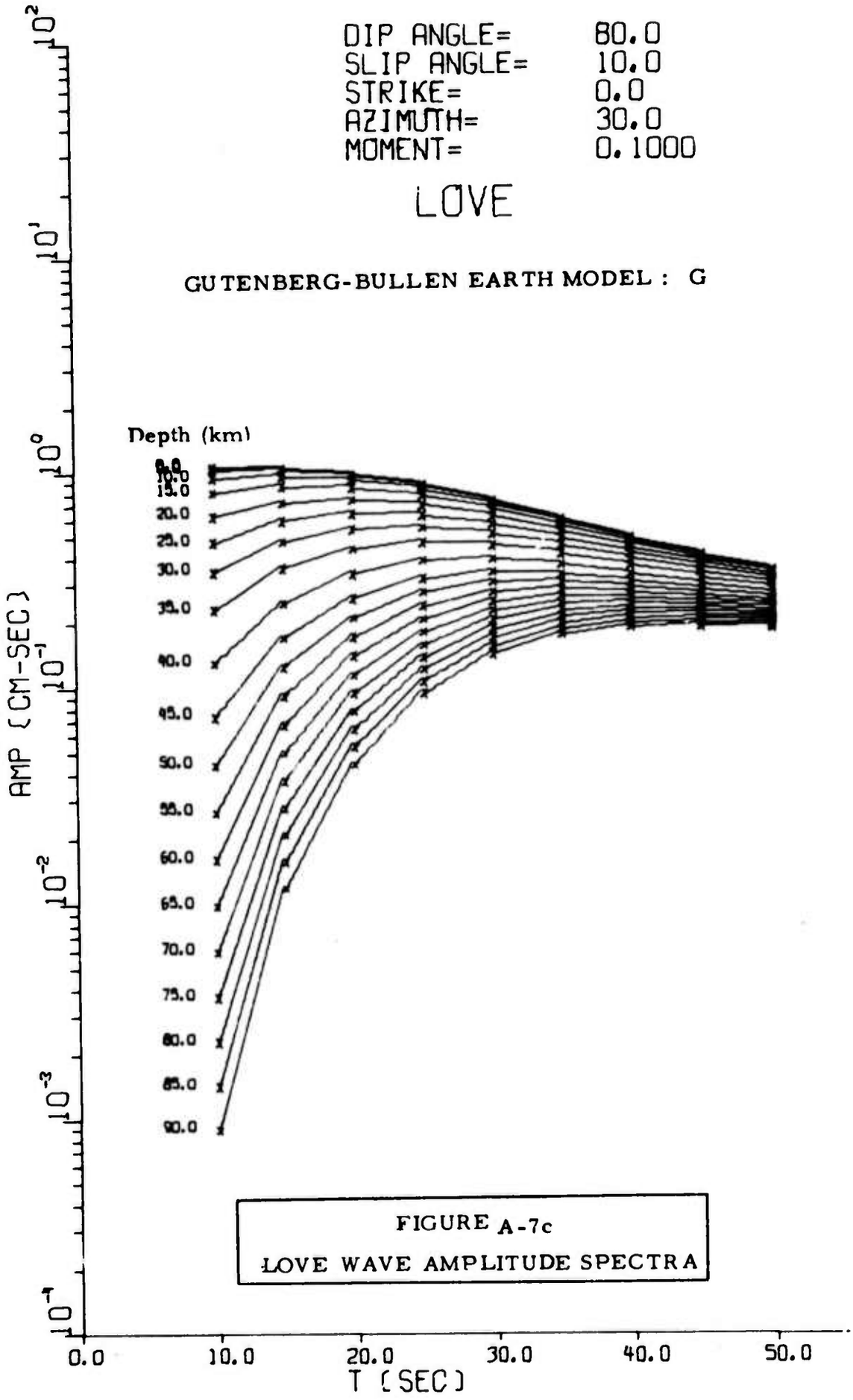

FIGURE A-7c

LOVE WAVE AMPLITUDE SPECTRA

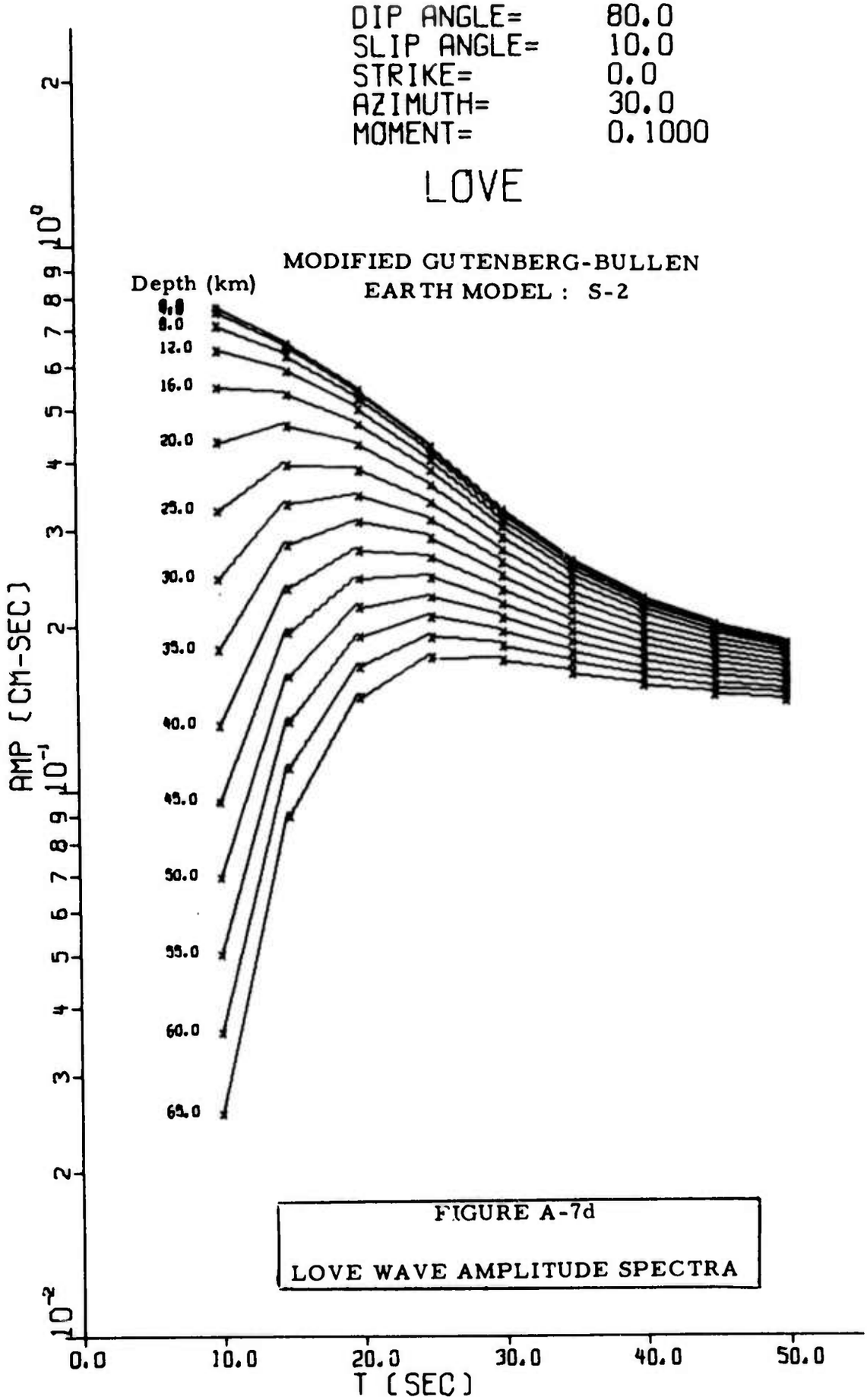

FIGURE A-7d

LOVE WAVE AMPLITUDE SPECTRA

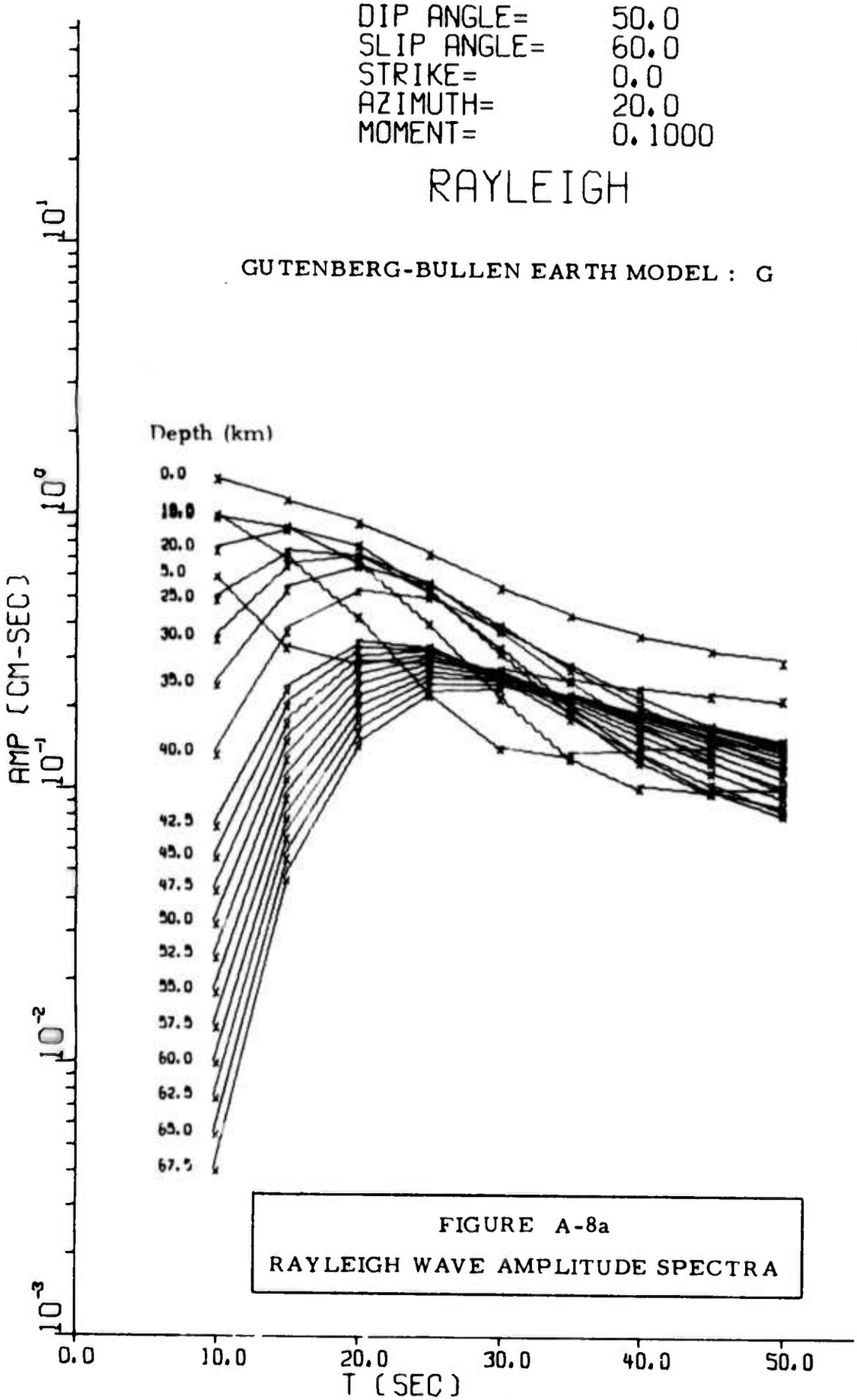

FIGURE A-8a

RAYLEIGH WAVE AMPLITUDE SPECTRA

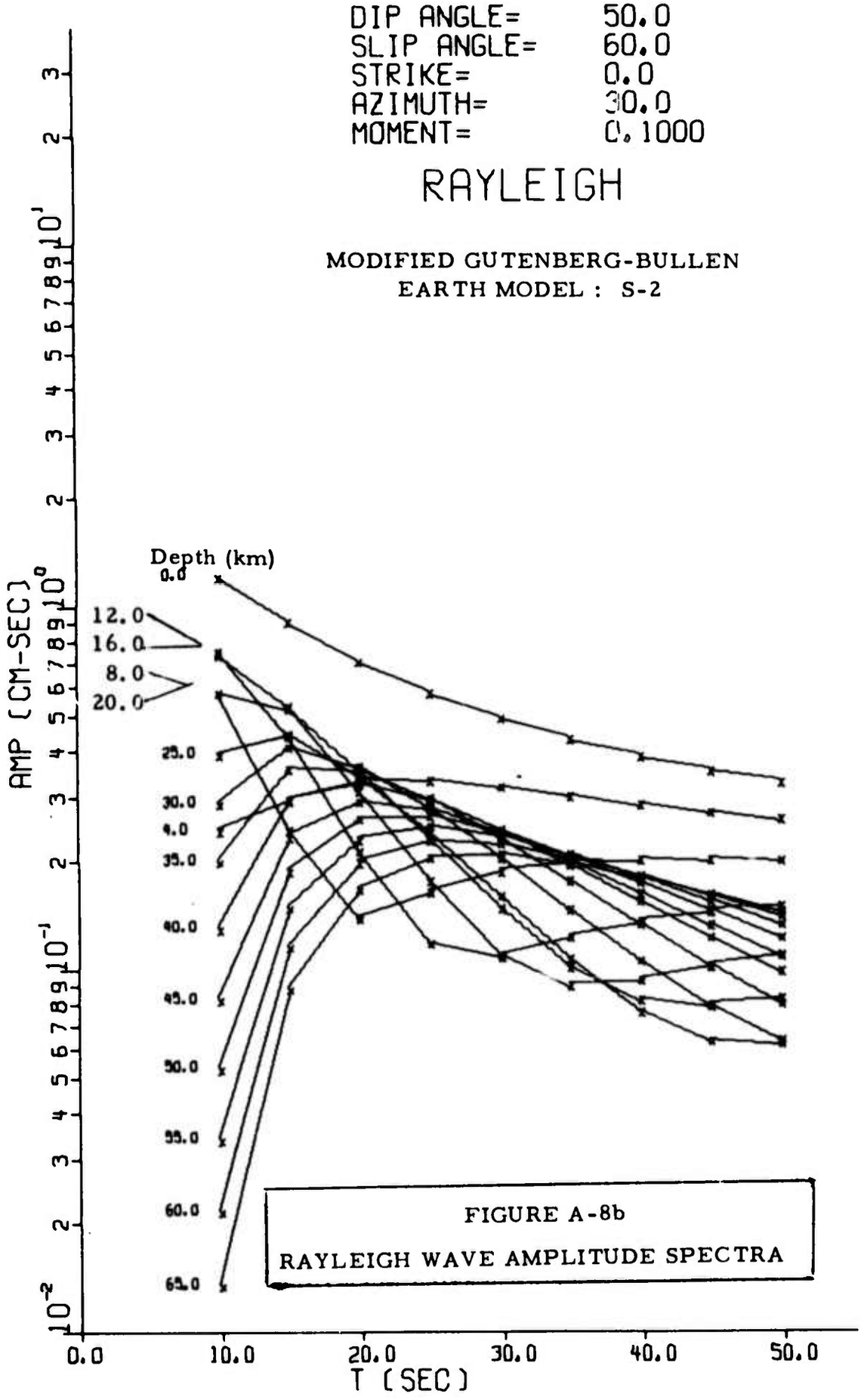

FIGURE A-8b

RAYLEIGH WAVE AMPLITUDE SPECTRA

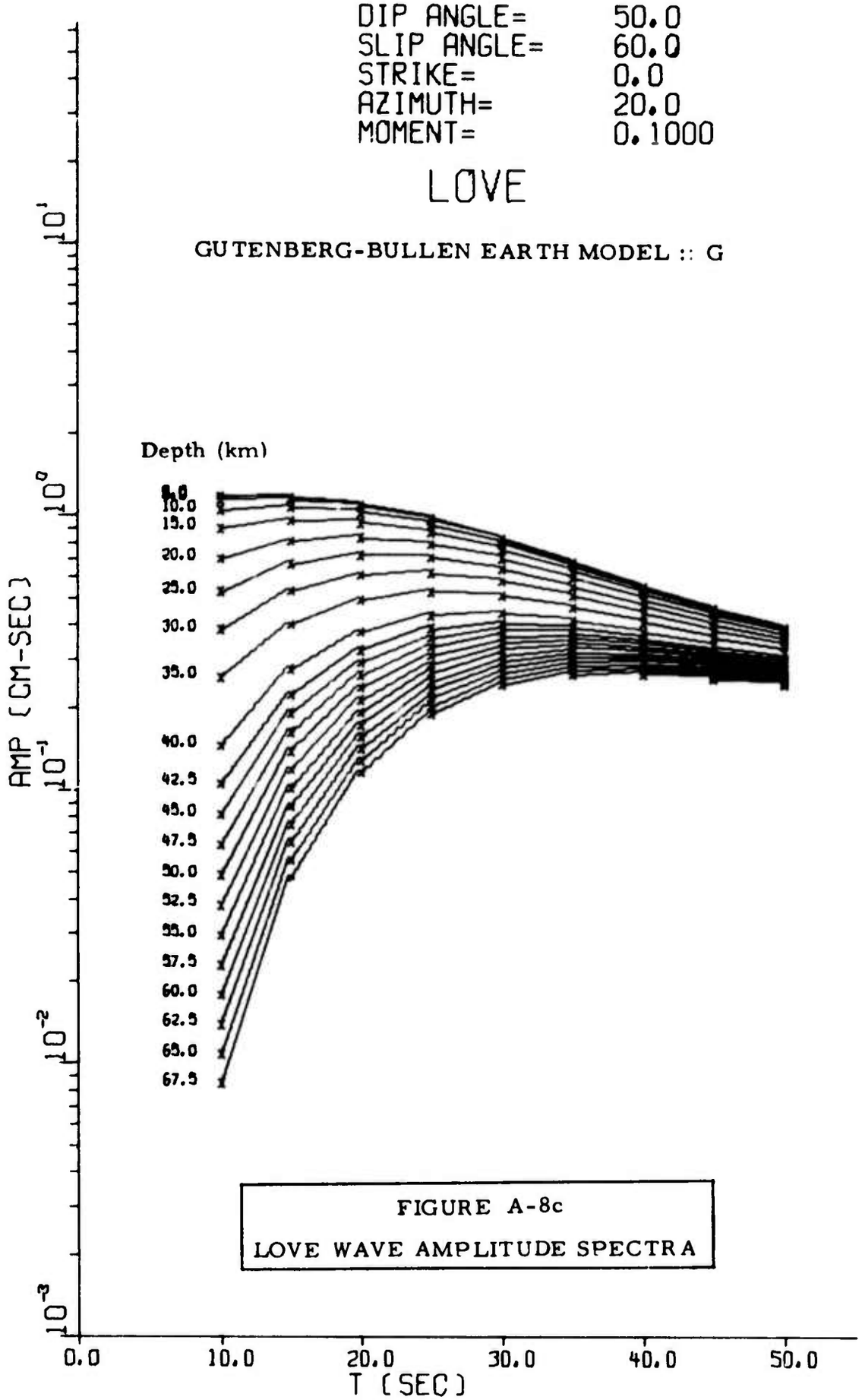

FIGURE A-8c

LOVE WAVE AMPLITUDE SPECTRA

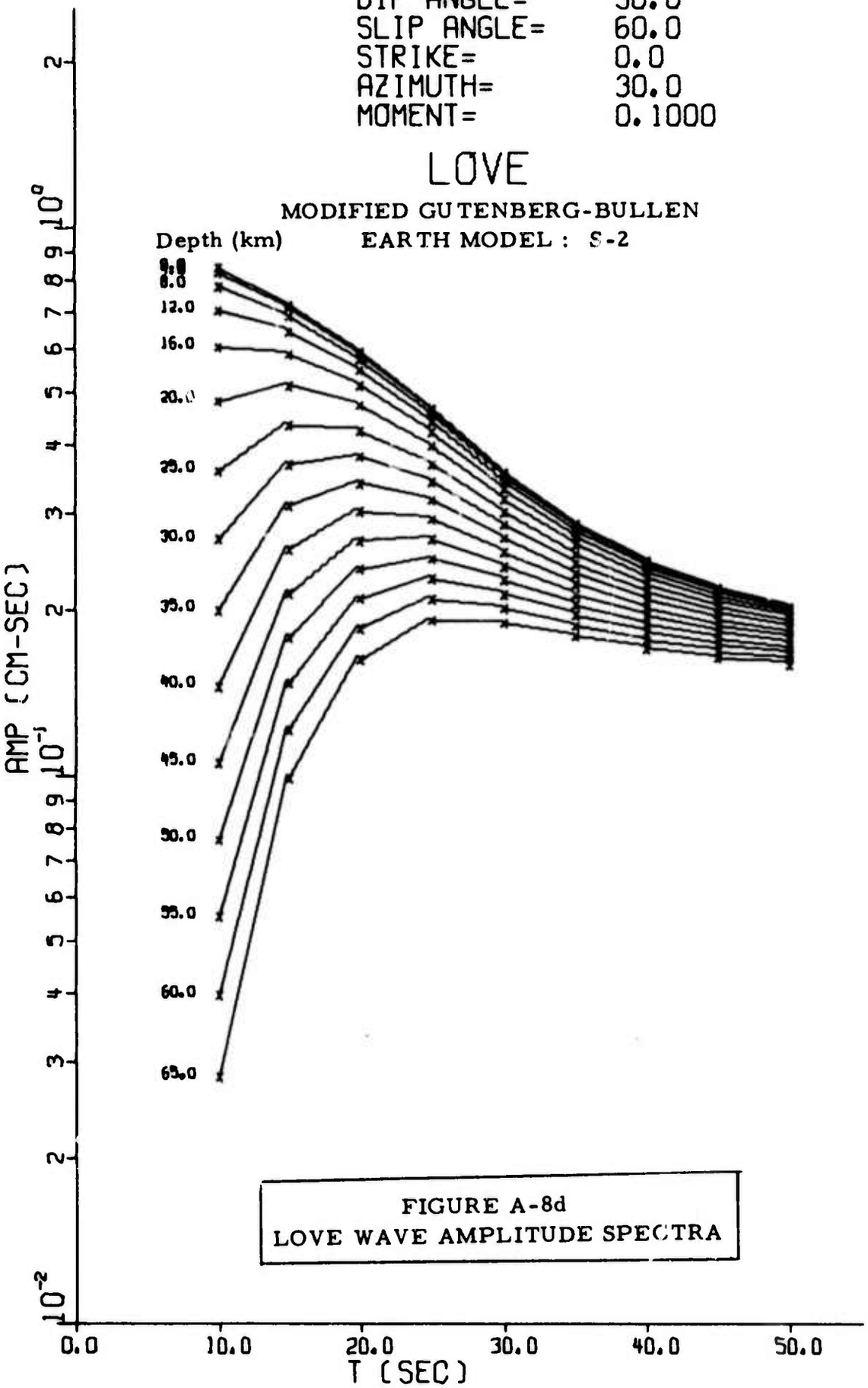

FIGURE A-8d
LOVE WAVE AMPLITUDE SPECTRA

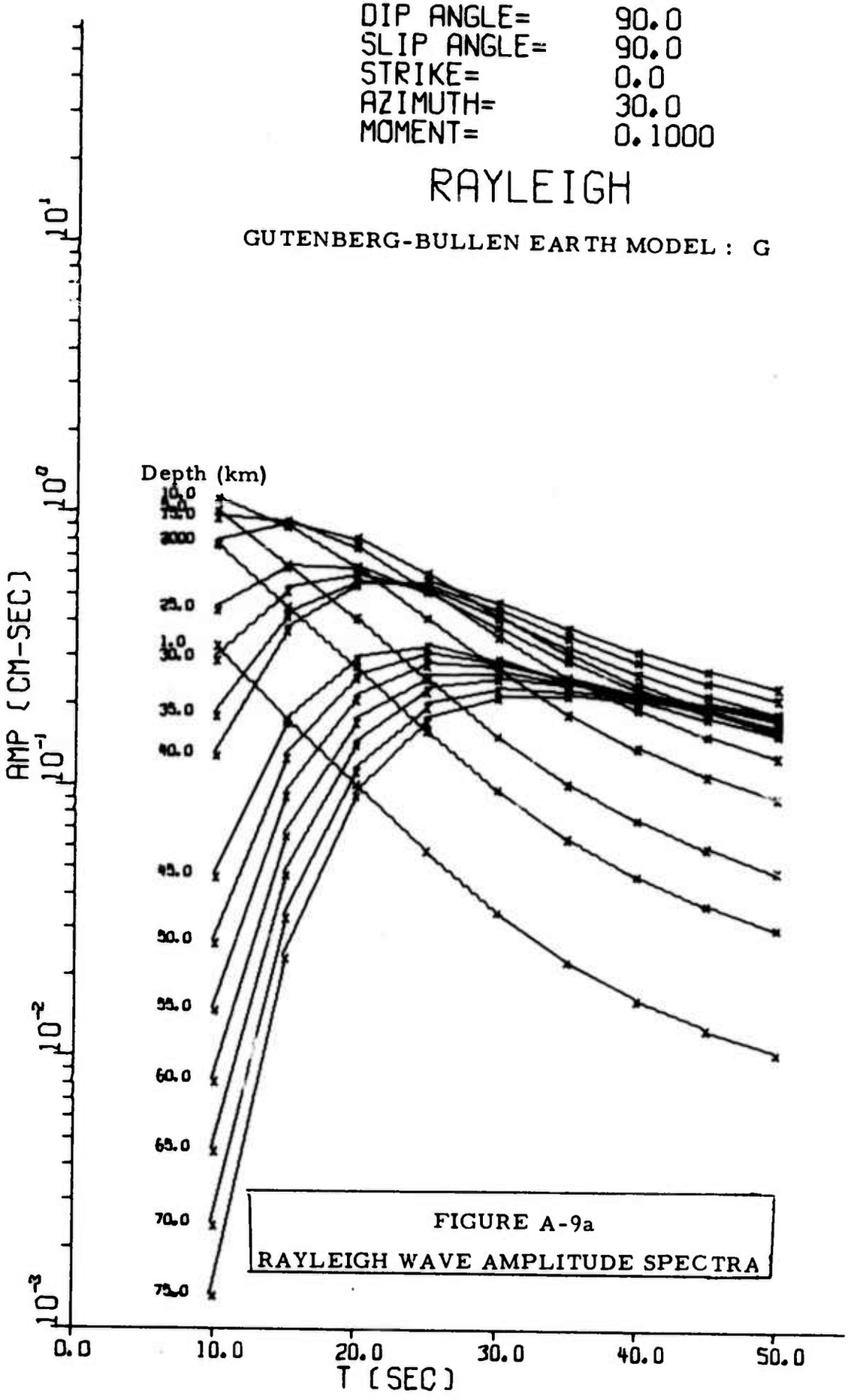

FIGURE A-9a

RAYLEIGH WAVE AMPLITUDE SPECTRA

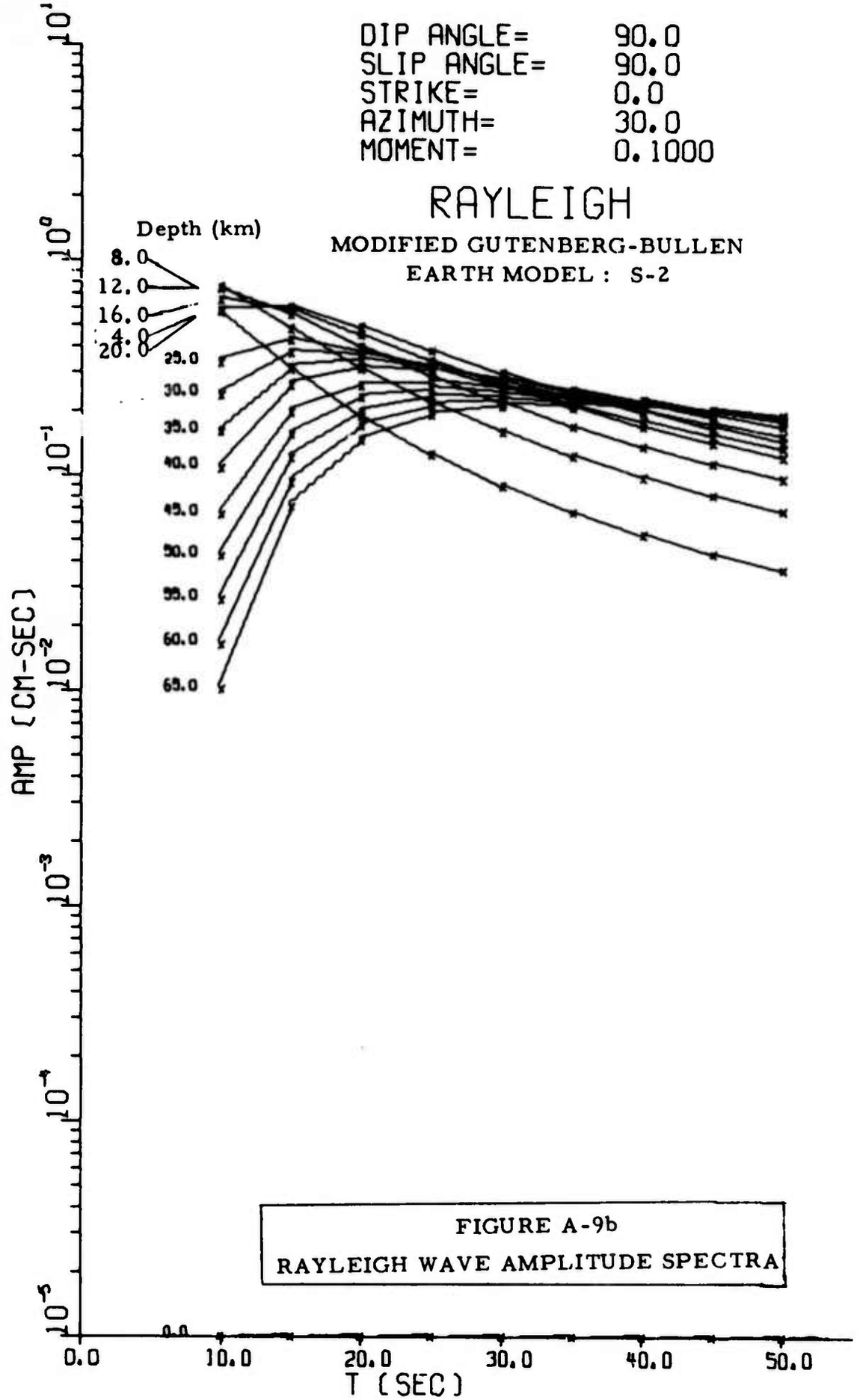

FIGURE A-9b

RAYLEIGH WAVE AMPLITUDE SPECTRA

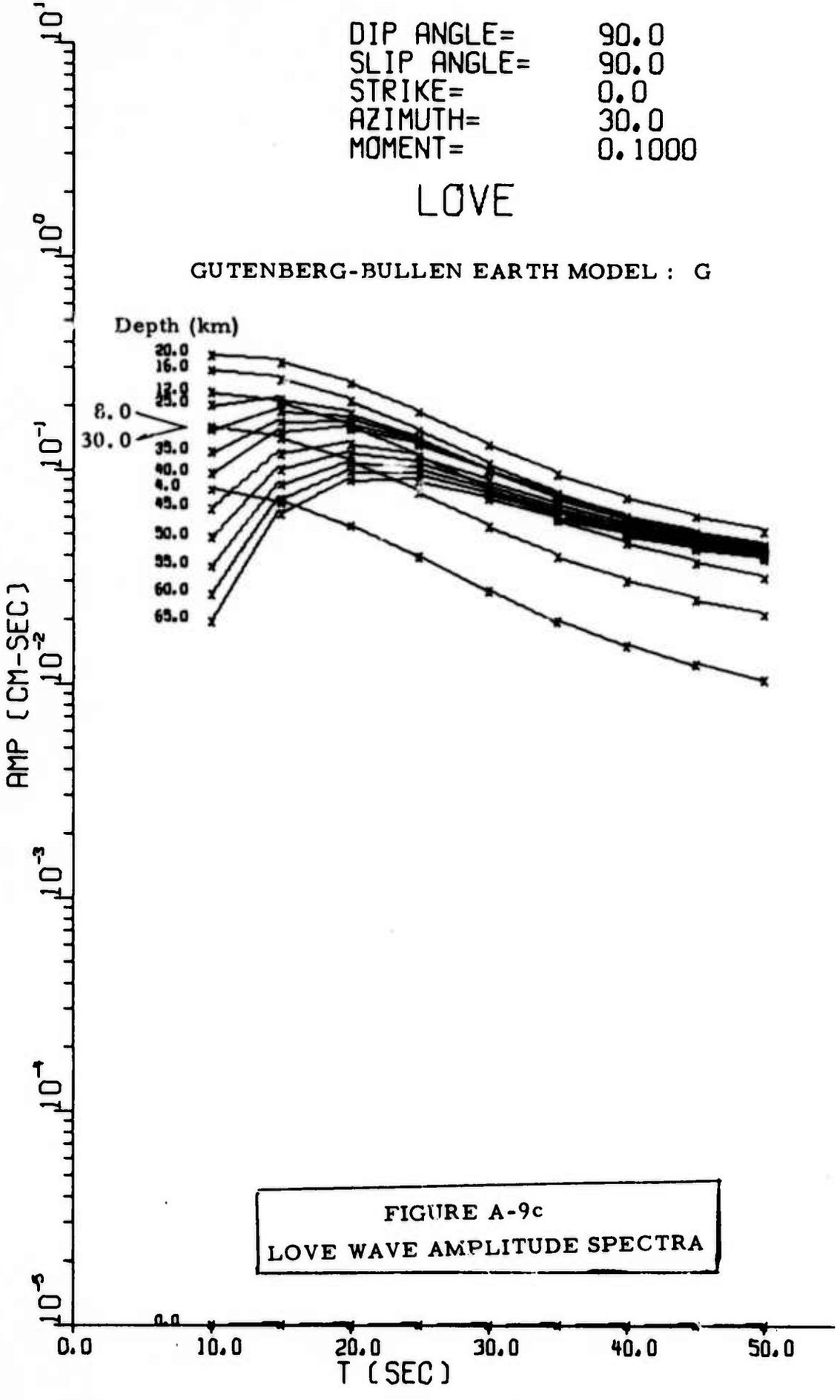

FIGURE A-9c
LOVE WAVE AMPLITUDE SPECTRA

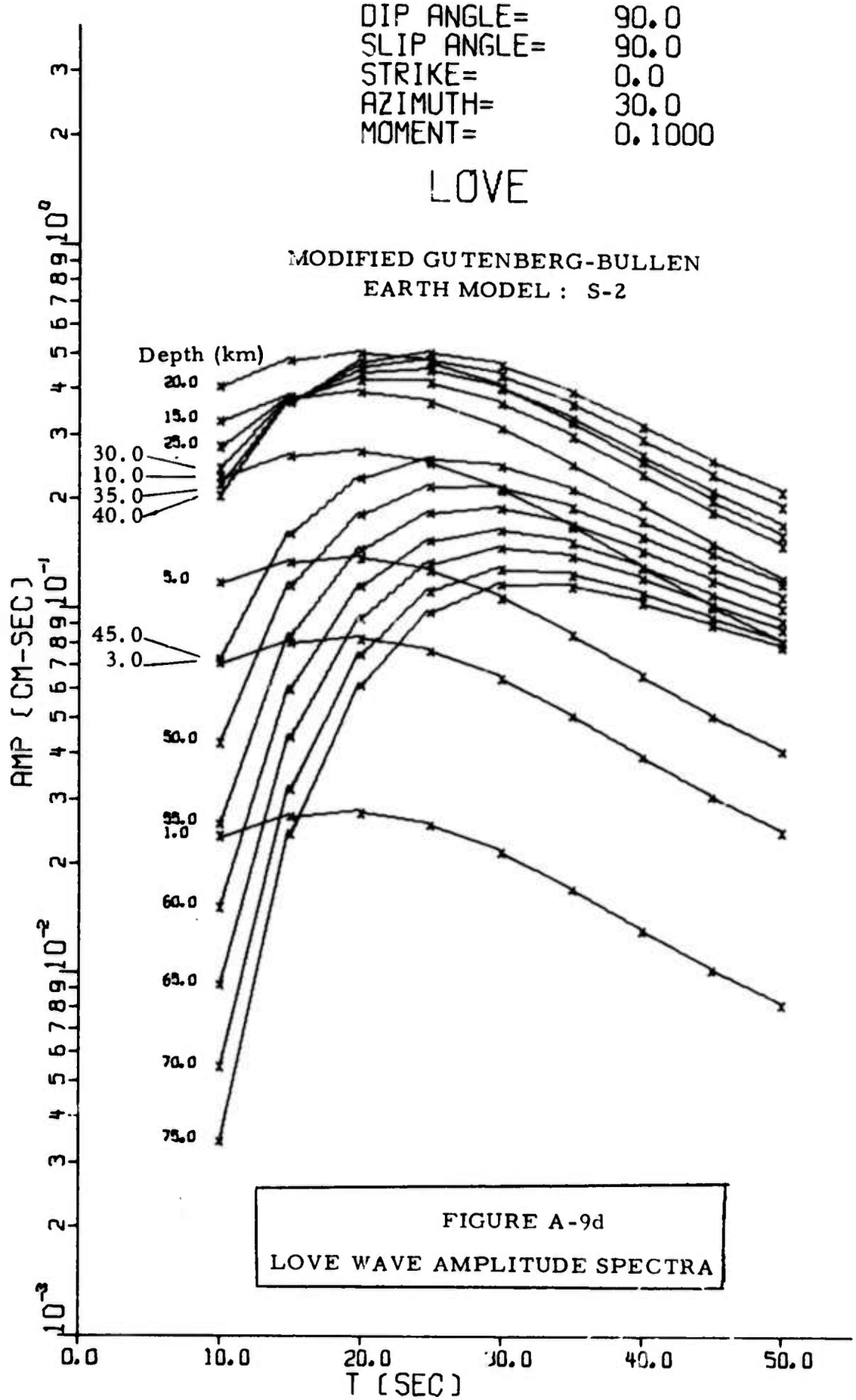

FIGURE A-9d

LOVE WAVE AMPLITUDE SPECTRA

APPENDIX B

COMPARISON OF THE INSTRUMENT RESPONSE AT SELECTED VLPE STATIONS, ALPA, AND NORSAR

The instrument response curves at selected VLPE stations were compared to those at NORSAR and ALPA to obtain some idea of the quality of the spectra we are using in 10 to 20 second period range. A summary of the vertical and horizontal response is given in Table B-1, with the actual curves shown in Figures B-1 to B-6 for ALQ, TLO, EIL, CHG, ALPA, and NORSAR. The important differences between the VLPE and array instruments are the response peaks (35-40 seconds vs 25 seconds respectively) and the dB down at 10 seconds (25 to 35 dB down vs 12 to 20 dB down).

If the VLPE instruments were to be modified to an array type response, the question arises as to the possible loss of long period information. A study by Massé (1970) showed that no information is lost, with the response curves of the instruments he used shown in Figure B-7, and the comparitive spectra of a typical event shown in Figure B-8.

TABLE B-1

INSTRUMENT RESPONSE AT 10 SECOND PERIOD FOR SELECTED VLPE STATIONS, ALPA, AND NORSAR

Station	Vertical Component		Horizontal Component	
	Period of Peak Response	dB Down From Peak At 10 Sec.	Period of Peak Response	dB Down From Peak At 10 Sec.
VLPE Sites				
ALQ	35	22.4	50	27.4
TLO	40	25.0	45	30.2
EIL	35	34.0	40	27.2
CHG	40	28.2	45	28.0
ALPA	25	20.0	25	20.0
NORSAR	25	12.0	25	12.0

FIGURE B-1

SYSTEM RESPONSE FOR ALQ

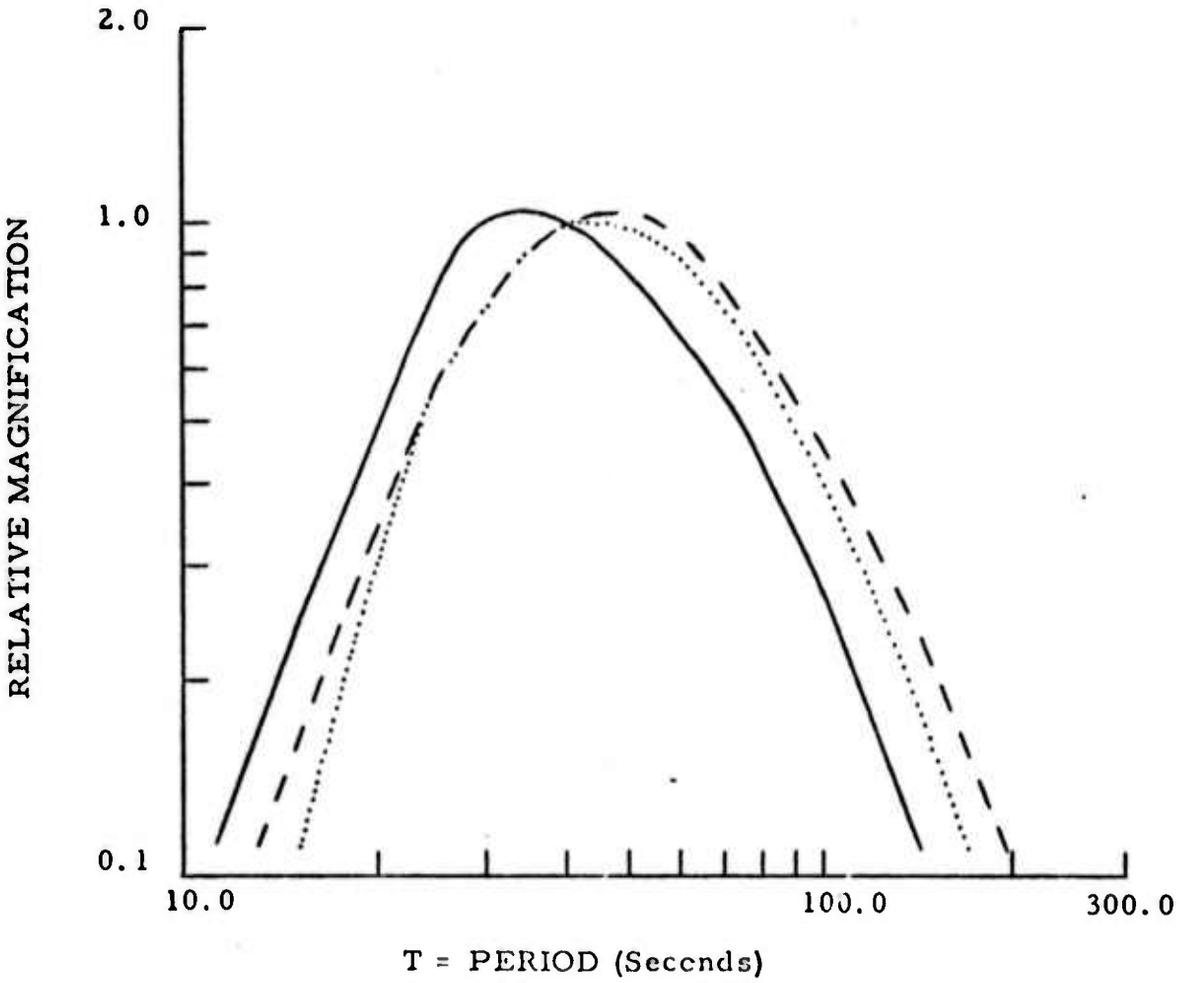

Gain at T = 40.0 Sec.

——— Z 1.12 mμ/count

- - - N 0.697 mμ/count

. . . . E 0.819 mμ/count

FIGURE B-2

SYSTEM RESPONSE FOR TLO

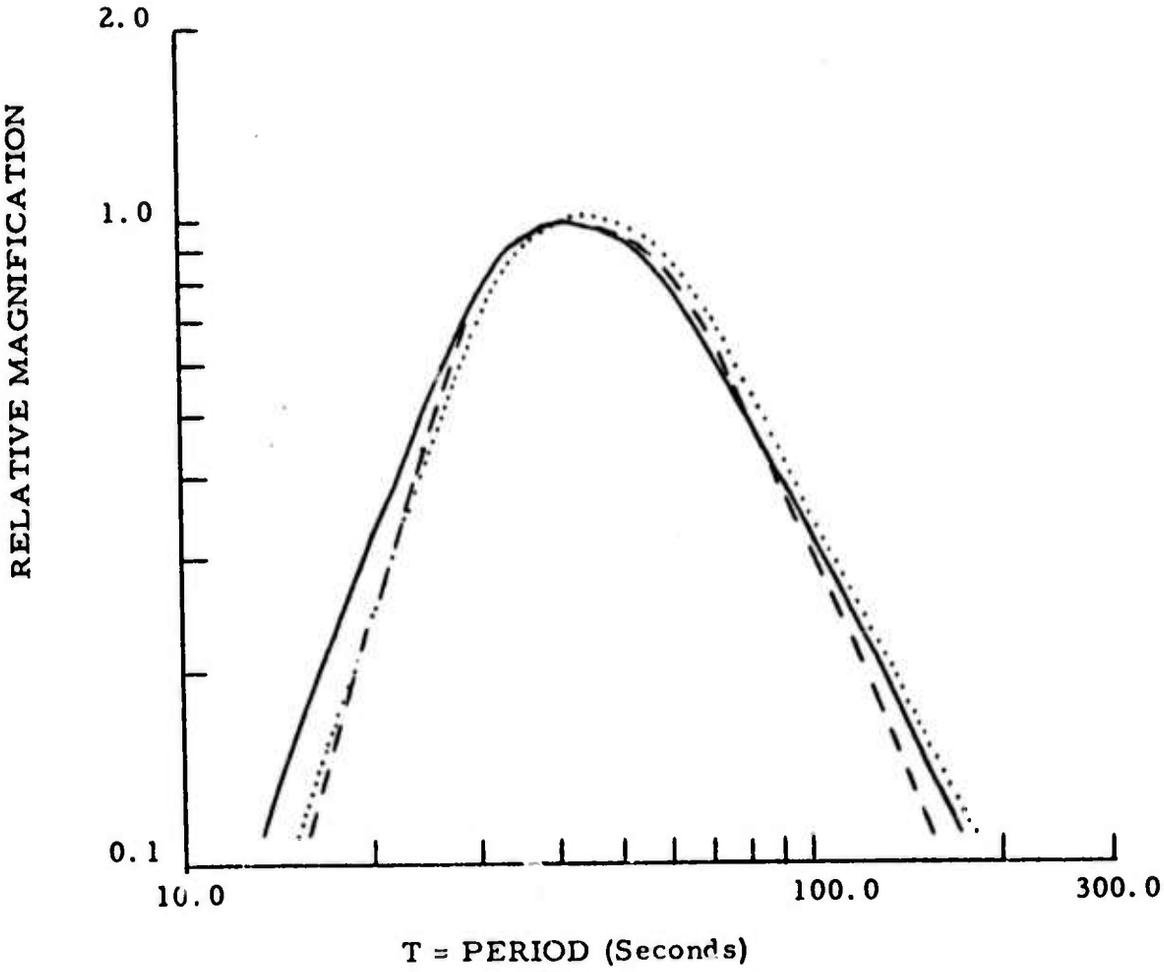

Gain at T = 40.0 Sec.

———	Z	0.708 mμ/count
- - -	N	0.625 mμ/count
. . . .	E	0.584 mμ/count

FIGURE B-1

SYSTEM RESPONSE FOR ALQ

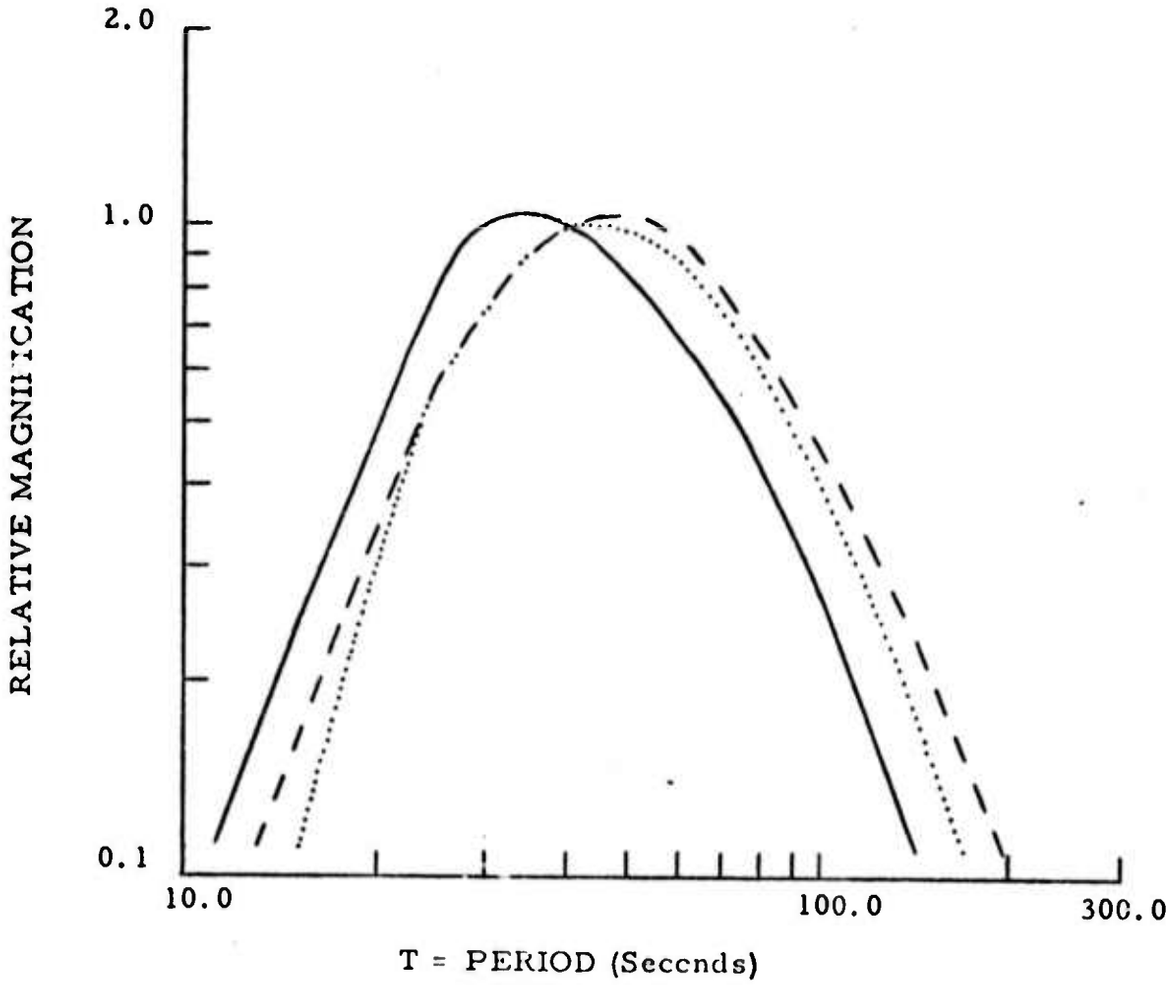

Gain at T = 40.0 Sec.

——— Z 1.12 mμ/count

- - - N 0.697 mμ/count

. . . . E 0.819 mμ/count

FIGURE B-2

SYSTEM RESPONSE FOR TLO

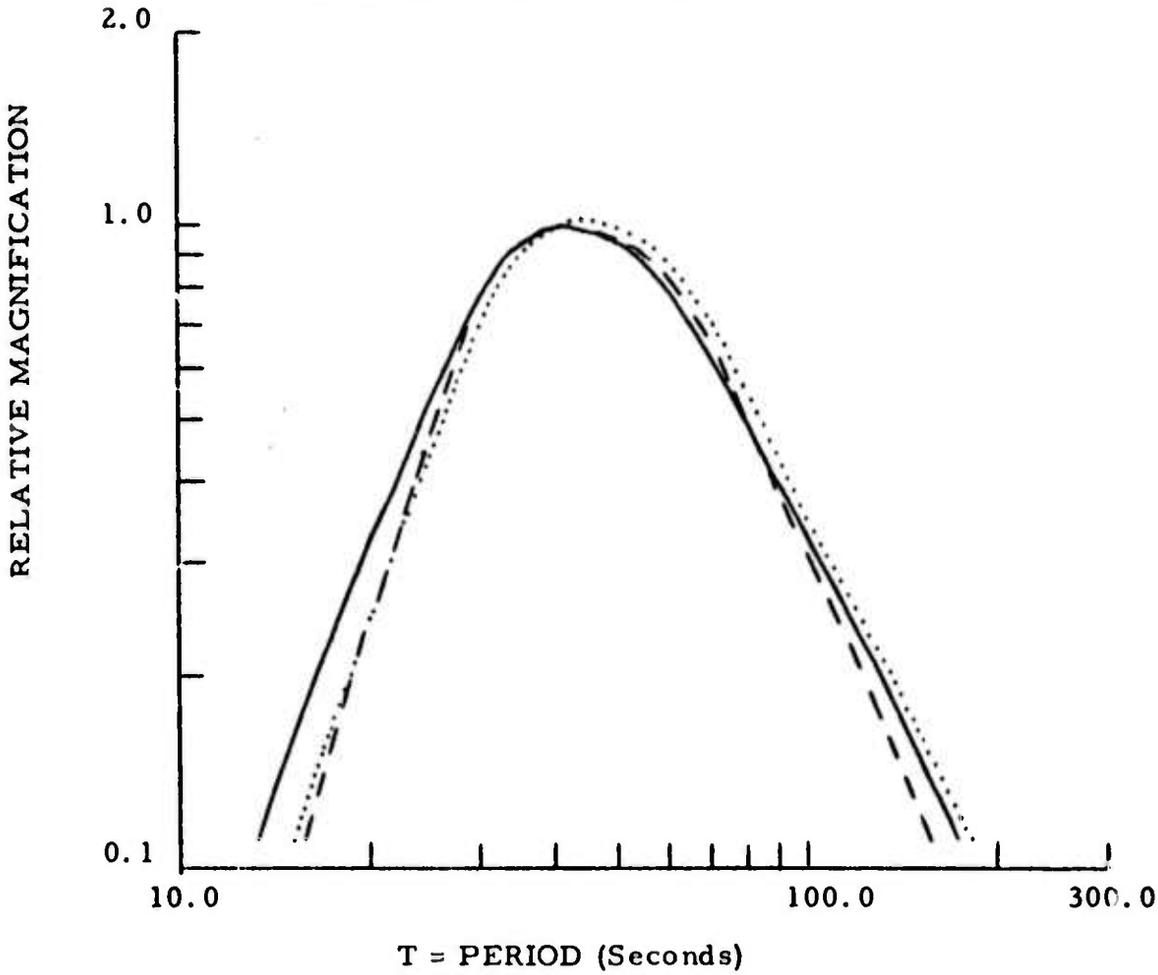

Gain at T = 40.0 Sec.

——— Z 0.708 mμ/count

- - - N 0.625 mμ/count

. . . . E 0.584 mμ/count

FIGURE B-3

SYSTEM RESPONSE FOR EIL
NOVEMBER 1972 TO PRESENT

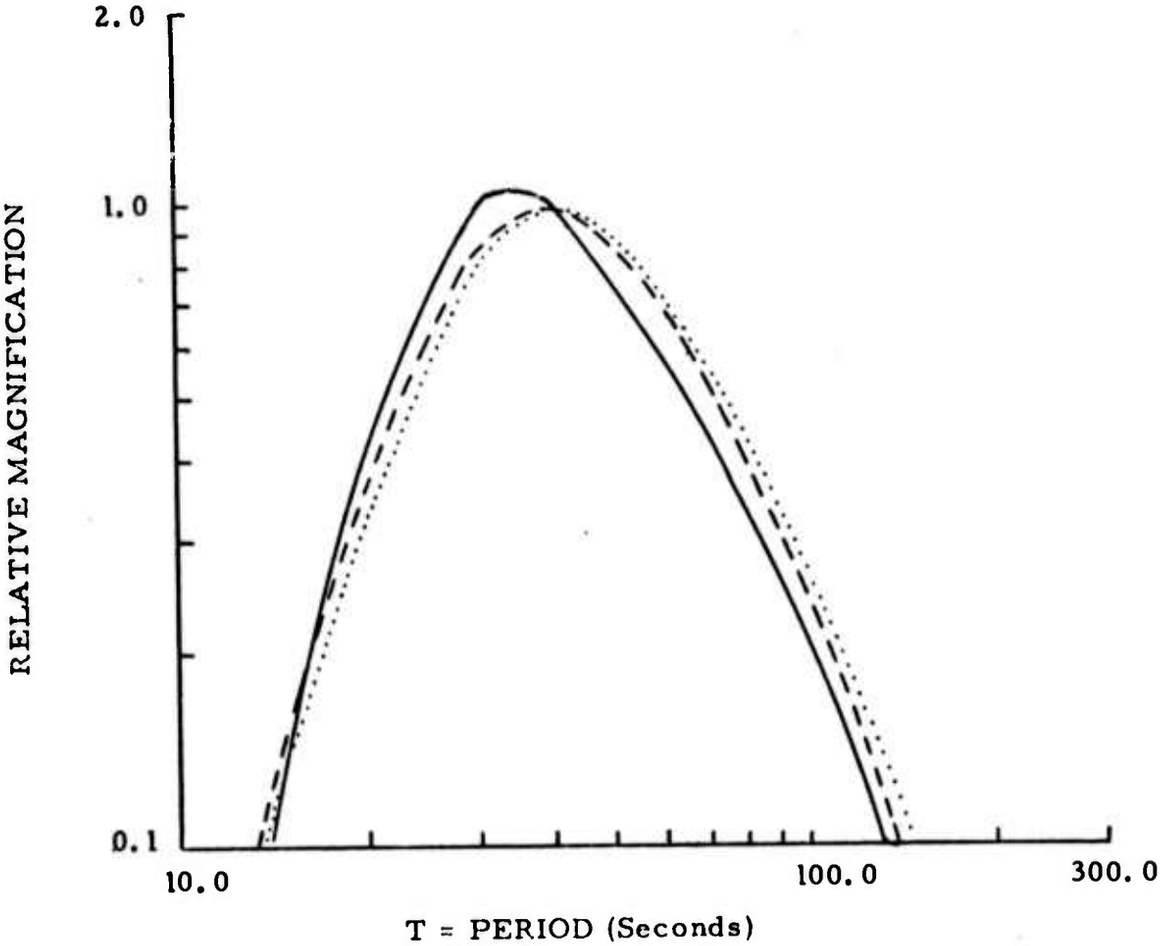

Gain at T = 40.0 Sec.

——— Z 1.701 mμ /count

- - - N 1.441 mμ /count

. . . . E 1.774 mμ /count

FIGURE B-4

SYSTEM RESPONSE FOR CHG

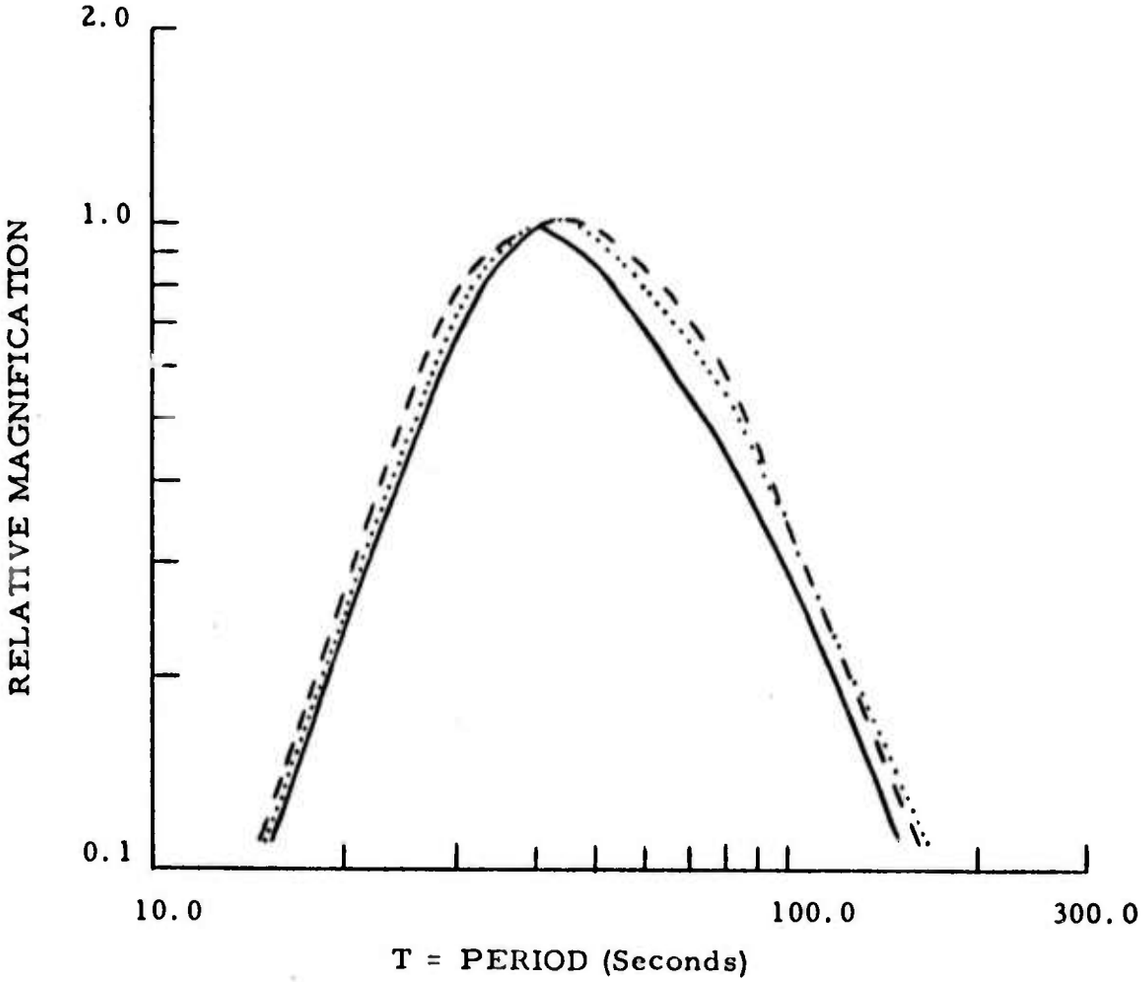

Gain at T = 40.0 Sec.

——— Z 0.806 mμ/count

- - - N 1.14 mμ/count

. . . . E 0.806 mμ/count

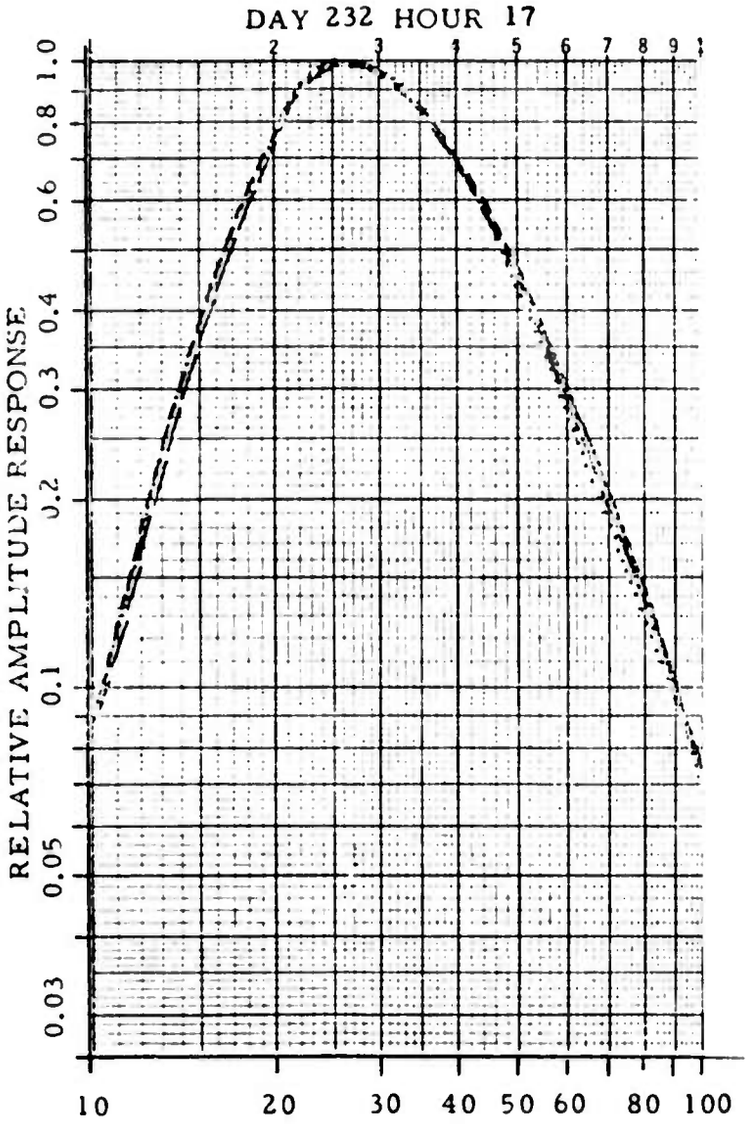

FIGURE B-5

NOMINAL AMPLITUDE RESPONSE OF LP SEISMOMETER AT ALPA

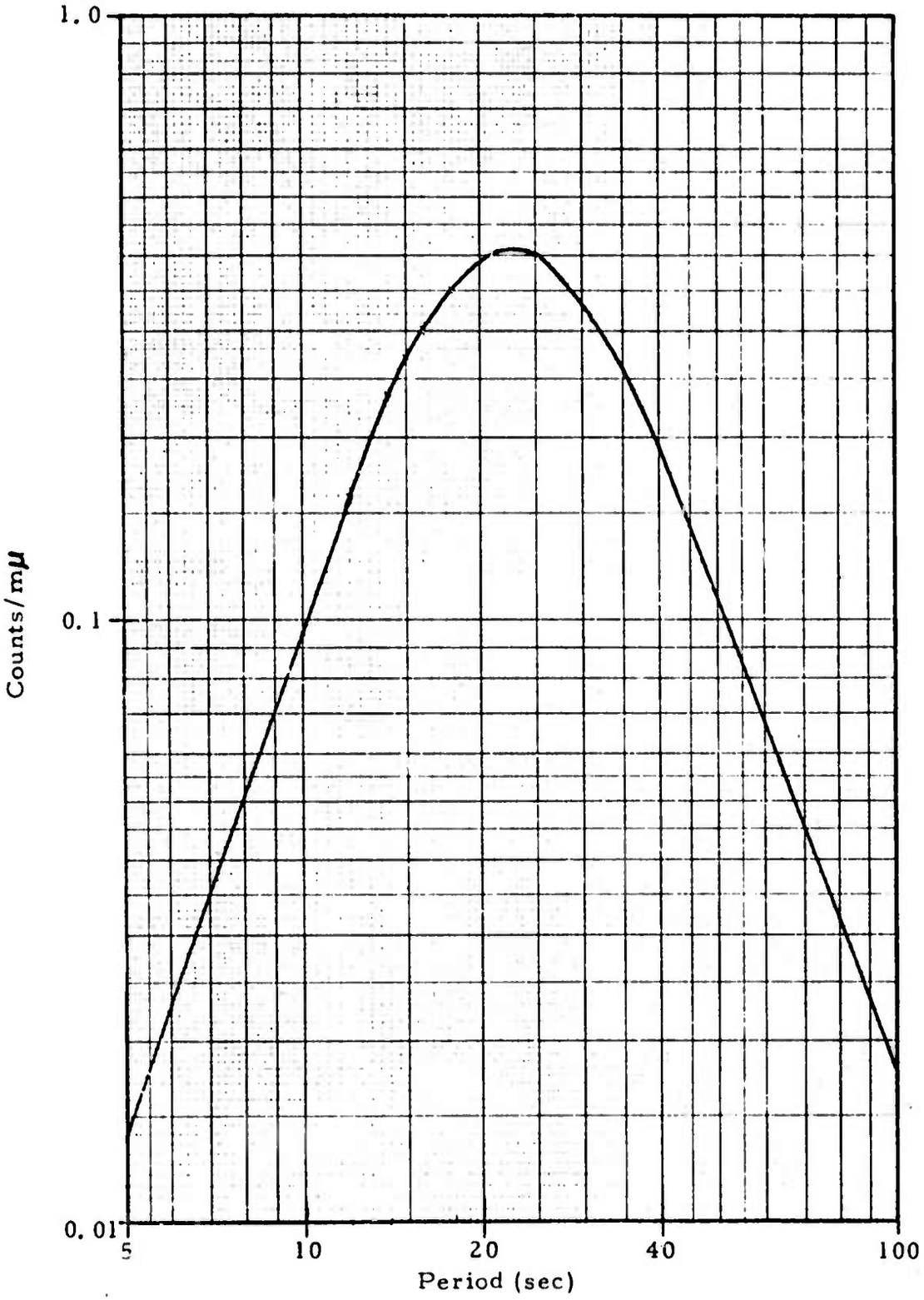

FIGURE B-6

NOMINAL AMPLITUDE RESPONSE OF LP SEISMOMETER AT NORSAR

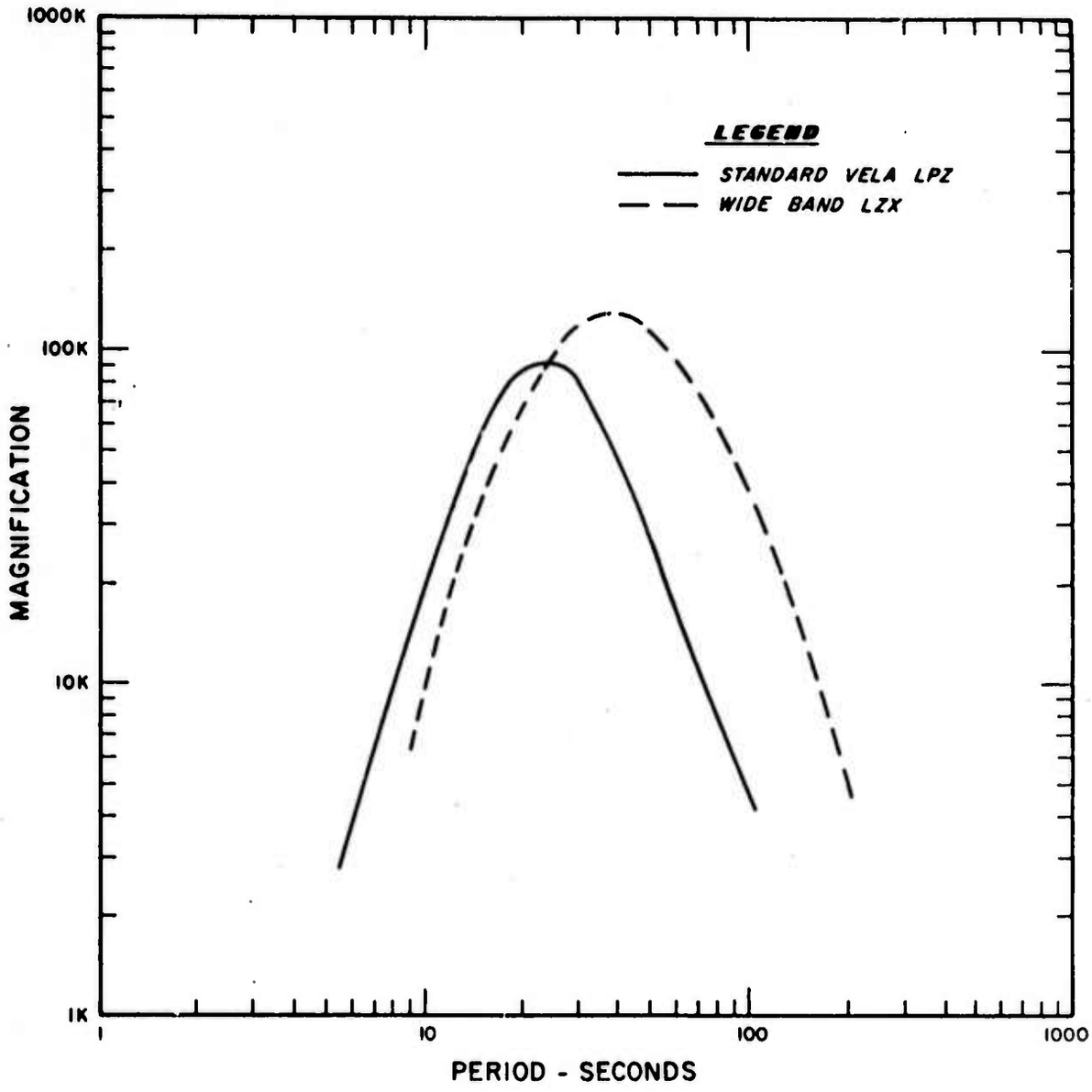

FIGURE B-7

SYSTEM RESPONSE OF STANDARD VELA LONG PERIOD AND OF WIDE BAND LONG PERIOD SEISMOGRAPHS

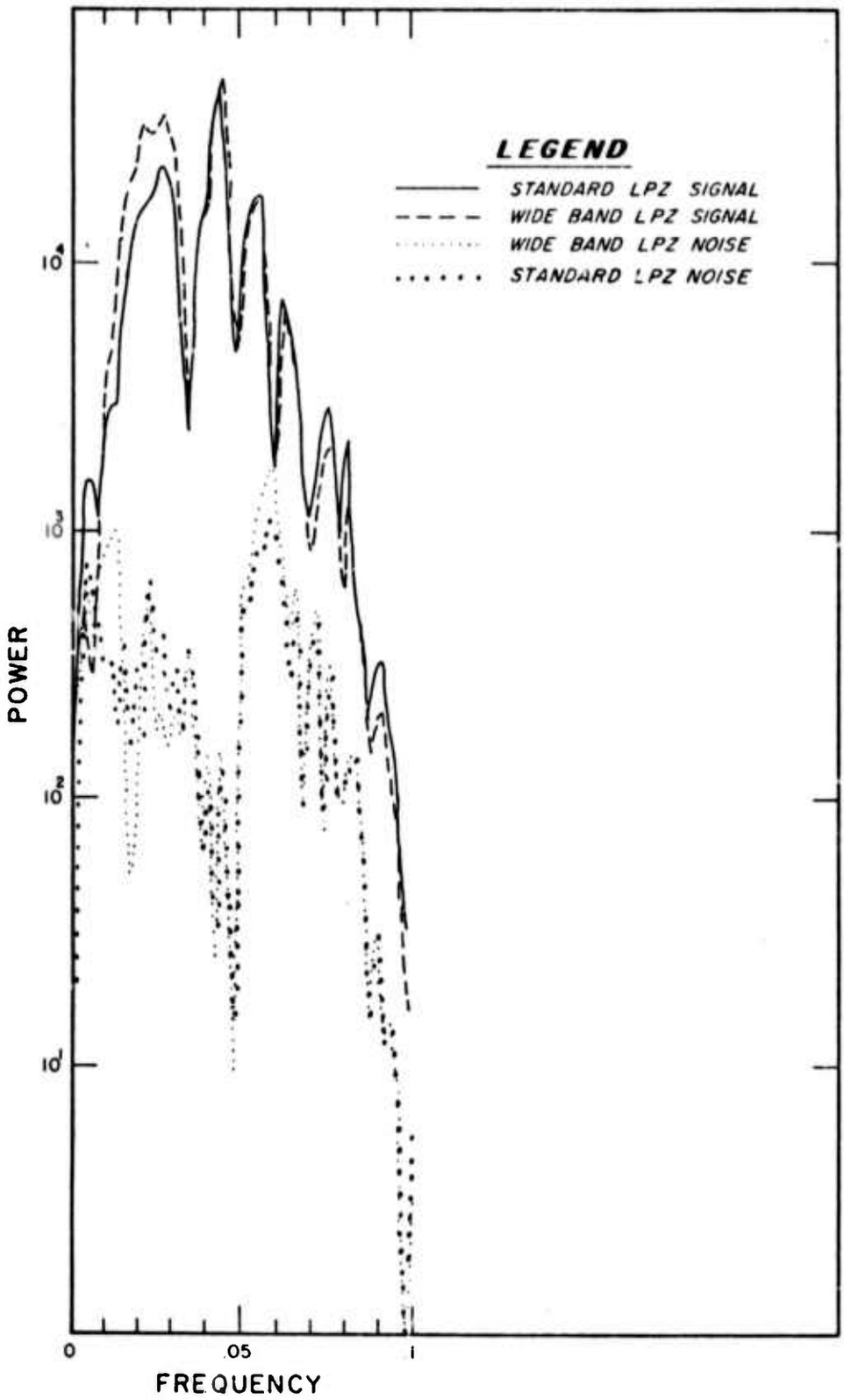

FIGURE B-8

POWER SPECTRA OF RAYLEIGH WAVES FROM AN EVENT IN THE CENTRAL PACIFIC OCEAN ON 4 NOVEMBER 1969

APPENDIX C

DETERMINATION OF FUNDAMENTAL MODE AMPLITUDE SPECTRA AND GROUP VELOCITIES BY NARROW BAND FILTERING

The background for the use of narrow band filters for de-multipathing has been discussed in an earlier report (Turnbull, et. al., 1973). We applied this technique to a pari of Italian events as well as Eurasian events with a reasonable degree of success. A recent examination of some of the developmental software has revealed a minor error, which resulted in an incorrect seismic moment (M_o) for the Italian events only. The corrected results are given in Appendix D.

We are in the process of automating the de-multipathing procedure. An example of some of the software objectives is shown in Figure C-1. The top trace shows the Rayleigh wave as recorded on the vertical component at CHG. The second trace shows the instantaneous period (Bracewell, 1965, and Newton, 1973). By calculating the instantaneous period (or its reciprocal, the instantaneous frequency), we obtain the period at which the phase of the analytic signal is changing. The abrupt phase changes caused by signal interference (multipathing) show up as sharp peaks. The third trace shows the result of applying a narrow band filter centered about 25 seconds period, with the fourth trace giving the envelope function of that result. The fifth and sixth traces represent the application of a narrow band filter center about 10 seconds period with its associated envelope function.

Presently, we pick the peaks of the narrow band filter results for an ensemble of periods (say 10 - 60 seconds), and compute their group velocity. These values are then plotted against standard curves as shown

LXTRAN

SIGNAL LX+CENAP+ 45
DATE 73015 (1/15/73)
TIME 46544 (12:55:44)
LAT 40.4
LONG 91.1
MAG-USCGS 5.1
SCALE: MMU/INCH

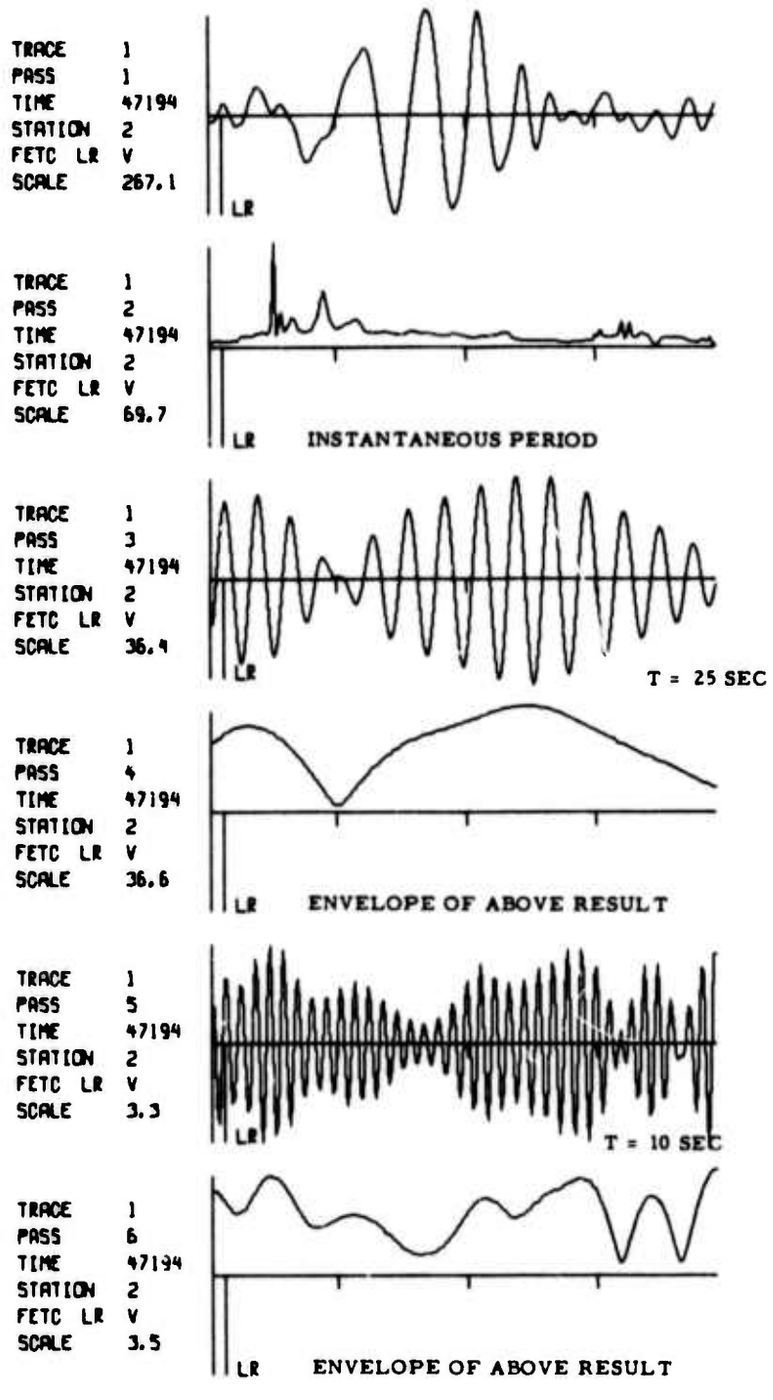

FIGURE C-1

NARROW BAND FILTER ANALYSIS

in Figure C-2, which shows the result for this analysis for CENAP+75 as recorded at CHG (see Section III for discussion of the abnormally low group velocities). The de-multipathed spectra is then chosen by estimating the trend of the peaks with the standard curves as reference. We are presently automating this selection of the proper wave packet.

OBSERVED GROUP VELOCITIES FROM NARROW BAND FILTERS

CENAP + 75 to CHG

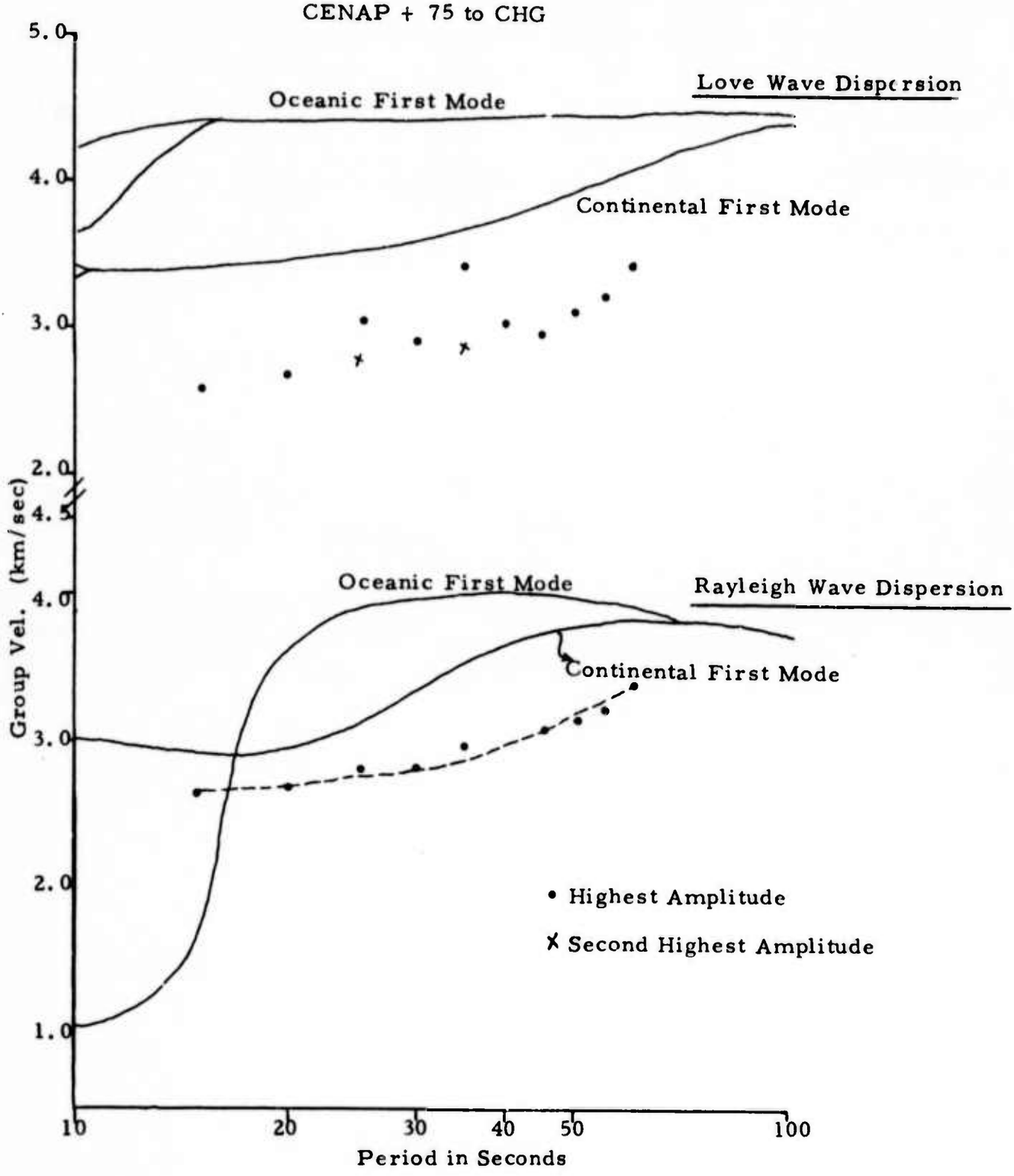

FIGURE C-2

APPENDIX D

ANALYSIS OF ITALIAN EVENTS

The solutions to these events were presented in an earlier report (Turnbull, et. al., 1973). Due to an error in the developmental software, incorrect values of the seismic moment (M_o) was obtained for the pair of Italian Events that were presented. The event locations are shown in Figure D-1, and the correct source parameter estimates are given in Table D-1. In each case, both from the individual and spectral ratio analysis, the seismic moment (M_o) is approximately a factor of 35 greater than the value previously determined.

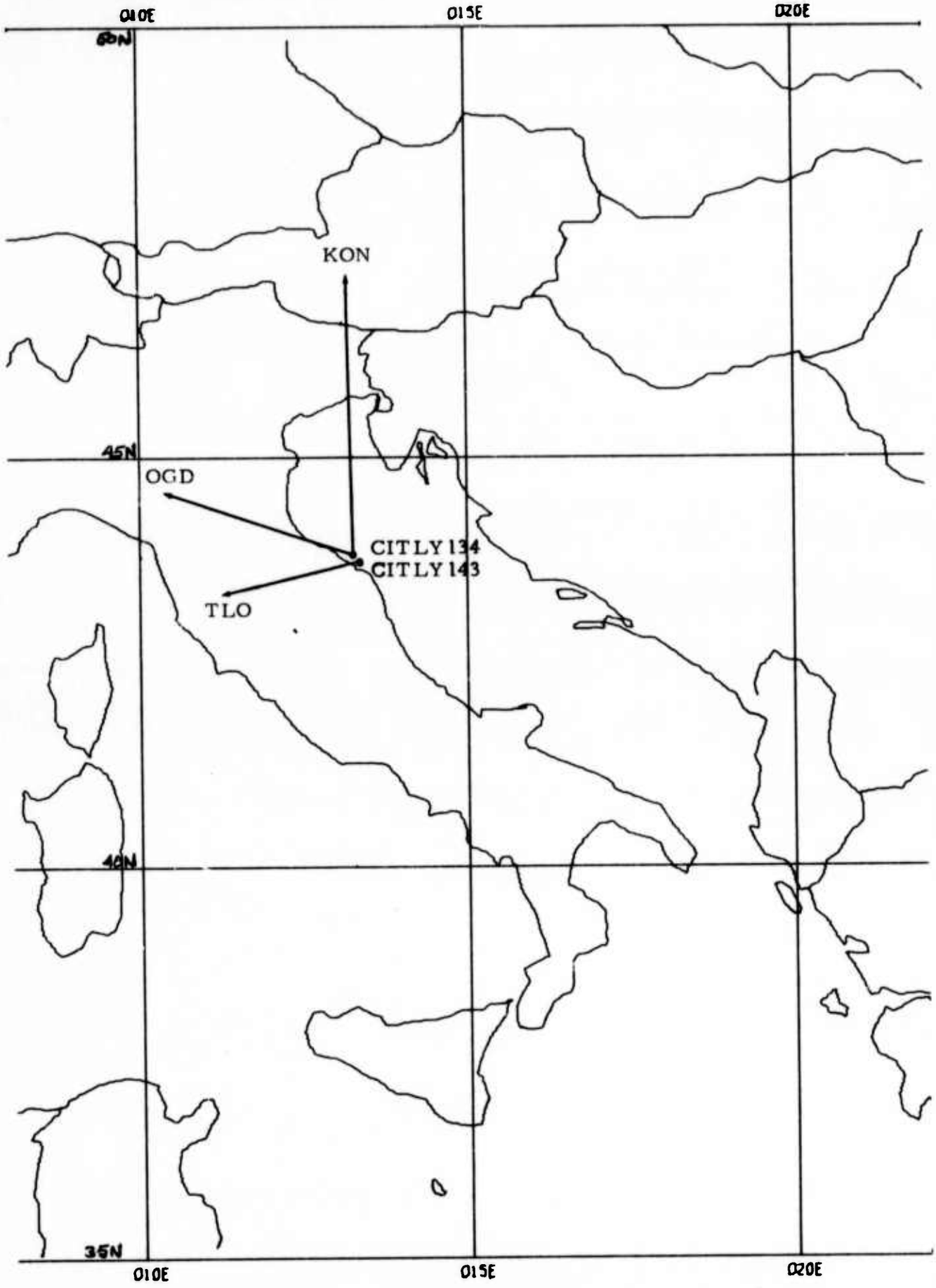

FIGURE D-1

LOCATIONS OF TWO, LOW MAGNITUDE ITALIAN EVENTS
RECORDED AT THREE VLPE STATIONS

TABLE D-1

SOLUTIONS FOR ITALIAN EVENTS

Analyzed Individually

Parameters	LX/CITLY/134 (2/4/72)		LX/CITLY/143 (2/5/72)	
	Value	Statistics	Value	Statistics
h (km)	22	20-26 ; 88%	20	18-24 ; 81%
δ	50°	40°-60°; 68%	50°	50°-70°; 65%
γ	-30°	$\pm 60^{\circ} \pm 30^{\circ}$; 89%	0°	-30°-30° ; 99%
ϕ	N110°E	80°-110°; 34%	N105°E	95°-115°; 37%
M (dyne-cm)	4.28×10^{22}		4.98×10^{22}	

Analyzed Using Spectral Ratio's of Events

$$\frac{S^{T}(\omega)_{\text{Trial Event}}}{S^{T}(\omega)_{\text{Ref. Event}}} = \frac{R^{OB}(\omega)_{TE}}{R^{OB}(\omega)_{RE}} = \frac{I(\omega)_{TE} G(\omega)_{TE} S^{OB}_{TE}(\omega)}{I(\omega)_{RE} G(\omega)_{RE} S^{OB}_{RE}(\omega)}$$

LX/CITLY/134 With LX/CITLY/143 As Reference

Parameters	Value	Statistics
h (km)	18	16-20 ; 87%
δ	40°	40° - 70°; 74%
λ	30°	$\pm 30^{\circ}$; 61%
ϕ	N90°E	80°-110°; 34%
M (dyne-cm)	4.64×10^{22}	

APPENDIX E

EXAMPLES OF MULTIPATHING FOR TYPICAL SOURCE STATION PATHS

In this section, we review some of the multipathing problems encountered in the analysis of Eurasian events. Using the data from CENAP + 45 as an example, we shall examine six travel paths from Central Asia to NORSAR, ALPA, KON, KIP, ALQ, and CHG (see Figure III-1 for the approximate paths). For each path, we are concerned with fundamental mode Rayleigh and Love wave dispersion.

CENAP+45 to NORSAR (Figure E-1): Because of the response characteristics of the NORSAR instrumentation, narrow band filters were applied from 20 to 10 seconds period at 2 second increments, as well as every 5 seconds period above 20 seconds to 60 seconds. Since the path is mostly continental, the dispersion curves followed along the expected continental modes. In the analysis of all the events discussed in Section III, NORSAR data was considered the most reliable.

CENAP+45 to ALPA (Figure E-2): These data were analyzed at intervals similar to those for NORSAR, again because of the favorable instrument response characteristics. The path is mostly continental, but a significant continental margin is crossed. Hence, more multipaths occur in the 10 to 20 second period range. In general, though, the curves were fairly regular.

CENAP+45 to KON(Figure E-3): For all VLPE data, only one period was examined below 20 seconds (15 seconds), because of their unadvantageous

OBSERVED GROUP VELOCITIES FROM NARROW BAND FILTERS

CENAP + 45 to NORSAR

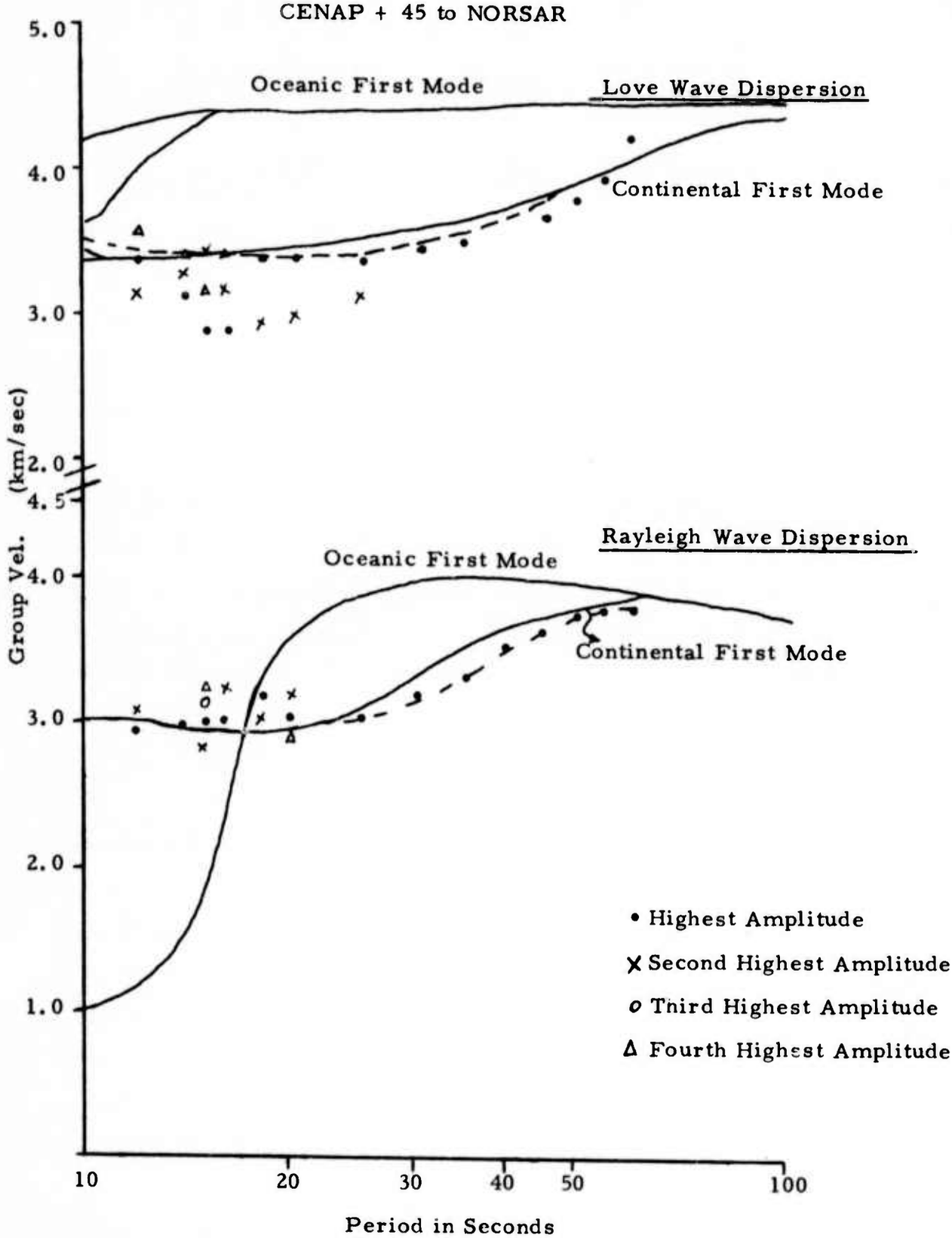

FIGURE E-1

OBSERVED GROUP VELOCITIES FROM NARROW BAND FILTERS

CENAP + 45 to ALPA

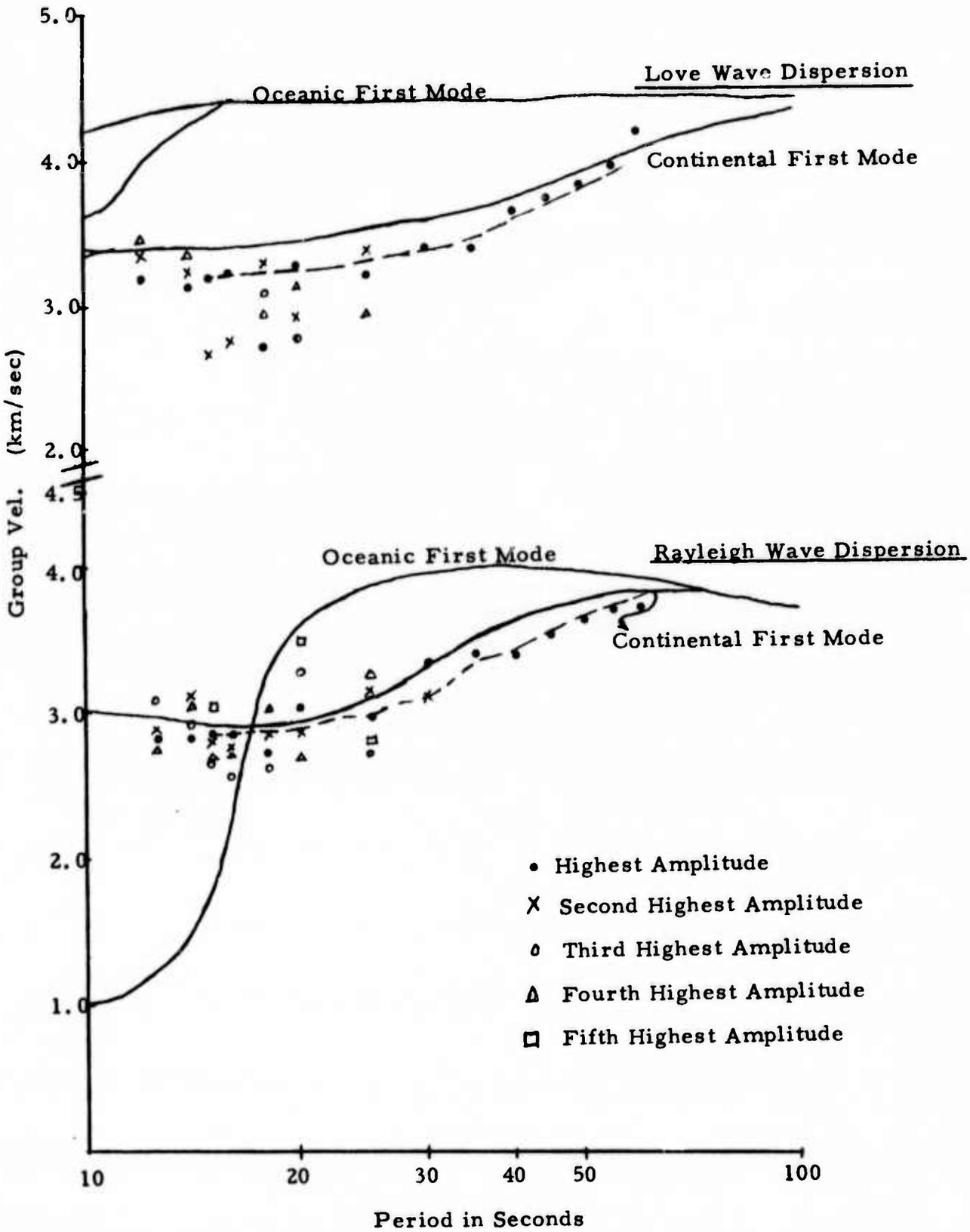

FIGURE E-2

OBSERVED GROUP VELOCITIES FROM NARROW BAND FILTERS

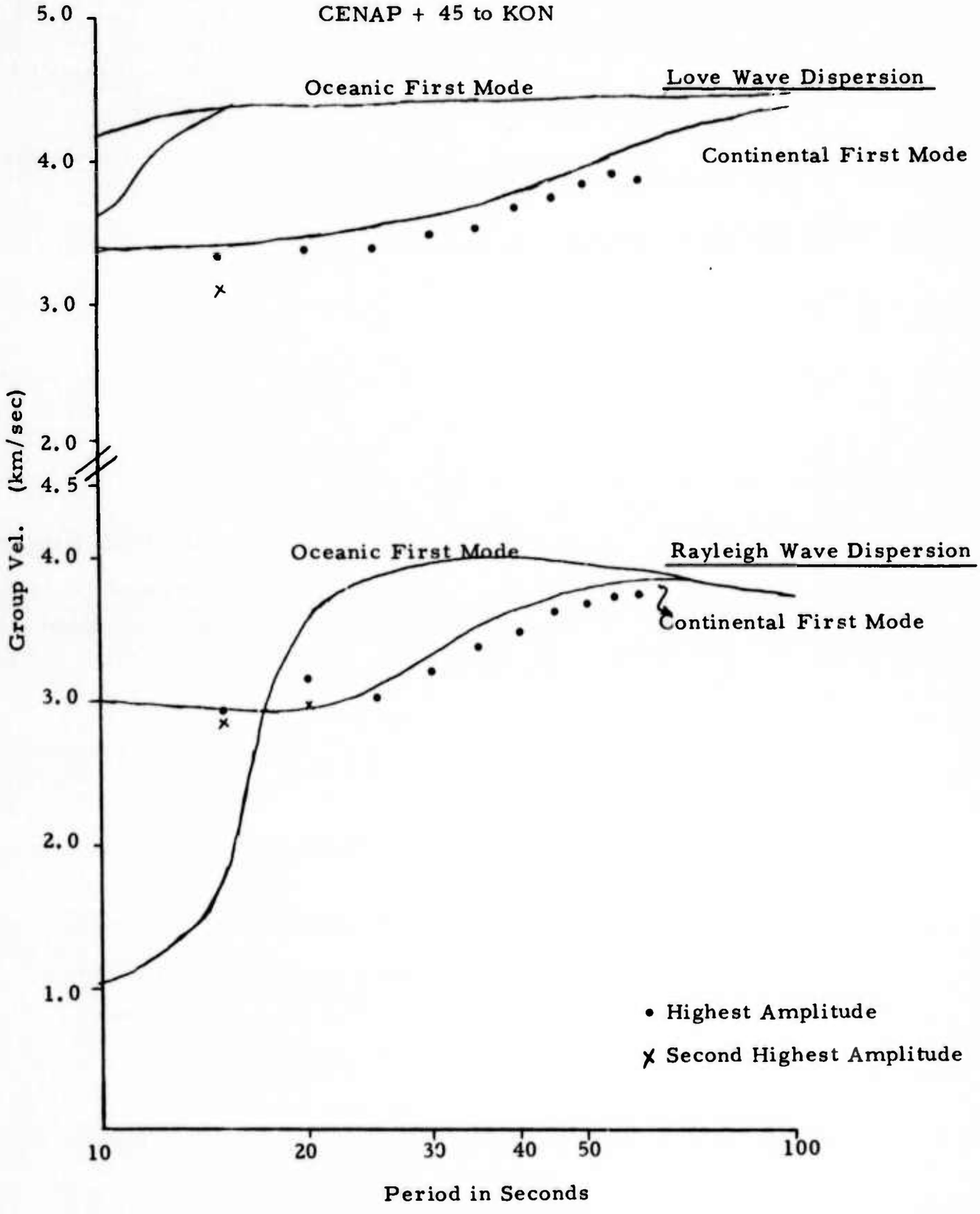

FIGURE E-3

instrument response characteristics. The data for this particular path was quite similar to that obtained for NORSAR, as should be expected.

CENAP+45 to KIP (Figure E-4): Because this path is approximately half continental and half oceanic, interpretation of the multipathing was very difficult. For several events, the Love wave spectra was completely eliminated from the fitting procedure. In many cases, several multipaths occurred for each period and the amplitudes were very close to each other. The Rayleigh wave dispersion approximated the mean of the oceanic and continental curves, especially below 30 seconds period.

CENAP+45 to ALQ (Figure E-5): The data obtained at ALQ was generally considered quite reliable. Although the travel path is polar, the dispersion curves closely follow the continental reference curve.

CENAP+45 to CHG (Figure E-6): This data probably constitutes the most irregular set observed. The path is entirely continental, but follows a course parallel and through some of the major Central Asian fold systems. It is characterized by severe Rayleigh and Love wave group delays, and severe Love wave multipathing. In many cases, the Love wave spectra had to be eliminated from the spectral fitting procedure.

OBSERVED GROUP VELOCITIES FROM NARROW BAND FILTERS

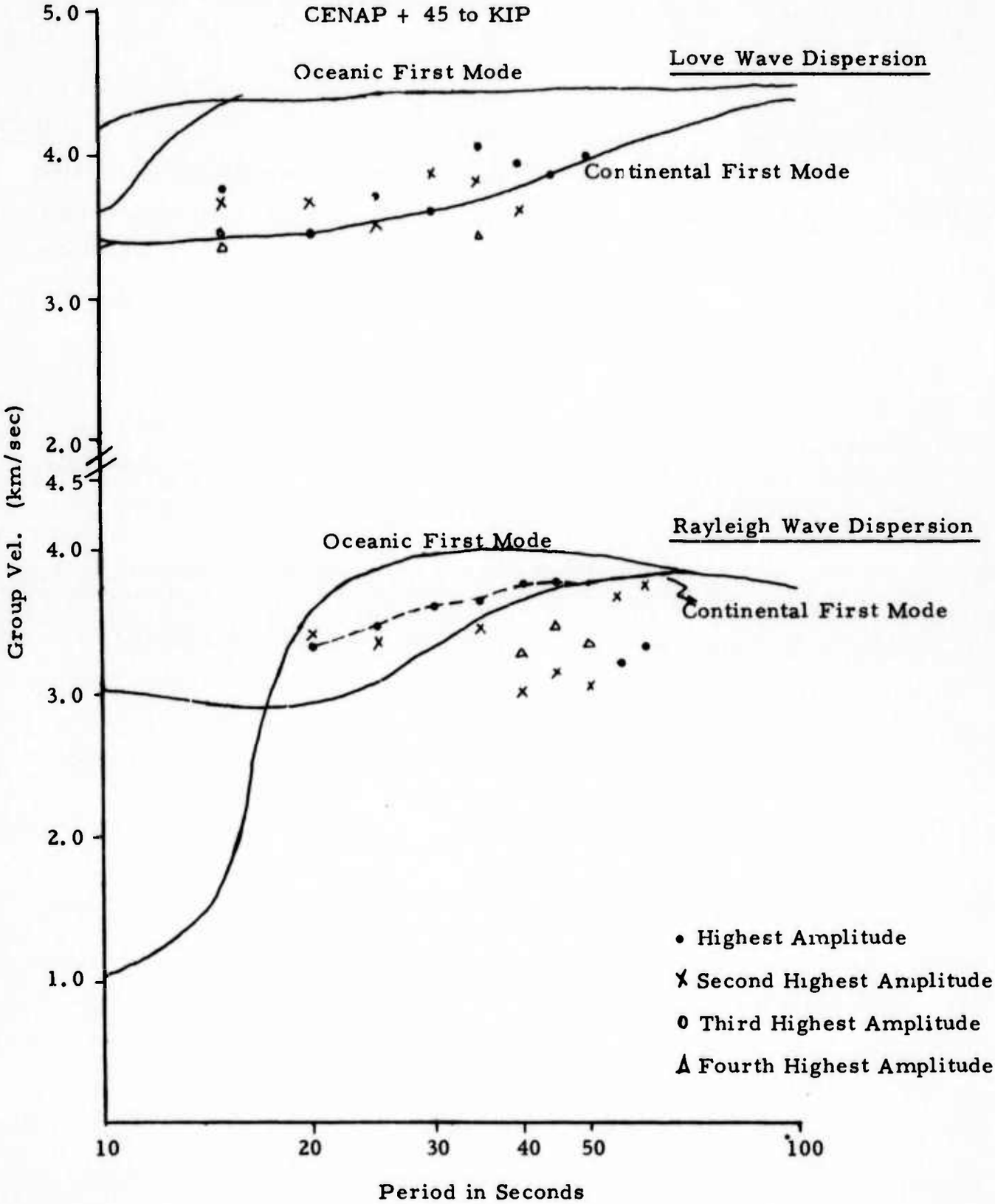

FIGURE E-4

OBSERVED GROUP VELOCITIES FROM NARROW BAND FILTERS

CENAP + 45 to ALQ

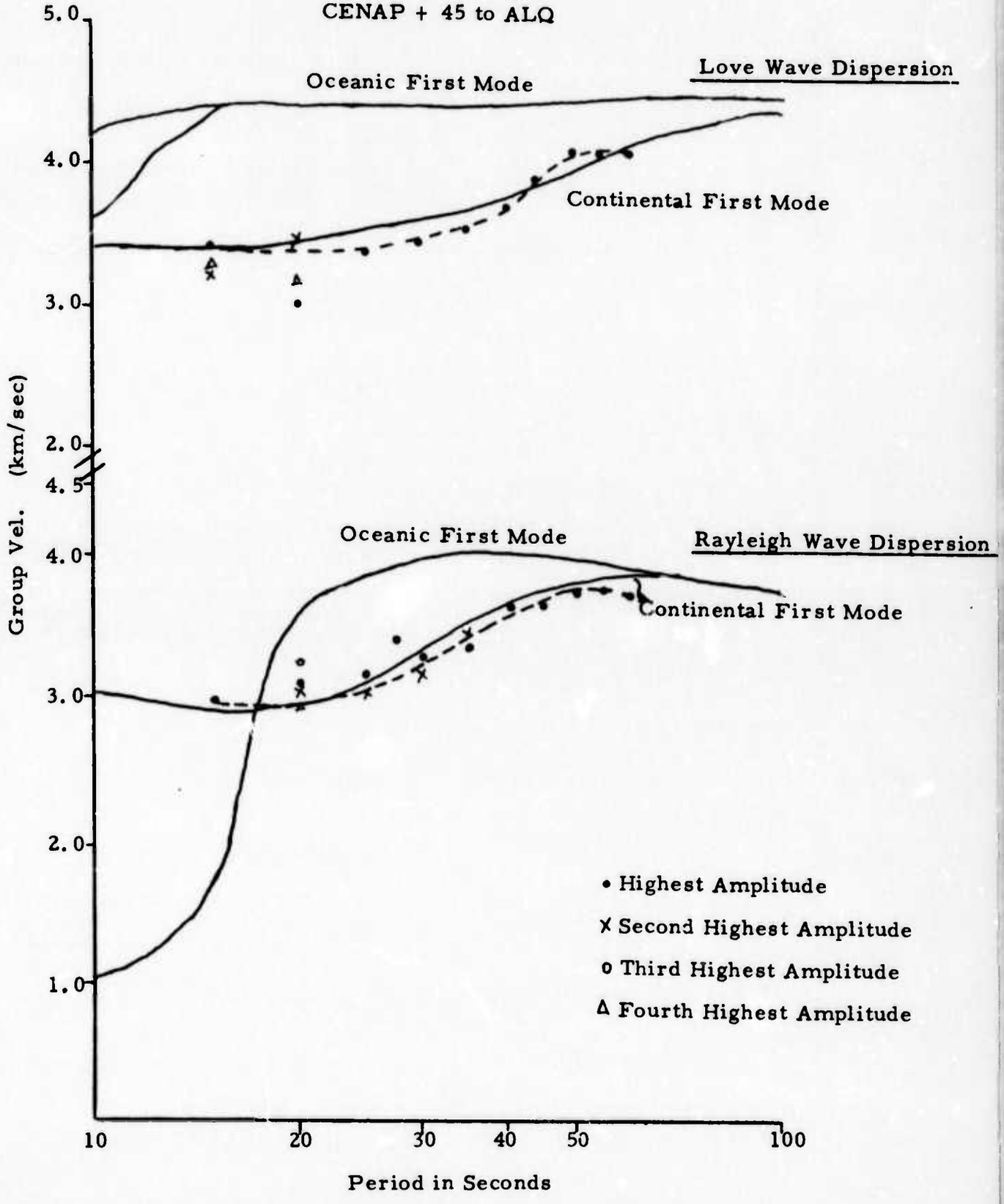

FIGURE E-5

OBSERVED GROUP VELOCITIES FROM NARROW BAND FILTERS

CENAP + 45 to CHG

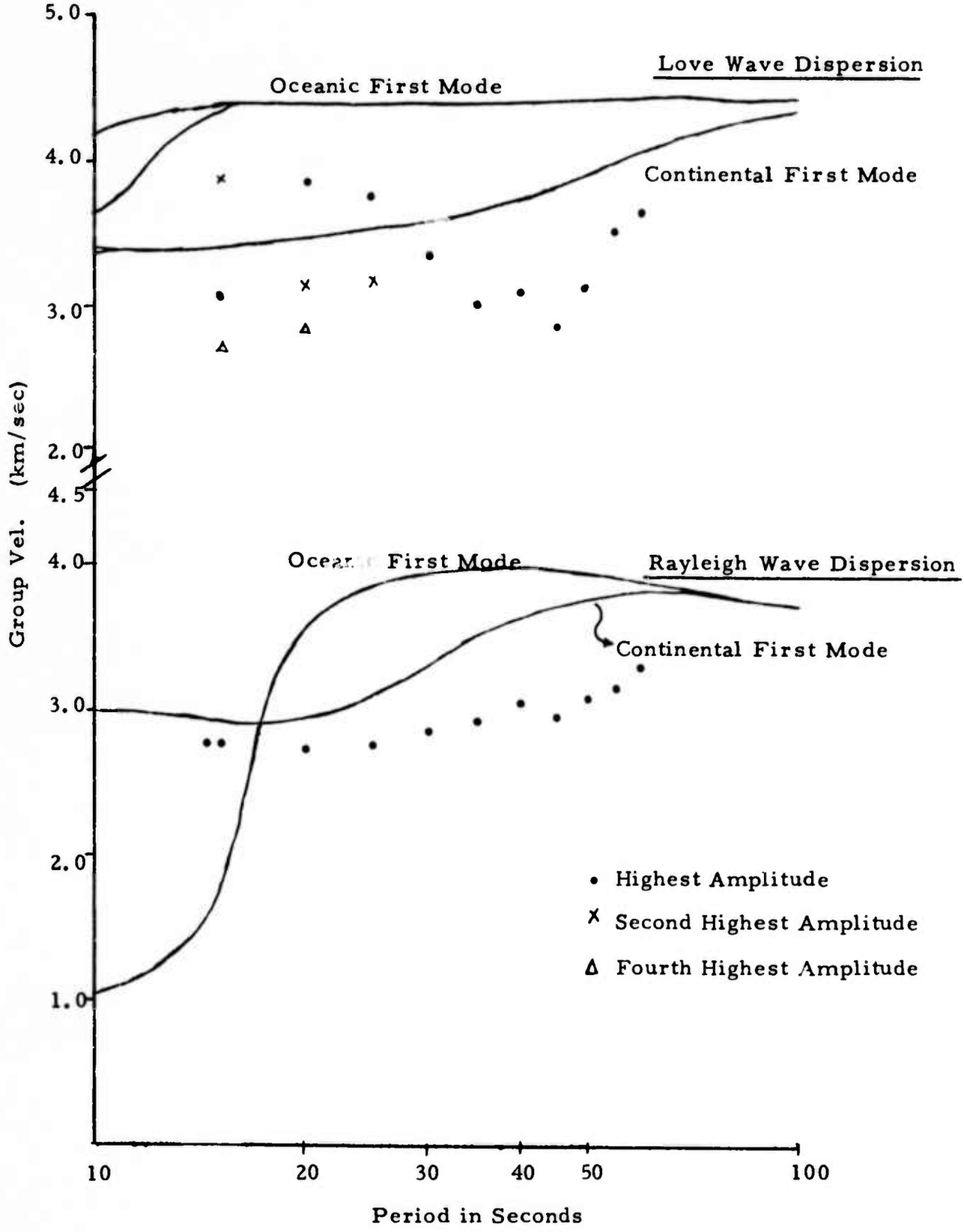

FIGURE E-6